

**Studies on the Coupling of Opioid and  
Cannabinoid Receptors to Adenylyl Cyclase.**

**Submitted in 1997 for the degree of Doctor of  
Philosophy to the University of Leicester by:**

**Robert Anthony Hirst BSc (hons).**

UMI Number: U551678

All rights reserved

INFORMATION TO ALL USERS

The quality of this reproduction is dependent upon the quality of the copy submitted.

In the unlikely event that the author did not send a complete manuscript and there are missing pages, these will be noted. Also, if material had to be removed, a note will indicate the deletion.



UMI U551678

Published by ProQuest LLC 2013. Copyright in the Dissertation held by the Author.  
Microform Edition © ProQuest LLC.

All rights reserved. This work is protected against  
unauthorized copying under Title 17, United States Code.



ProQuest LLC  
789 East Eisenhower Parkway  
P.O. Box 1346  
Ann Arbor, MI 48106-1346

## **Studies on the Coupling of Opioid and Cannabinoid Receptors to Adenylyl Cyclase.**

**Robert Anthony Hirst.**

This thesis represents a detailed study of the regulation of adenylyl cyclase (AC) by opioid and cannabinoid ligands which act at transmembrane spanning Gi-protein coupled receptors.

In SH-SY5Y human neuroblastoma cells carbachol (CCh) and  $K^+$  caused a time and dose dependent increase in cAMP formation and also increased  $[Ca^{2+}]_i$ .  $Ni^{2+}$  essentially abolished CCh stimulated  $[Ca^{2+}]_i$  plateau phase and blocked  $K^+$  stimulated  $[Ca^{2+}]_i$ . Preincubation with  $Ni^{2+}$ , did not affect the initial CCh mediated rise in cAMP but significantly reduced the 5 and 10min levels. CCh in  $Ca^{2+}$  free buffer increased cAMP and when  $Ca^{2+}$  was re-introduced to the buffer there was a further increase in cAMP. These studies suggest that SH-SY5Y cells express type 1 AC.

The previously characterised SH-SY5Y ( $[^3H]$ Diprenorphine (DPN)  $B_{max}$  (an estimate of opioid receptor density)=98fmol/mg protein) and NG108-15 ( $[^3H]$ DPN  $B_{max}$ =280fmol/mg protein) cells were used as a model system for the study of endogenous  $\mu$ - and  $\delta$ - opioid receptors respectively. In SH-SY5Y membranes, fentanyl, DAMGO and in NG108-15 membranes, DPDPE, DADLE displaced  $[^3H]$ DPN revealing high affinity binding sites. Fentanyl, DAMGO (SH-SY5Y) and DPDPE, DADLE (NG108-15) dose dependently inhibited forskolin stimulated cAMP formation with  $IC_{50}$  values of 18, 202nM and 0.8, 0.5nM respectively. Maximal inhibition ( $I_{max}$ ) in both cell lines with all agonists were relatively constant, 47-65%. The ORL-1 receptor agonist, nociceptin also inhibited forskolin stimulated cAMP formation in SH-SY5Y cells with  $IC_{50}$  and  $I_{max}$  values of 72nM and 47% respectively. These studies in SH-SY5Y cells, report the regulation by opioid and ORL-1 receptors of type 1 AC.

Endogenous opioid receptors in SH-SY5Y and NG108-15 cells were then compared with recombinant receptors expressed in CHO cells. Opioid receptor subtypes ( $\mu$ -,  $\delta$ -, and  $\kappa$ -) bound  $[^3H]$ DPN in a dose dependent and saturable manner, ( $B_{max}$ , range=35-561fmol/mg protein). Fentanyl and  $[D-Ala^2, Me-Phe^4, Gly-ol]$ enkephalin (DAMGO) displaced  $[^3H]$ DPN from CHO $\mu$  membranes with high affinity. Spiradoline displaced  $[^3H]$ DPN from CHO $\kappa$  cells.  $[D-Pen^2, D-pen^5]$ enkephalin (DPDPE) and  $[D-Ala^2, D-Leu^5]$ enkephalin (DADLE) displaced  $[^3H]$ DPN from CHO $\delta$  cell membranes revealing the presence of a high affinity binding site. All opioid agonists used in displacement studies inhibited forskolin stimulated cAMP formation in there respective CHO $\mu$ ,  $\delta$ , or  $\kappa$  cells.

The cannabinoid receptor is also an example of a transmembrane spanning G-protein coupled receptor. In order to study the cannabinoid receptor in detail, an assay was developed using the first central cannabinoid receptor (CB1) selective antagonist, SR141716A. In rat cerebella membranes,  $[^3H]$ SR141716A bound with a  $K_d$  of around 0.7nM. A range of cannabinoid agonists displaced  $[^3H]$ SR141716A from cerebella membranes. In addition, basal cAMP levels were inhibited by WIN55212-2 in rat cerebella membranes in an SR141716A reversible manner.

CB1 cDNA was expressed in CHO cells and the resulting CHO $CB1$  cells bound  $[^3H]$ SR141716A, which was displaced dose dependently by unlabeled SR141716A yielding a  $K_i$  of 2.2nM. These receptors were functionally coupled to adenylyl cyclase. Collectively, these findings add significantly to our current understanding of opioid and cannabinoid receptor regulation of AC.

## **Acknowledgement.**

This thesis is dedicated to my late father, Richard Anthony Hirst, who influenced and inspired my work. Also to my mother, who continues to give me her unconditional love.

Thank you to my brother and sister who have supported me throughout.

I would also like to thank the members of the Department of Anaesthesia who have helped me with proof reading etc., namely Jim, Bev, Charlotte, Ed, Dave C, Rob C, Kaz and Thor. Thanks also to Sarah Almond for help with cannabinoid experiments. A big thank you goes to Dave Lambert, who had faith in my ability, and who gave unlimited supervision and encouragement.

Thanks to all my friends for keeping me sane through the last four years, especially Gilly, Pip, Matt, Kul, Soph, Neil, Sarah, Gord, Bob, Viv, Gabs, Derick, Sarah O, Ant, Tasha, and anyone else I have missed.

Finally, special thanks to T. J. M. Simmons. for the love and support she has given me.

## **List of Abbreviations**

All abbreviations are defined in the text, and this list is in order of appearance.

<b>AC</b>	<b>Adenylyl cyclase</b>
<b>G-proteins</b>	<b>guanylyl nucleotide binding proteins</b>
<b>cAMP</b>	<b>cyclic adenosine 3'5' monophosphate</b>
<b>ATP</b>	<b>adenosine triphosphate</b>
<b>PDE</b>	<b>phosphodiesterase</b>
<b>PKA</b>	<b>protein kinase A</b>
<b>PLC</b>	<b>phospholipase C</b>
<b>I<sub>h</sub></b>	<b>inwardly rectifying cation current</b>
<b>5-HT</b>	<b>5-hydroxytryptamine</b>
<b>GABA</b>	<b>gamma aminobutyric acid</b>
<b>N-</b>	<b>amino</b>
<b>C-</b>	<b>carboxyl</b>
<b>GTP</b>	<b>guanylyl triphosphate</b>
<b>GDP</b>	<b>guanylyl diphosphate</b>
<b>P<sub>i</sub></b>	<b>phosphate</b>
<b>Mg<sup>2+</sup></b>	<b>magnesium</b>
<b>CaM</b>	<b>Ca<sup>2+</sup>/calmodulin</b>
<b>PKC</b>	<b>protein kinase C</b>
<b>cDNA</b>	<b>cloned DNA</b>
<b>[Ca<sup>2+</sup>]<sub>i</sub></b>	<b>intracellular calcium concentration</b>
<b>LTP</b>	<b>long term potentiation</b>
<b>PIP<sub>2</sub></b>	<b>phosphatidylinositol diphosphate</b>
<b>DAG</b>	<b>diacylglycerol</b>
<b>IP<sub>3</sub></b>	<b>inositol 1,3,5 triphosphate</b>
<b>SERM</b>	<b>smooth endoplasmic reticular membrane</b>
<b>SMOCC</b>	<b>second messenger operated Ca<sup>2+</sup> channels</b>
<b>ROCC</b>	<b>receptor operated Ca<sup>2+</sup> channels</b>
<b>GOCC</b>	<b>G-protein operated Ca<sup>2+</sup> channels</b>

<b>I<sub>crac</sub></b>	intracellular Ca <sup>2+</sup> store recharging Ca <sup>2+</sup> channels
<b>VOCC</b>	voltage operated Ca <sup>2+</sup> channels
<b>Na<sup>+</sup></b>	sodium
<b>K<sup>+</sup></b>	potassium
<b>Ba<sup>2+</sup></b>	barium
<b>NT</b>	neurotransmission
<b>Ach</b>	acetylcholine
<b>AFDX116</b>	(11[[2-[(diethylamino)methyl]-1-piperidinyl]acetyl]-5,11-dihydro-6H-pyrido[2,3-b][1,4]benzodiazepine-6-one
<b>HHS</b>	hexahydrosiladifenadol
<b>4-DAMP</b>	4-diphenylacetoxy-N-methyl piperidine methiodide
<b>DAMGO</b>	[D-Ala <sup>2</sup> ,Me-Phe <sup>4</sup> ,Gly-ol]enkephalin
<b>DPDPE</b>	[D-Pen <sup>2</sup> ,D-pen <sup>5</sup> ]enkephalin
<b>DADLE</b>	[D-Ala <sup>2</sup> ,D-Leu <sup>5</sup> ]enkephalin
<b>DSLET</b>	[D-Ser <sup>2</sup> ,Leu <sup>5</sup> ]enkephalyl-Thr
<b>Nor-BNI</b>	nor-binaltorphimine
<b>CTOP</b>	D-Phe-Cys-Tyr-D-Orn-Thr-Pen-Thr-NH <sub>2</sub>
<b>NMDA</b>	N-methyl-D-aspartate
<b>α</b>	alpha
<b>β</b>	beta
<b>δ or Δ</b>	delta
<b>γ</b>	gamma
<b>κ</b>	kappa
<b>λ</b>	lamda
<b>μ</b>	mu
<b>ω</b>	omega
<b>CNS</b>	central nervous system
<b>CGRP</b>	calcitonin gene related peptide
<b>AP</b>	action potential
<b>NT</b>	neurotransmission
<b>Δ<sup>9</sup>-THC</b>	Δ <sup>9</sup> -tetrahydrocannabinol
<b>CB1</b>	central cannabinoid receptor

<b>CB2</b>	peripheral cannabinoid receptor
<b>TFP</b>	trifluoperazine
<b>IBMX</b>	4-isobutyl-1-methylxanthine
<b>CCh</b>	carbachol
<b>Fura2-AM</b>	Fura2-acetoxymethylester
<b>EDTA</b>	ethylenediaminetetracetic acid
<b>EGTA</b>	ethyleneglycol-di-(aminoethyl)-N,N,N',N'-tetraacetic acid
<b>CK</b>	creatine kinase
<b>PC</b>	phosphocreatinine
<b>BSA</b>	bovine serum albumin
<b>DMSO</b>	dimethylsulphoxide
<b>MOPS</b>	3-(N-morpholino)propanesulphonic acid
<b>HEPES</b>	N-2-hydroxyethylpiperazine-N'-2-ethanesulphonic acid
<b>AMPA</b>	alpha amino-3-hydroxy-5-methyl-4-isoxazolepropionic acid
<b>HCl</b>	hydrochloric acid
<b>HAT</b>	hypoxanthine aminopterin thymidine
<b>PEI</b>	polyethanolamine
<b>DNA</b>	deoxyribose nucleic acid
<b>Cl<sup>-</sup></b>	chloride ion
<b>NaCl</b>	sodium chloride
<b>KCl</b>	potassium chloride
<b>MgCl<sub>2</sub></b>	magnesium chloride
<b>NaOH</b>	sodium hydroxide
<b>H<sub>2</sub>PO<sub>4</sub><sup>2-</sup></b>	hydrogen phosphate ion
<b>SO<sub>4</sub><sup>2-</sup></b>	sulphate ion
<b>EU</b>	enzyme units
<b>μl</b>	microlitres
<b>ml</b>	millilitres
<b>l</b>	litre
<b>g</b>	gram
<b>mg</b>	milligram
<b>μg</b>	microgram

<b>cm</b>	<b>centimeter</b>
<b>mm</b>	<b>milimeter</b>
<b>sec</b>	<b>seconds</b>
<b>min</b>	<b>minutes</b>
<b>M</b>	<b>molar</b>
<b>mM</b>	<b>milimolar</b>
<b>μM</b>	<b>micromolar</b>
<b>nM</b>	<b>nanomolar</b>
<b>pM</b>	<b>picomolar</b>
<b>fM</b>	<b>femtamolar</b>
<b>nm</b>	<b>nanometers</b>
<b>CO<sub>2</sub></b>	<b>carbon dioxide</b>
<b>g</b>	<b>gravity</b>
<b>Sfb</b>	<b>ratio of baseline fluorescence</b>
<b>CuSO<sub>4</sub></b>	<b>copper sulphate</b>
<b>Na<sub>2</sub>HCO<sub>3</sub></b>	<b>sodium hydrogen carbonate</b>
<b>NSB</b>	<b>non-specific binding</b>
<b>Kd</b>	<b>dissociation constant</b>
<b>Ki</b>	<b>equilibrium dissociation constant</b>
<b>Bmax</b>	<b>maximum binding sites</b>
<b>K<sub>+1</sub></b>	<b>on rate</b>
<b>K<sub>-1</sub></b>	<b>off rate</b>
<b>K<sub>ob</sub></b>	<b>observed on rate</b>
<b>IC<sub>50</sub></b>	<b>50% inhibitory concentration</b>
<b>EC<sub>50</sub></b>	<b>50% effective concentration</b>
<b>I<sub>max</sub></b>	<b>maximum inhibition</b>
<b>KiH</b>	<b>high affinity receptor</b>
<b>KiL</b>	<b>low affinity receptor</b>
<b>pIC<sub>50</sub></b>	<b>log IC<sub>50</sub></b>
<b>pKi</b>	<b>log equilibrium dissociation constant</b>
<b>pEC<sub>50</sub></b>	<b>log 50% effective concentration</b>
<b>ANOVA</b>	<b>analysis of variance</b>

<b>SEM</b>	<b>standard error of the mean</b>
<b>SD</b>	<b>standard deviation</b>
<b>p</b>	<b>probability</b>
<b>[<sup>3</sup>H]NMS</b>	<b>tritiated N-methyl scopolamine</b>
<b>[<sup>3</sup>H]DPN</b>	<b>tritiated diprenorphine</b>
<b>HBS</b>	<b>hepes buffered saline</b>
<b>BAPTA</b>	<b>1,2-di-(o-aminophenoxy)ethane-N,N,N'N'-tetraacetic acid</b>
<b>[Ca<sup>2+</sup>]<sub>e</sub></b>	<b>extracellular calcium concentration</b>
<b>HEK</b>	<b>human embryonic kidney</b>
<b>CHO</b>	<b>Chinese hamster ovary</b>
<b>PMSF</b>	<b>Phenylmethysulfonyl Fluoride</b>
<b>CBM</b>	<b>cerebella membranes</b>
<b>SR141716A</b>	<b>N-piperidino-5-(4-chlorophenyl)-1-(2,4-dichlorophenyl)-4-methylpyrozole-3-carboxamide hydrochloride</b>
<b>WIN55212-2</b>	<b>R-(+)-(2,3-dihydro-5-methyl-3-[4-morponolinylmethyl]pyrol[1,2,3-de]-1,4-benzoxazin-6-yl(1-napthalenyl) methanone mono-methanesulfonate</b>
<b>CP55,940</b>	<b>6S-[3(R),6α,6aα,9α,10aβ]-(-)-5,6,6a,7,8,9,10,10a-octahydro-6-methyl-3-(1-methyl-4-phenylbutoxy)-1,9-phenanthridinediol 1-acetate hydrochloride</b>
<b>anandamide</b>	<b>arachidonylethanolamide</b>
<b>RbCl</b>	<b>rubidium chloride</b>
<b>pH</b>	<b>log hydrogen ion concentration</b>
<b>UV</b>	<b>ultra violet</b>
<b>mv</b>	<b>milivolts</b>

<b><u>Contents.</u></b>	<b><u>Page Number.</u></b>
<b>Abstract.</b>	2
<b>Acknowledgment.</b>	3
<b>List of Abbreviations</b>	4
<b>Chapter 1. General Introduction.</b>	12
1.1. Adenylyl cyclase signalling	13
1.1.1. Functional consequences of cAMP inhibition	16
1.2. G-protein coupled receptors	17
1.3. G-proteins	18
1.4. Adenylyl cyclase	20
1.5. Phospholipase C, IP <sub>3</sub> and Ca <sup>2+</sup>	23
1.6. Voltage operated calcium channels.	25
1.7. Cholinergic muscarinic receptors	26
1.8. Opioid receptors	28
1.9. Opioid pharmacology and pain	35
1.10. Cannabinoid receptors.	38
1.11. Cell culture	42
1.12. General aims	43
<b>Chapter 2. Materials and Methods.</b>	45
2.1. Sources of chemicals	46
2.2. Buffer composition	47
2.3. Tissue culture	48
2.4. Harvesting and washing procedure	49
2.5. Membrane preparation	49
2.6. cAMP experiment and assay	49
2.7. Measurement of intra- and extracellular Ca <sup>2+</sup>	53
2.8. Lowry protein assay	57
2.9. Binding assay protocols	57
2.10. Receptor binding principles	57
2.11. Saturation studies	58
2.11.1 Why use Scatchard analysis?	59
2.12. Displacement studies	60

2.13. Kinetic analysis of Kd	61
2.14. Data analysis	62
<b>Chapter 3. Characterization of Adenylyl Cyclase in SH-SY5Y Human Neuroblastoma cells.</b>	63
3.1. Introduction	64
3.2. Methods	66
3.3. Results	68
3.4 Discussion	80
<b>Chapter 4. Characterisation of Endogenous <math>\mu</math>- and <math>\delta</math>-Opioid Receptors on SH-SY5Y and NG108-15 cells.</b>	84
4.1. Introduction	85
4.2. Methods	87
4.3. Results	87
4.4 Discussion	97
<b>Chapter 5. Recombinant <math>\mu</math>-, <math>\delta</math>-, and <math>\kappa</math>-opioid Receptors Expressed in CHO cells are Negatively Coupled to Adenylyl Cyclase.</b>	101
5.1. Introduction	102
5.2. Methods	104
5.3. Results	104
5.4 Discussion	115
<b>Chapter 6. Neuronal Cannabinoid Receptor Binding and Inhibition of Adenylyl Cyclase in Rat Cerebella, SH-SY5Y and NG108-15 Cell Membranes.</b>	118
6.1. Introduction	119
6.2. Method development	121
6.3. Final method	131
6.4. Results	132
6.5. Discussion	141
<b>Chapter 7. Functional Expression of the Recombinant Central Cannabinoid Receptor.</b>	143
7.1. Introduction	144
7.2. Methods	147
7.3. Results	151

7.4. Discussion	154
<b>Chapter 8. Discussion and Summary.</b>	156
8.1. Summary of Results.	157
8.2. Regulation of AC in SH-SY5Y cells by muscarinic and depolarisation induced increases in $[Ca^{2+}]_i$	160
8.3. Opioid receptor agonist affinity and potency-Effect of assay conditions.	164
8.4. Opioid Receptor pharmacology	165
8.5. Central cannabinoid receptor pharmacology.	171
8.6. Future work.	173
<b>Chapter 9. References.</b>	174
9.1. Publications arising from this thesis.	197

**CHAPTER 1. GENERAL INTRODUCTION.**

### **1.1. Adenylyl cyclase signaling.**

Cellular communication relies on membrane mediated biochemical events involving membrane bound proteins. Adenylyl cyclase (AC) is an enzyme used to relay extracellular signals into the cell. A chemical first messenger binds to a receptor which then transduces the signal across the plasma membrane via guanylyl nucleotide binding proteins (G-proteins). Activated G-proteins regulate the activity of AC to generate the second messenger, cAMP. The second messenger is then free to activate cAMP-dependent protein kinase enzymes which are responsible for phosphorylation of target proteins (Figure 1.1).

AC activity was first discovered in 1957, by investigations into the mechanisms of glucagon and adrenaline regulation of glycogen metabolism in liver homogenates [Rall et al]. AC is an enzyme which catalyses the formation of the second messenger, cyclic adenosine 3'5' monophosphate (cAMP) from the energy rich molecule adenosine triphosphate (ATP). The activity of AC is regulated by a variety of hormones and neurotransmitters (see table 1.1). Robison and coworkers [1968] demonstrated that cAMP bound to an intracellular enzyme which caused many intracellular proteins to be phosphorylated. The enzyme responsible for the phosphorylation events was named cAMP-dependent protein kinase A. It was soon clear that many types of cAMP-dependent protein kinase A existed. The ultimate role of the phosphorylation events is to cause a cellular response (some examples are shown in table 1.1). Phosphodiesterase (PDE) is the enzyme which is responsible for termination of the cAMP signal and this enzyme also exists as a family of structurally related isoforms [Beavo, 1996].

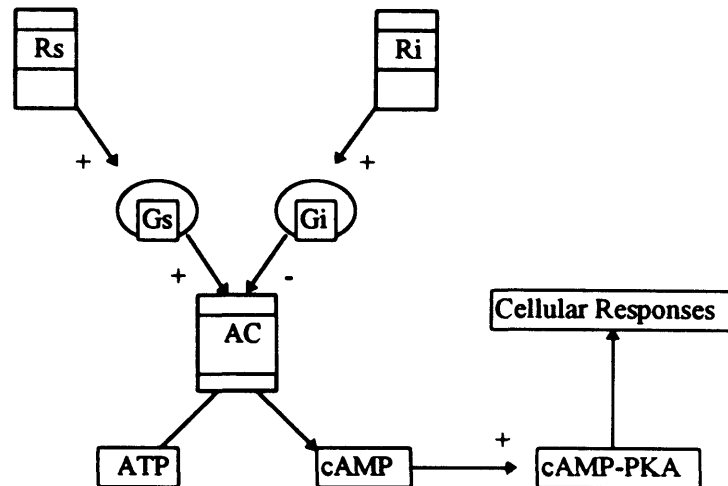


Figure 1.1. Schematic representation of AC signaling. Inhibitory (R<sub>i</sub>) or stimulatory (R<sub>s</sub>) receptors activate G<sub>i</sub> or G<sub>s</sub>, respectively. G proteins increases or decreases AC activity, thereby regulating intracellular cAMP levels, which in turn controls cAMP dependent protein kinase A activity. - = inhibition and + = stimulation.

The involvement of G-proteins in transmembrane signaling was first suggested by Rodbell and colleagues [1971], close examination of glucagon activation of AC activity in liver homogenates revealed the requirement for GTP. The discovery of S49 (*cyc-*) cell mutant, which lacked GTP-dependent AC activity was published in 1977 [Ross and Gilman]. A few years later both the GTP-binding component involved in phototransduction (transducin) and the GTP-binding regulatory component of AC (G/F and N now named G<sub>s</sub>) had been purified [Godchaux and Zimmerman, 1979; Kuhn, 1980; Bitensky et al, 1981; Stryer et al, 1981]. AC is regulated by heterotrimeric G-proteins in the cell membrane [Gilman, 1987]. AC activity is regulated by different types of G-protein [Birnbaumer et al, 1990]. If a receptor is linked to the inhibitory G-protein (G<sub>i</sub>) then the agonist for the receptor will cause a decrease in intracellular cAMP concentration by inhibiting AC activity. Receptors working via the stimulatory G-protein (G<sub>s</sub>) will stimulate AC activity and hence increase intracellular cAMP concentrations [Birnbaumer et al, 1990].

Agonist	Receptor	Cell type	G-protein	Effector	Effect
Adrenaline	$\beta 2$ adrenoceptors	Hepatocytes	$G_s$	AC	Glycogen catabolism
Adrenaline	$\beta 1$ adrenoceptors	Adipocytes	$G_s$	AC	Lipid catabolism
Vasopressin	V-2 receptors	Kidney cells	$G_s$	AC	Water reabsorption.
Acetylcholine	$M_2$ muscarinic receptors	Cardiac Myocytes	$G_i$	Potassium channels	Reduced heart rate and cardiac output
Enkephalins, endorphins, opioids	$\mu$ , $\delta$ and $\kappa$ - opioid receptors	Neurons	$G_i/G_o$	$Ca^{2+}/K^+$ channels AC	Modulate electrical activity of neurons
Angiotensin	Angiotensin II receptors	Vascular smooth muscle cells	$G_q$	PLC	vasoconstriction
Odorants	Oderant receptors	Nasal neuroepithelia l cells.	$G_{olf}$	AC	Oderant detection
Light	photoreceptors	Retinal rod and cone cells	$G_t$	cGMP PDE	Sight

Table 1.1. A small sample of physiological effects mediated by receptor-G-protein-effector coupling. PDE=Phosphodiesterase, PLC=Phospholipase C, AC=Adenylyl cyclase.

### **1.1.1. Functional consequences of cAMP inhibition.**

Receptors which couple to  $G_o$  or G inhibitory proteins cause no change or a reduction in  $[cAMP]_i$ . cAMP is responsible for the direct activation of cAMP dependent protein kinase A [Gilman, 1987]. This enzyme is responsible for the catalysis of ATP hydrolysis to ADP and transfer of a phosphate to serine and/or threonine amino acid residues within protein structures. The effects of this extra highly electronegative phosphate group is to disrupt the conformation of the protein and hence its function. Target proteins for phosphorylation are numerous throughout the cell and are different depending on the tissue. Therefore if cAMP levels are decreased by  $G_i/G_o$  inhibition of adenylyl cyclase, there will be a reduced level of protein phosphorylation which will effect cellular responses (table 1.1).

In addition,  $G_i$  coupled opioid receptors have been shown to modulate the inwardly rectifying cation current ( $I_h$ ) in guinea pig nodose ganglion neurones via inhibition of adenylyl cyclase [Ingram and Williams, 1994]. The consequence of the inhibition of  $I_h$  is that neuronal firing frequency is slowed down, and this may be mechanism by which opioid receptors decrease pain.

It was later shown in the brainstem that 5-HT depolarises motoneurones and that  $I_h$  activation was independent of protein phosphorylation by PKA, the effect on the channel being due to direct cAMP interactions [Larkman, et al, 1995].

In addition,  $I_h$  can be inhibited by the  $GABA_B$  agonist baclofen in rat midbrain, by activating an outward potassium current, the effect on  $I_h$  was shown to be independent of adenylyl cyclase inhibition [Watts et al, 1996]. In addition, it has been recently shown that  $G_i$ -coupled opioid receptors can decrease  $Ca^{2+}$  currents [Taddese et al, 1995].

Other non-G-protein coupled receptors have been described, these include tyrosine kinase, ion channel linked, and intracellular receptors. These classes of receptors will not be discussed and the reader is directed to the following book [Rang and Dale, 1987].

## **1.2. G-protein Coupled Receptors.**

The family of G-protein coupled receptors contains literally hundreds of members, and they share some common structural characteristics [Birnbaumer et al, 1990]. All are membrane proteins, containing seven transmembrane spanning domains which are rich in hydrophobic amino acids [Kyte and Doolittle, 1982]. In addition, they all have a bulky extracellular N-terminus. The C-terminus is rich in potential phosphorylation sites (serine and threonine residues) and is orientated on the intracellular face of the membrane [Tobin et al, 1996](see figure 1.2). All the receptors are glycoproteins, the consensus sequence required for N-linked oligosaccharide additions is Asn-Xaa-Ser/Thr, and these are usually present on the extracellular N-terminus, however in some cases sites also exist on the second extracellular loop [Rands et al, 1990]. There are also a number of conserved cysteine residues present in most G-protein linked receptors, two cysteine residues form covalent bonds with sulphur atoms to form a disulphide bridge between the first and second extracellular loop of the receptor. It has been suggested that the function of the energetically stable disulphide bridge is to constrain the conformation of the extracellular domain of the protein [Karnik et al, 1988] (see figure 1.2). In order to study structure/function relationships of receptors, many site directed mutagenesis studies have been published. This thesis is concerned with muscarinic, opioid and cannabinoid receptors and molecular studies with these receptors will be reviewed later.

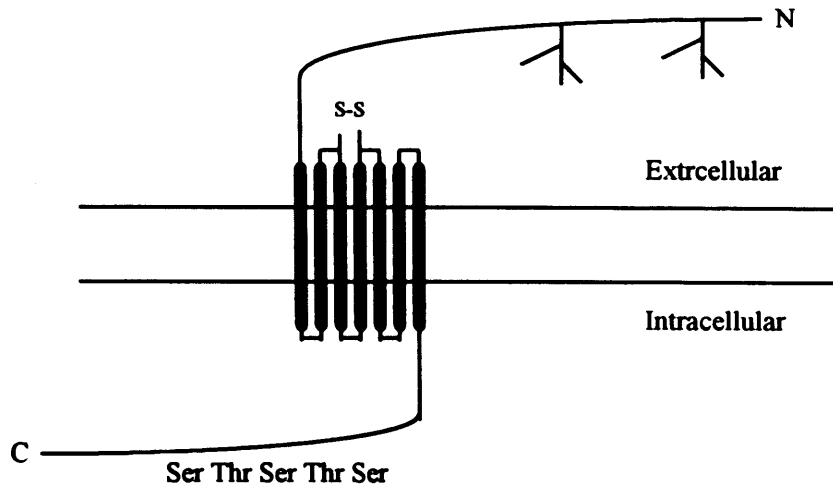


Figure 1.2. A schematic representation (not to scale) of a G-protein coupled receptor. Seven transmembrane spanning domains with an extracellular N- and an intracellular C-terminus. Glycosylation sites are shown as branches, and a disulphide bridge is shown between the first and the second extracellular loop. Repeated serine and threonine residues, which are potential phosphorylation sites, are shown on the C-terminus.

### **1.3. G-Proteins.**

The relay of transmembrane signals is mediated in part by Guanine nucleotide binding proteins (G-proteins). A G-protein is a heterotrimeric protein associated with the plasma membrane. It consists of an  $\alpha$ ,  $\beta$  and  $\gamma$  subunit, which on activation dissociates into  $\alpha$ -GTP and  $\beta\gamma$  dimers [Birnbaumer et al, 1990].  $\beta\gamma$  dimers exist as a tightly associated complex which function as a specific unit, and can only be separated under denaturing conditions. The  $\alpha$  subunits bind and hydrolyse GTP, define the receptor and effector specificity and differ from G-protein to G-protein [Manning and Gilman, 1983]. Originally, it was thought that only  $\alpha$  subunits were able to regulate effector systems, however, recent reports have suggested a role for  $\beta\gamma$  dimers [Tang and Gilman 1991; Birnbaumer, 1992; Taussig et al, 1993]. The rate limiting factor for G-protein mediated signaling is the kinetics of GTP binding and its hydrolysis by the  $\alpha$  subunit, this is shown in figure 1.3. In the inactive state G-proteins exist in the tertiary structure ( $\alpha\beta\gamma$ ) with guanine diphosphate (GDP) bound to the  $\alpha$  subunit. When an appropriate receptor is activated by a ligand the receptor-ligand complex stimulates the dissociation of GDP

from the  $\alpha$  subunit, probably by changing the conformation of the GTP binding site from closed to open [Bourne, 1993]. When this occurs the receptor has a high affinity for agonists, and in the absence of GTP (under experimental conditions) agonist-receptor-G-protein complexes are stable. However, when GTP is freely available, G-protein activation occurs. Binding of GTP to the  $\alpha$ -subunit reduces its affinity for  $\beta\gamma$  subunits.  $\alpha$ -GTP is responsible for the regulation of effector enzymes. However, the  $\beta\gamma$  subunits are free to dissociate and act upon targets such as adenylyl cyclase or phospholipase C [Gilman, 1995] (table 1.1).

Upon activation the G-protein also dissociates from the receptor. Deactivation of the G-protein is dependent upon the intrinsic GTPase activity of the  $\alpha$  subunit. This is the rate of hydrolysis of the bound GTP to GDP+Pi by the  $\alpha$  subunit. Deactivation also allows  $\beta\gamma$  reassociation with  $\alpha$ -GDP to reform the heterotrimeric G-protein (see figure 1.3).

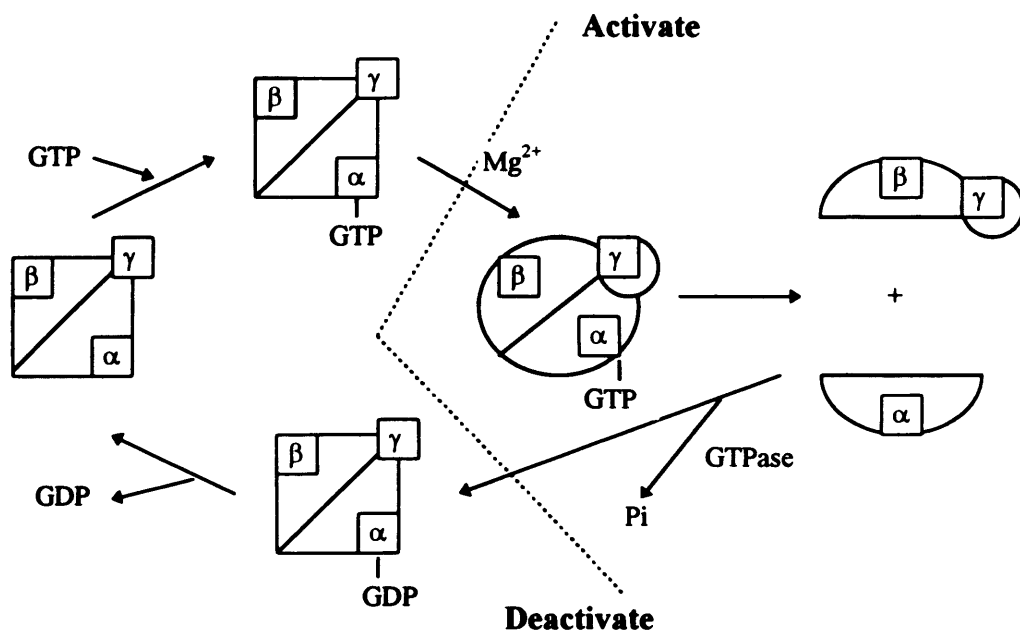


Figure 1.3. The G protein cycle, squares represent the inactive states. Circular shapes represent activated G protein. Activation is  $Mg^{2+}$  and GTP dependent and is stabilised by subunit dissociation to give activated  $\alpha$ -GTP plus the  $\beta\gamma$  dimer.

$\alpha$  subunits of many G proteins are target substrates for bacterial toxins. Cholera toxin, from *Vibrio cholera*, catalyses the transfer of ADP-ribosylated nicotinamide adenine dinucleotide (NAD<sup>+</sup>) to a specific arginine residue on G $\alpha$ . This modification has the effect of inhibiting GTPase activity and hence locking the G protein in an active conformation [Northrup et al, 1980; Codina et al, 1984]. The main physiological effect of these  $\alpha$  subunit modifications is inhibition of water reabsorption in the gut, which leads to dehydration and death (cholera).

In addition, pertussis toxin (from *Bordetella pertussis*) acts in a similar way to cholera toxin except the substrates here are mainly G $\beta\gamma$  and G $\alpha_o$ . Pertussis toxin ADP-ribosylates a specific cysteine residue four amino acids from the C-terminus which is common among G $\beta\gamma$  and G $\alpha_o$ . The modification blocks receptor mediated activation of the G protein [Hildebrandt et al, 1983; Sternweis and Robishaw, 1984]. These two toxins have proved invaluable tools for the identification of the G-proteins involved in specific signal transduction pathways.

#### **1.4. Adenylyl cyclase.**

AC is the enzyme responsible for the formation of the second messenger cAMP from ATP. The cloning of the first AC revealed a complex structure [Krupinski et al, 1989]. The enzyme was very large (over 1000 amino acids) with 12 transmembrane spanning domains which are split into 2 cassettes with each cassette followed by a large cytosolic domain [Tang and Gilman, 1992]. The structure resembles that of ion channels and transporters [Krupinski et al, 1989]. To date, eight subtypes of the enzyme have been cloned, and the transmembrane domains are not highly conserved between them and share little or no homology with the highly conserved domains of ion channels [Catterall, 1994]. The two cytosolic domains contain ATP binding sites on each and are thought to act in a cooperative manner [Tang et al, 1991]. Recent studies indicate that non-overlapping regions on the enzymes may be responsible for allowing separate interaction with G protein G $\alpha_s$ , G $\alpha_i$  and  $\beta\gamma$  subunits [Taussig et al, 1994; Taussig et al, 1993]. The first cytoplasmic loop has also been connected with an auto inhibitory action of AC as the presence of amino acids 425-444 profoundly inhibits type 5 AC [Kawabe

et al, 1994].  $\text{Ca}^{2+}$ /calmodulin (CaM) complexes also interact with AC isoforms, the binding site for this interaction is also thought to be in the first cytoplasmic loop near the plasma membrane [Vorherr et al, 1993; Wu et al, 1993]. A schematic representation of AC can be seen in figure 1.4.

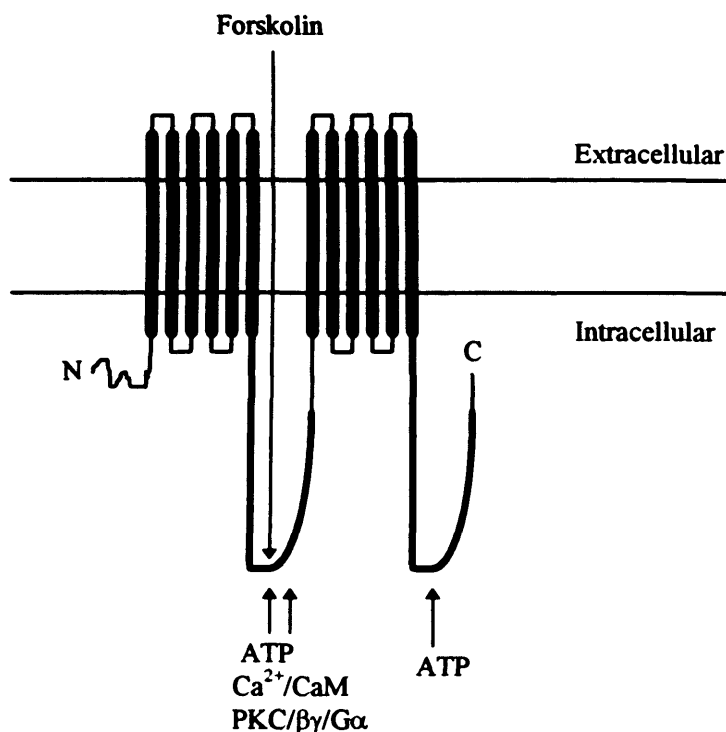


Figure 1.4. Cartoon (not to scale) of the structure of AC. 2 cassettes consisting of six transmembrane spanning domains, both N- and C-termini are on the intracellular face. Arrows indicate possible Forskolin, ATP,  $\text{Ca}^{2+}$ /CaM, PKC,  $\beta\gamma$  or  $G\alpha$  subunit binding sites.

Individual AC isoforms are regulated by a variety of molecules. The diterpene, forskolin was first discovered in the late seventies [Bhat et al, 1977], and soon after its effects (smooth muscle relaxation and positive inotropic effects) were attributed to activation of AC [Metzger and Lindner, 1981]. Forskolin has the ability to directly activate all AC isoforms independently of receptor-G protein interactions. Since then, forskolin has been used widely for studying the role of elevated levels of intracellular cAMP in signal transduction pathways. The traditional view that  $G\alpha$  subunits were the dominant natural regulator of AC, has recently been questioned by the fact that protein

kinase C (PKC) [Lustig et al, 1993],  $Ca^{2+}$  [Cooper et al, 1994] and  $\beta\gamma$  subunits of G proteins [Tang and Gilman, 1991] can stimulate or inhibit particular AC's far more effectively than G protein  $\alpha$  subunits [Cooper et al, 1995]. When the cloned type 2 AC was transfected into mammalian cells, phorbol esters (PKC activators) elicited twice the activity than that caused by  $Gs\alpha$  [Jacobowitz et al, 1993]. In addition, receptors working through  $Gs\alpha$  stimulated types 1 and 8 AC by approximately 10%, whereas  $Ca^{2+}$  stimulated these subtypes up to fourfold [Yoshimura and Cooper, 1992; Cali et al, 1994]. Another recent observation was that type 6 AC can be inhibited to a greater extent by elevations of intracellular  $Ca^{2+}$  than by  $G_i$  linked receptors [DeBernardi et al, 1991]. Table 1.2 summarises the regulation of the subtypes of AC.

AC type	$Ca^{2+}$ effect	$\beta\gamma$ effect	Gs activation	PKC activation	Richest mRNA source
1	Stimulation	Inhibition	Mild	None	DG/HO
3	Stimulation	?	Yes	None	OE
8	Stimulation	?	Mild	None	HO
2	None	Stimulation	Yes	Yes	CBM
4	None	Stimulation	Yes	None	Rare
7	None	?	Yes	Yes	CBM
5	Inhibition	None	Yes	None	CN
6	Inhibition	None	Yes	None	Heart

Table 1.2. Cloned AC isoforms are grouped according to their structural similarity. The regulation of each isoform is shown, note that  $\beta\gamma$  activation must originate from activated  $G\alpha\beta\gamma$ . The  $\beta\gamma$  data comes from in-vitro reconstitution studies [Taussig et al, 1994], however the other data comes from studies of cDNAs expressed in intact HEK293 cells, which have been subjected to a physiological elevation of intracellular calcium [ $Ca^{2+}$ ]<sub>i</sub>, receptor activated Gs or phorbol ester activation of PKC [modified from Cooper et al, 1995]. DG=Dentate gyrus, HO= Hippocampus, OE= Olfactory neuroepithelium, CBM=Cerebellum and CN= Caudate nucleus.

Some AC isoforms are very specific for particular brain regions, type 1 occurs predominantly in the dentate gyrus of the hippocampus and in the granule layers of the cerebellum and is stimulated by  $\text{Ca}^{2+}/\text{CaM}$  and Gs [Xai et al, 1991; Mons et al, 1993]. Type 5, is only found in the striatum and is inhibited by  $\text{Ca}^{2+}/\text{CaM}$  [Glat and Snyder, 1993]. The stimulation of types 1 and 8 AC by  $\text{Ca}^{2+}$  and their presence in the hippocampus implicates them in the brain function of memory and learning via regulation of long term potentiation (LTP). One important component of LTP is glutamate receptor (NMDA) mediated  $\text{Ca}^{2+}$  entry [Bliss and Collingridge, 1993], and is associated with an elevation of cAMP [Chetcovitch et al, 1991]. Direct evidence for the involvement of type 1 AC in learning was provided by its deletion in a strain of transgenic mice. The mice showed impaired hippocampus-dependent learning ability and a 40-60% decrease in  $\text{Ca}^{2+}/\text{CaM}$  stimulated cAMP formation in ex-vivo hippocampal tissue [Wu et al, 1995]. The organisation of AC isoforms suggests that specific targeting information may be within the enzyme structure, and genetic studies are continuing in order to address these questions.

### **1.5. Phospholipase C (PLC), $\text{IP}_3$ and $\text{Ca}^{2+}$**

PLC is a receptor-G protein linked membrane bound effector enzyme which is responsible for the hydrolysis of phosphatidylinositol diphosphate ( $\text{PIP}_2$ ) into Diacylglycerol (DAG) and Inositol 1,3,5 triphosphate ( $\text{IP}_3$ ). DAG remains associated with the plasma membrane and is able to activate PKC, whereas  $\text{IP}_3$  is free to diffuse into the cytosol and binds to its intracellular ( $\text{IP}_3$ ) receptor located on smooth endoplasmic reticulum  $\text{Ca}^{2+}$  stores. Inositol polyphosphates are metabolised and the membrane inositol store is replenished. The main steps are shown below in figure 1.5, and for further information the reader is directed to the following review [Shears, 1991].

PLC exists as a family of isoforms ( $\gamma 1$ ,  $\delta 1$ , and  $\beta 1-4$ ) each regulated by various agonists and intracellular messengers ( $\beta\gamma$  subunits,  $\text{Ca}^{2+}$ ) [Lee et al, 1993]. For example,  $\text{G}\beta\gamma$  activates  $\text{PLC}\beta 2$  but has no effect on  $\text{PLC}\beta 1$  [Ito et al, 1992]. A recent study has shown that  $\text{PLC}\beta 3$  is activated by both  $\text{G}_q$  and a pertussis toxin sensitive G

protein [Blayney et al, 1996]. In another study, Dickenson and Hill (1995) suggested that pertussis toxin sensitive PLC $\beta$  isoforms may result from  $\beta\gamma$  activation liberated following Gi activation.

Subtypes of IP<sub>3</sub> receptors have also been cloned [Furuichi and Mikoshiba, 1995]. They act as calcium channels and are mainly located on the smooth endoplasmic reticular membrane (SERM). Once occupied IP<sub>3</sub> receptors gate the release Ca<sup>2+</sup> from the intracellular store. The free intracellular Ca<sup>2+</sup> is then able to regulate Ca<sup>2+</sup>-dependent proteins involved in cellular functioning such as proteins involved in fertilization [Berridge, 1993]. In addition, when Ca<sup>2+</sup> is bound to CaM, these complexes have regulatory properties over other proteins such as adenylyl cyclase [Cooper et al, 1994] and IP<sub>3</sub> receptors [Furuichi and Mikoshiba, 1995].

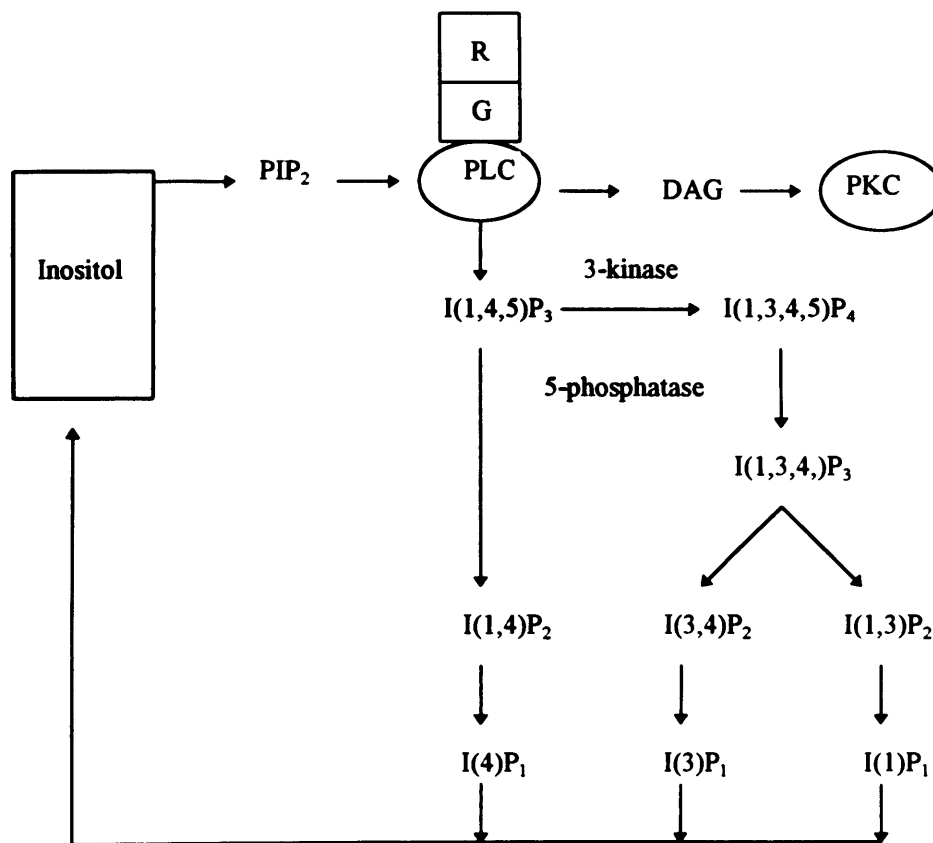


Figure 1.5. Synthesis and metabolism of IP<sub>3</sub> where R=receptor, G= G protein, and phosphate positions on the inositol ring are in brackets. Modified from Lambert et al, 1990.

CaM is one of many calcium binding proteins which include calmodulin and calquestrin, these high capacity ( $4\text{Ca}^{2+}:1$  for CaM), low affinity proteins are partly responsible for turning off the  $\text{Ca}^{2+}$  response. The  $\text{Ca}^{2+}$  signal is mainly switched off by  $\text{Ca}^{2+}$  ATPases which are a group of enzymes located in many cellular membranes, a high proportion are located on the plasma and SER membranes and are responsible for the active transport of  $\text{Ca}^{2+}$  up its concentration gradient utilizing ATP hydrolysis as energy. Extracellular  $\text{Ca}^{2+}$  can also be utilised as a second messenger. The types of  $\text{Ca}^{2+}$  channel which are opened include, second messenger operated  $\text{Ca}^{2+}$  channels (SMOCC), receptor operated  $\text{Ca}^{2+}$  channels (ROCC), G-protein operated  $\text{Ca}^{2+}$  channels (GOCC) and intracellular  $\text{Ca}^{2+}$  store recharging  $\text{Ca}^{2+}$  channels ( $I_{\text{crac}}$ ) [Clementi and Meldolisi, 1996]. In addition to these are the voltage sensitive  $\text{Ca}^{2+}$  channels, and these are discussed in some detail later. The study of intracellular  $\text{Ca}^{2+}$  homeostasis has been greatly enhanced by the introduction of fluorescent indicator dyes such as Fura-2 [Cobbold and Rink, 1987]. The practical use of Fura-2 will be discussed in chapter 2.

### **1.6. Voltage Operated Calcium Channels (VOCC).**

Synaptic transmission is a  $\text{Ca}^{2+}$ -dependent process. High (mM) concentrations of extracellular  $\text{Ca}^{2+}$  represent a pool which the cell (containing nM levels) can utilise in order to drive cellular processes. Embedded within the plasma membrane are  $\text{Ca}^{2+}$  channels which gate extracellular  $\text{Ca}^{2+}$  into the cell, these include receptor-G-protein coupled and second messenger operated  $\text{Ca}^{2+}$  channels [Dolphin, 1991]. In addition, multiple subtypes of VOCC's exist, each has been characterised according to conductance activity and blockade by dihydropyridines, inorganic ions and  $\omega$ -conotoxin [Bertilino and Llinas, 1992] and subgrouped into L-, T-, N-, and P-type channels (table 1.3), although others have been described [Bertilino and Llinas, 1992].

Using excitable cells in low  $\text{Na}^+$  (~40mM, in order to maintain tonicity of the cell) buffer, it is possible to cause membrane depolarization and opening of VOCC's using high concentrations of  $\text{K}^+$ . The subsequent rise in intracellular  $\text{Ca}^{2+}$  acts as the second messenger which is thought to be the essential stimulus for the secretion of neurotransmitters [Lipton, 1991].

Property	L	T	N	P
Conductance (pS)	~25	~8	~10-20	~10-12
Activation Threshold	High	Low	High	Moderate
Inactivation Rate	Slow	Fast	Rapid	None
Permeation	$Ba^{2+} > Ca^{2+}$	$Ba^{2+} = Ca^{2+}$	$Ba^{2+} > Ca^{2+}$	$Ba^{2+} > Ca^{2+}$
Function	Smooth muscle endocrine cells, some neurons	Cardiac SA node, spiking: repetitive activity in neurons and endocrine cells.	Neuronal only, N.T release.	Neuronal only, N.T release.
Nimodipine	Sensitive	Insensitive	Insensitive	Insensitive
Verapamil	Sensitive	Insensitive	Insensitive	Insensitive
Diltiazem	Sensitive	Insensitive	Insensitive	Insensitive
$\omega$ -conotoxin	Insensitive	Insensitive	Sensitive	Insensitive
$\omega$ -Agatoxin	Insensitive	Insensitive	Insensitive	Sensitive

Table 1.3. Classification of VOCC subtypes, Taken from RBI handbook of receptor classification, 1994. NT=neurotransmission.

### **1.7. Cholinergic Muscarinic receptors.**

Pre-synaptic cholinergic nerve terminals release the neurotransmitter acetylcholine (ACh) into the synaptic cleft, whereby it can act on its cholinergic receptors or be catabolised by the enzyme cholinesterase into choline and acetate. These products are then taken up into the nerve in order for ACh resynthesis or for use in other metabolic pathways. Cholinergic receptors are separated into two distinct receptor types according to their selectivity for the agonists nicotine and muscarine, namely nicotinic and muscarinic [Rang and Dale, 1987]. The continually growing family [Dendris et al, 1991] of nicotinic receptors exist as pentameric, water filled, membrane bound ion channels located on the post-synaptic cell body. The excitatory responses associated

with nicotinic receptor activation include membrane depolarization and increased neuronal firing rate, and are mainly due to Na<sup>+</sup> entry into the cell [Clarke, 1993].

Muscarinic receptors are also activated by ACh, however they are G-protein coupled receptors. Specific agonists and antagonists have been used to characterise five distinct muscarinic receptor isoforms [see Hulme et al, 1990; Lambert et al, 1992](see table 1.4). Their structural identity was revealed from cloning studies [Hulme, 1990].

Receptor	Selective Antagonists	Tissue	Preferred Effector
M <sub>1</sub>	Pirenzepine	Neuronal	PLC stimulation
M <sub>2</sub>	AFDX 116 Methoctramine	Cardiac	AC inhibition
M <sub>3</sub>	4-DAMP HHS	Neuronal Glandular	PLC stimulation
M <sub>4</sub>	none	Neuronal	AC inhibition
M <sub>5</sub>	none	Neuronal	PLC stimulation

Table 1.4. Muscarinic receptor subtypes, pharmacology, tissue location and second messenger coupling (modified from Lambert et al, 1992). AFDX116= (11[[2-[(diethylamino)methyl]-1-piperidinyl]acetyl]-5,11-dihydro-6H-pyrido[2,3-b][1,4]benzodiazepine-6-one, HHS=hexahydrosiladifenadol, 4-DAMP=4-diphenylacetoxy-N-methyl piperidine methiodide.

Five isoforms (M<sub>1</sub>-M<sub>5</sub>) have been cloned and sequenced [for review see Hulme et al, 1990] and all possess predicted structural homology. M<sub>1</sub>, M<sub>3</sub> and M<sub>5</sub> isoforms all couple to G<sub>q</sub> which is responsible for activation of PLC, increasing intracellular Ca<sup>2+</sup> concentrations and activating PKC. M<sub>2</sub> and M<sub>4</sub> receptors are coupled to an inhibition of AC via Gi. The main difference in structure between M<sub>1</sub>, <sub>3</sub>, <sub>5</sub> and M<sub>2</sub>, <sub>4</sub> receptors is observed in the third intra-cellular loop [Richards, 1991; Lambert et al, 1992]. This suggests that this region of the receptor may be important for G-protein selectivity. Indeed, when a construct M<sub>2</sub> receptor containing the third intracellular loop of an M<sub>3</sub> receptor was expressed in a mammalian cell, it was found to couple to the activation of

PLC, confirming the involvement of the third intracellular loop in G protein selectivity [Wess et al, 1989; Wess et al, 1990].

### **1.8. Opioid receptors.**

Noxious stimulation which causes actual or potential tissue damage is referred to as pain. Analgesics such as morphine have the ability to relieve the subjective component of pain without interfering with other sensory perceptions such as vision, hearing and touch. Opium has been used for many centuries for the relief of pain, and the identification of morphine as the active constituent in 1806 [Sertuner] led to the medicinal use of morphine throughout the developed world. However, the effects of morphine at a molecular level were not discovered until 1973, when several laboratories reported stereospecific opioid binding sites in the central nervous system [Pert and Snyder, 1973; Simon et al, 1973; Terenius, 1973]. The discovery of the endogenous ligand for the opioid receptor in 1975 [Hughes, 1975; Hughes et al, 1975] led to a series of reports of similar ligands acting at opioid receptors (see table 1.5).

Ligand	Structure	Group and Year
[Met <sup>5</sup> ] enkephalin	Tyr-Gly-Gly-Phe-Met	Hughes, 1975
[Leu <sup>5</sup> ] enkephalin	Tyr-Gly-Gly-Phe-Leu	Hughes and Kosterlitz, 1975
β-Endorphin	Tyr-Gly-Gly-Phe-Met-Thr-Ser-Glu-Lys- Ser-Gln-Thr-Pro-Leu-Val-Thr-Leu-Phe- Lys-Asn-Ala-Ile-Ile-Lys-Asn-Ala-Tyr- Lys-Lys-Gly-Glu	Bradbury et al, 1976
Dynorphin A	Tyr-Gly-Gly-Phe-Leu-Arg-Arg-Ile-Arg- Pro-Lys-Leu-Lys-Trp-Asp-Asn-Gln	Goldstein et al, 1979

Table 1.5. Peptide sequence and year of discovery of endogenous ligands for opioid receptors.

Due to the presence of multiple endogenous ligands it was suggested that each ligand acted at a particular receptor subtype. Direct evidence came from the work of Martin et al in 1976, who identified  $\mu$ - (from Morphine) and  $\kappa$ - (from Ketocyclazocine) opioid receptors using cross-tolerance (the ability of one drug to alleviate the withdrawal symptoms of another) studies in dogs. A year later the presence of the  $\delta$ - (vas deferens) opioid receptor was reported [Lord et al, 1977]. Endogenous ligands for the opioid receptors show very little subtype specificity, however, dynorphin related peptides preferentially bind to  $\kappa$ -receptors [Chavkin et al, 1982] whereas deltorphin has a higher affinity for  $\delta$ -receptors [Kreil et al, 1989]. Ligands have been synthesised which are opioid receptor subtype selective, these are numerous and the most commonly used ligands are shown in table 1.6.

Receptor subtype	Agonists	Antagonists
$\mu$ -	DAMGO Fentanyl	CTOP cyprodime
$\delta$ -	DADLE DPDPE DSLET	Naltrindole
$\kappa$ -	Spiradoline Dynorphin	Nor-BNI

Table 1.6. Commonly used subtype specific opioid receptor agonists and antagonists. DAMGO= [D-Ala<sup>2</sup>,Me-Phe<sup>4</sup>,Gly-ol]enkephalin; DPDPE = [D-Pen<sup>2</sup>,D-pen<sup>5</sup>]enkephalin; DADLE= [D-Ala<sup>2</sup>,D-Leu<sup>5</sup>]enkephalin; DSLET = [D-Ser<sup>2</sup>,Leu<sup>5</sup>]enkephalyl-Thr; Nor-BNI = nor-binaltorphimine; CTOP = D-Phe-Cys-Tyr-D-Orn-Thr-Pen-Thr-NH<sub>2</sub>.

Multiple isoforms of a specific subtype of opioid receptor have also been proposed by differences in affinity for various ligands,  $\mu$ -opioid receptors are thought to exist as  $\mu_1$  and  $\mu_2$  [Pasternak and Wood, 1986];  $\delta$ - as  $\delta_1$  and  $\delta_2$  [Traynor and Elliott, 1993] and  $\kappa$ - as  $\kappa_1$ ,  $\kappa_2$  and  $\kappa_3$  [Pasternak, 1993; Cheng et al, 1995]. In addition, a third isoform of the  $\mu$ -opioid receptor has been identified [Cruciani et al, 1994]. It was also hypothesised

that the  $\delta$ -opioid receptor could exist as a single receptor or as a dimer complex [Traynor and Elliott, 1993].

Recent major advances in opioid pharmacology came with the cloning of the rat  $\delta$ -opioid receptor from NG108-15 cells by two separate groups [Evans et al, 1992; Kieffer et al, 1992]. Soon after the mouse  $\kappa$ - [Yasuda et al, 1993], rat  $\kappa$ - [Chen et al, 1993; Minami et al, 1993], and rat  $\mu$ - [Chen et al, 1993; Fukuda et al, 1993; Wang et al, 1993] opioid receptors were also cloned (figure 1.6). In recent studies the human forms of the  $\mu$ -,  $\delta$ -, and  $\kappa$ -opioid receptors have also been cloned and sequenced [Wang et al, 1994; Knapp et al, 1994; Simonin et al, 1995]. Recent molecular biological studies have revealed more information about opioid receptor structure and function and some of the findings can be seen in table 1.7.



Subtype	Genetic manipulation	Functional consequence	Reference
μ-	Deletion of 64 N-terminal amino acids.	No effect on receptor function.	Surratt et al, 1994
	Further deletion of 33 C-terminal amino acids.	Prevents DAMGO but not morphine inhibiting AC.	
	Replacement of charged amino acids in transmembrane domains 2, 3 and 6.	Increased naloxone affinity, Reduced agonist binding affinities and increased inhibition of AC.	
δ-	Mutation of Asp <sup>393</sup> to Asn.	Decreased agonist binding affinity, without affecting antagonist binding. Reversed Na <sup>+</sup> inhibition of agonist binding.	Reisine et al, 1994.
	Mutation of Thr <sup>353</sup> to Ala	Reversed desensitisation of prolonged inhibition of AC.	Cvejic et al, 1996.
κ-	Chimeric μ/κ constructs	The second extracellular loop and the fourth transmembrane helix were found to be essential for dynorphin binding, and the third extracellular loop and the sixth and seventh transmembrane helices were essential for NorBNI binding. κ-opioid receptor were found to have differential binding domains for peptide and non-peptide ligands.	Xue et al, 1994

Table 1.7. Alterations in opioid receptor structure by molecular techniques reveal details about functional domains.

The cloned opioid receptors have been further classified as the pharmacological  $\mu_1$ ,  $\kappa_1$ , and  $\delta_2$  [Raynor et al, 1994], and the cloned  $\kappa$ -opioid receptor has been designated as  $\kappa_{1b}$  [Lai et al, 1994].

Along with the classical opioid receptors ( $\mu$ -,  $\delta$ - and  $\kappa$ -), recent cloning studies have revealed an atypical opioid receptor [Bunzow et al, 1994; Mollereau et al, 1994; Wick et al, 1994]. The clone, loosely termed the orphan receptor but designated specifically as ORL-1 [Mollereau et al, 1994] or LC132 [Bunzow et al, 1994], had only 50% homology to  $\mu$ -,  $\delta$ - and  $\kappa$ -opioid receptors, bound etorphine with low affinity which causes an inhibition of AC. The ORL-1 receptor did not bind opioid ligands and was found in the central nervous system in areas involved in pain perception (Hypothalamus, brainstem and spinal cord dorsal horn) [Fukuda et al, 1994].

Soon after the discovery of this receptor two groups simultaneously identified its endogenous ligand, it was called nociceptin or orphanin FQ and was a heptadeca peptide [Meunier et al, 1995; Reinscheid et al, 1995] (see below).

#### Orphanin FQ or Nociceptin.

Phe-Gly-Gly-Phe-Thr-Gly-Ala-Arg-Lys-Ser-Ala-Arg-Lys-Leu-Ala-Asn-Gln-OH

The endogenous ligand for the ORL-1 receptor was structurally different to endogenous opioid peptides. The homology within the opioid peptide family is predominant in the first four C-terminal amino acids (Tyr-Gly-Gly-Phe). Nociceptin retains homology in the -Gly-Gly-Phe amino acids, however the C-terminal amino acid is Phe instead of the conserved Tyr. It was suggested that this amino acid played an important role in receptor selectivity. However, it was later shown that substitution of the N-terminal Phe with Try had no effect on agonist selectivity [Shimohigashi et al, 1996]. It has recently been shown that the internal basic amino acids of nociceptin are mainly involved in conveying receptor selectivity to the molecule [Butour et al, 1997].

The peptide, when injected intracerebroventricularly (ICV) into mice caused hyperalgesia, and it was hypothesised that the ligand may have a role to play in modulating nociception and locomotive behavior [Reinscheid et al, 1995]. In a recent study, it has been shown that nociceptin can affect wind up, which may be involved in analgesia if injected spinally in rats [Stanfa et al, 1996]. There is still some debate concerning the overall role of nociceptin in the production of analgesia or hyperalgesia.

In addition to these effects, nociceptin has also been shown to cause inhibition of forskolin stimulated cAMP formation in CHO cells expressing the ORL-1 receptor [Meunier et al, 1995]. The ORL-1 receptor is also naturally expressed in undifferentiated SH-SY5Y cells [Cheng et al, 1995]. In SH-SY5Y cells, nociceptin inhibits voltage operated calcium currents and in the presence of carbachol, increases intra-cellular calcium concentrations both effects being dose dependent and pertussis toxin sensitive [Connor et al, 1996].

Opioid receptors couple to an inhibition of AC via Gi and/or Go, close VOCC's and stimulate an outward K<sup>+</sup> conductance [Atcheson and Lambert, 1994; Childers, 1993]. Opioids have also been shown to increase intracellular cAMP concentrations in rat olfactory bulb,  $\mu$ -,  $\delta$ -, but not  $\kappa$ -opioid receptors stimulated basal cAMP formation but inhibited Ca<sup>2+</sup>/CaM and forskolin stimulated formation [Olianas and Onali, 1994]. Rhim and Miller [1994] have shown that  $\mu$ -opioid receptors close N-, P- and Q-type VOCC. L-type VOCC's are also modulated by opioids, Tang and coworkers [1995] recently showed that  $\delta$ -opioid receptors opened L-type VOCC in ND8-47 cells by virtue of the response being blocked by nifedipine. In agreement with this study, Smart et al [1995] also demonstrated in SH-SY5Y cells that  $\mu$ -opioid receptors may couple to an opening of L-type VOCC and the subsequent rise in intracellular calcium activated PLC. Calcium activation of PLC in SH-SY5Y cells increased IP<sub>3</sub> levels, the effect being blocked by pertussis toxin pretreatment and activation of protein kinase C [Smart and Lambert, 1995, Smart and Lambert, 1996].

These studies taken collectively indicate that opioids can act via specific receptors in specific tissues to cause inhibitory and also excitatory responses. While inhibitory effects of opioids are well characterised, the role of opioid mediated neuronal excitatory effects remain unclear.

### **1.9. Opioid Pharmacology and Pain.**

Opioid Receptors are distributed in specific regions throughout the CNS and the periphery.  $\mu$ -opioid receptors are found in many brain regions, including the cerebral cortex, caudate putamen, nucleus accumbens, olfactory tubercle, septal nuclei, thalamus, hippocampus and medial nucleus [Zastawny et al, 1994]. Yasuda and coworkers [1993] showed that the  $\kappa$ -opioid receptor was expressed in brain regions, which were similar to  $\delta$ -receptor expression. These brain regions include the neocortex, hippocampus, amygdala, hypothalamus, locus cerules and parabrachial nucleus, which implicate these receptors may have a role to play in arousal and regulation of autonomic and neuroendocrine functions [Yasuda et al, 1993]. Opioid receptors are also expressed in the spinal cord, where the  $\mu$ -opioid receptor predominates [Besse et al, 1991], these will not be discussed here and the reader is directed to the review by Borosdi, 1991.

Analgesia results from both spinal and supraspinal sites of action.  $\mu$ -opioid agonists selectively inhibit various nociceptive reflexes and induce analgesia when administered intrathecally or into the dorsal horn of the spinal cord. Opioid receptors on the primary afferent nerves mediate inhibition of the release of neurotransmitters such as substance P, calcitonin gene related peptide, Neurokinin A and glutamate [Schaible and Grubb, 1993](figure 1.7).

$\mu$ -opioid agonists also antagonise the effects of endogenously released substance P by causing postsynaptic inhibitory actions on interneurons and on the output neurons of the spinothalamic tract that conveys nociceptive information to the brain.  $\delta$ - and  $\kappa$ -opioid

agonists are thought to act in a similar way but with varying efficacy [Lewis et al, 1987; Magnuson and Dickenson, 1991].

Analgesia can also be produced by morphine ( $\mu$ ) injected directly into the third ventricle or in various sites in the midbrain and the medulla. In addition, electrical or chemical stimulation of these sites also causes naloxone reversible analgesia, suggesting the response is mediated by endogenous opioid peptides. The exact circuitry for this to occur remains to be elucidated [Dickenson, 1995]. Similar effects are seen with  $\delta$ - but not  $\kappa$ -opioid agonists [Gilman et al, 1990].

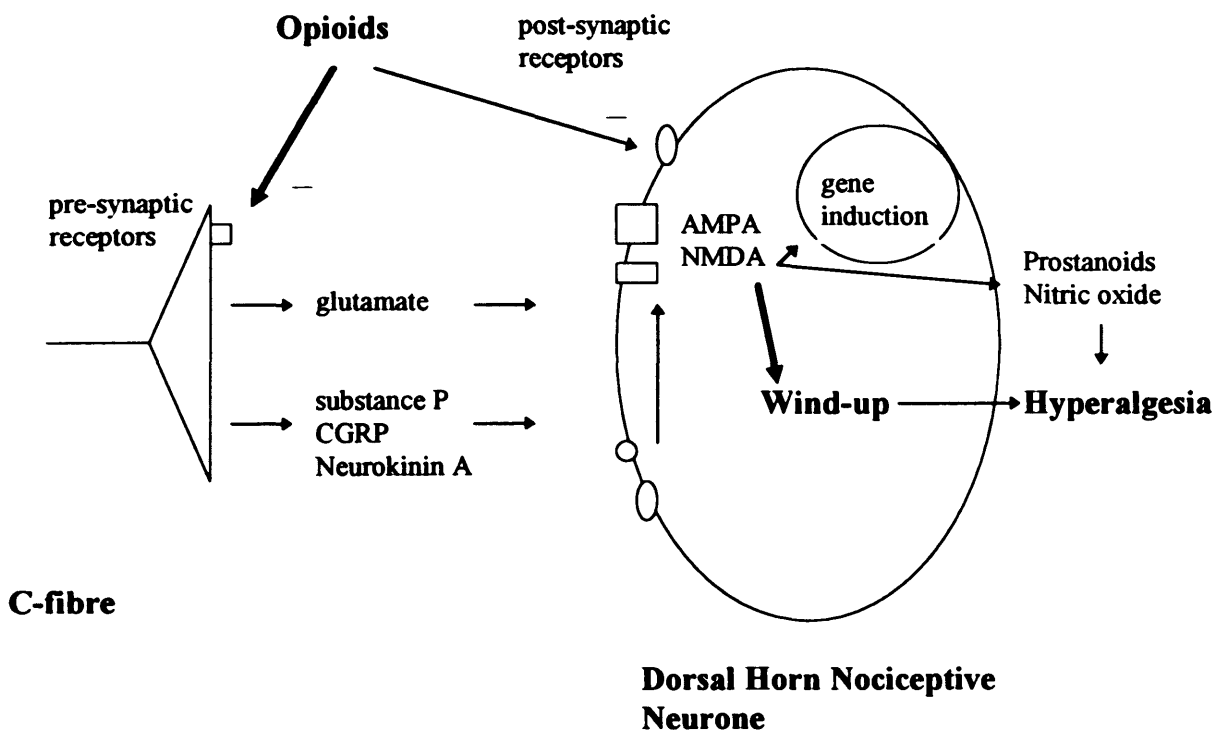


Figure 1.7. A diagram showing the release of excitatory transmitters from C-fibres and the subsequent effects on a dorsal horn nociceptive neurone. The predominant pre-synaptic action of opioids (reduction of neurotransmission) and the post-synaptic action (reducing neuronal activity) are shown. [modified from Dickenson, A. H. 1995].

The mechanisms by which opioids inhibit neurotransmitter release from pre-synaptic neurons are shown below (figure 1.8)

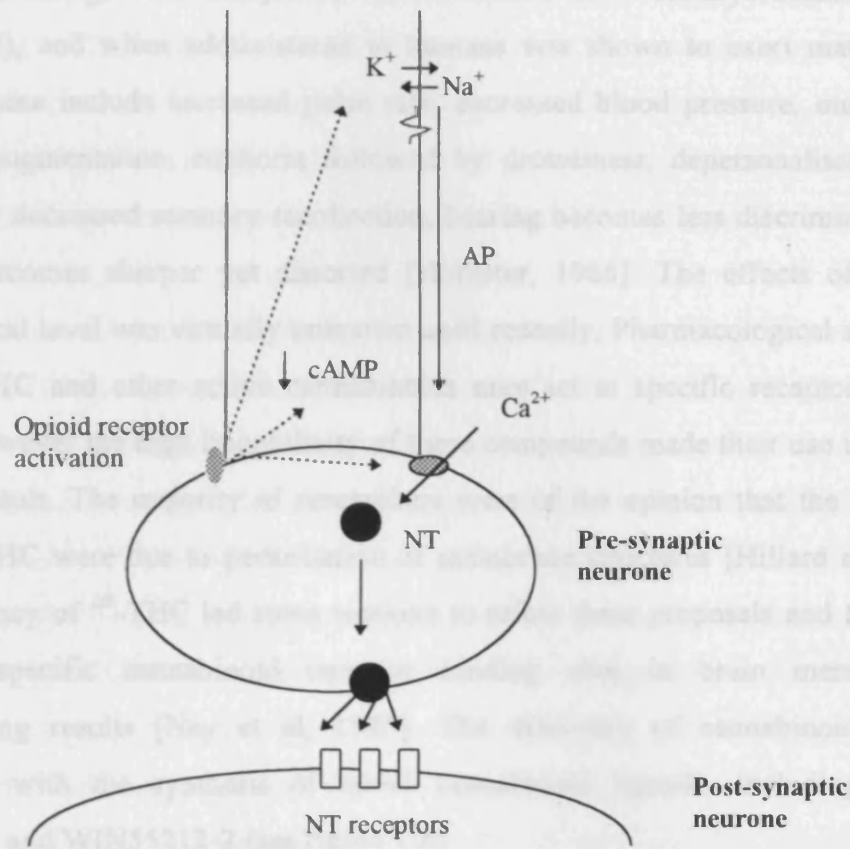


Figure 1.8. A simplified diagrammatic representation of the mechanisms of opioid inhibition of neurotransmission. The action potential (AP) travels along the membrane of the pre-synaptic neuron. The membrane depolarises and VOCC open and this is thought to initiate neurotransmitter (NT) release into the synaptic cleft. Opioid receptor activation leads to an inhibition of cAMP formation. This effect has been proposed as a mechanism by which opioids inhibit the inward rectifying cation current ( $I_h$ ) and inhibit primary afferent excitability and relieve pain [Ingram and Williams, 1994]. Opioids also stimulate the outward potassium current and inhibit voltage sensitive  $Ca^{2+}$  channels, both events decrease neurotransmission.

## 1.10. Cannabinoid receptors.

The major psychoactive constituent of *Cannabis sativa* was first isolated in 1964 [Gaoni and Mechoulam]. This compound was identified as  $\Delta^9$ -tetrahydrocannabinol ( $\Delta^9$ -THC, figure 1.8), and when administered to humans was shown to exert many physiological effects, these include increased pulse rate, decreased blood pressure, muscle weakening, appetite augmentation, euphoria followed by drowsiness, depersonalisation, time sense alteration, decreased memory recollection, hearing becomes less discriminative and visual signals becomes sharper yet distorted [Hollister, 1986]. The effects of  $\Delta^9$ -THC at the biochemical level was virtually unknown until recently. Pharmacological studies suggested that  $\Delta^9$ -THC and other active cannabinoids may act at specific receptor sites [Pertwee, 1988], however the high lipophilicity of these compounds made their use in binding assays very difficult. The majority of researchers were of the opinion that the effects observed with  $\Delta^9$ -THC were due to perturbation of membrane structures [Hillard et al, 1985]. The high potency of  $\Delta^9$ -THC led some workers to refute these proposals and early attempts to identify specific cannabinoid receptor binding sites in brain membranes showed encouraging results [Ney et al, 1985]. The discovery of cannabinoid receptors was enhanced with the synthesis of novel cannabinoid ligands, including levonantradol, CP55,940 and WIN55212-2 (see figure 1.8).

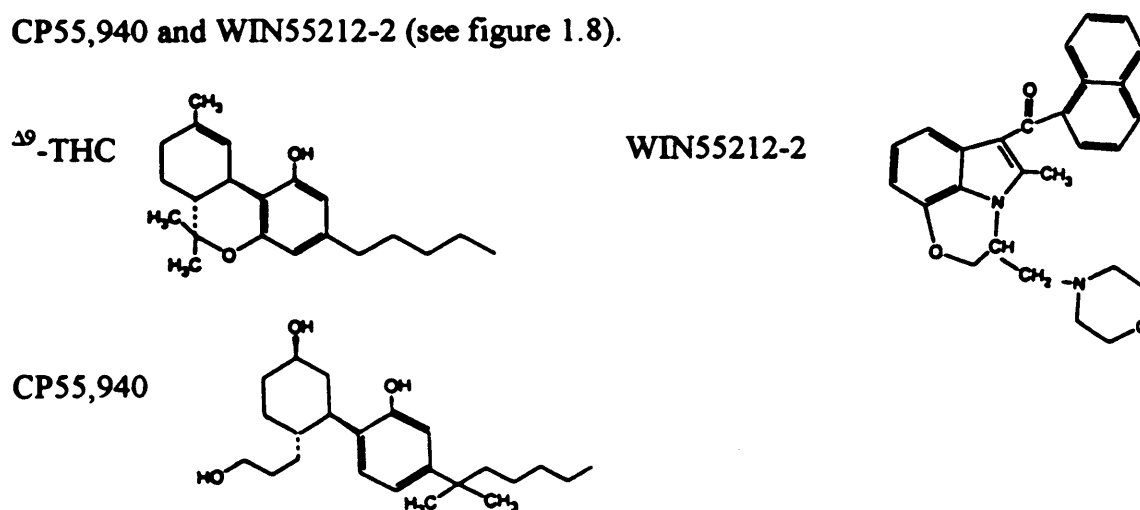


Figure 1.8. Structures of cannabinoid receptor agonists.

These compounds were more hydrophilic and were more potent than  $\Delta^9$ -THC [Johnson et al, 1988]. In addition, the compounds had inactive stereoisomers which distinguished the non-specific effects of cannabinoids. As early as 1984, Howlett and coworkers showed that cannabinoids caused inhibition of AC, later they showed that this effect was seen only in the presence of GTP and was sensitive to pertussis toxin pre-treatment, indicating a  $G_i/G_o$  mediated response [Howlett and Flemming, 1984; Howlett et al, 1986]. Using the radiolabelled agonist CP55,940 Devane et al [1988] demonstrated dose dependent and saturable binding to brain membranes, an effect that was also dependent on GTP.

The neuronal cannabinoid receptor (CB1) was first cloned from the rat DNA library in 1990 [Matsuda et al], soon after the human receptor was also cloned [Gerard et al, 1991]. The CB1 receptor belongs to the superfamily of G-protein coupled receptors, with seven transmembrane spanning domains and extracellular N- and intracellular C-termini as described previously (See figure 1.2). Recently, the presence of a truncated isoform of the central cannabinoid receptor was discovered [Shire et al, 1995], and termed CB1a. The pharmacology of CB1a was almost identical to CB1 except that agonist binding affinity to CB1a was slightly reduced when compared with CB1 [Rinaldi-Carmona, 1996a]. In addition, another isoform of the cannabinoid receptor was cloned from macrophages and spleen, this receptor showed only 44% homology with the CB1 receptor and was not expressed in the brain, this receptor was termed the peripheral cannabinoid receptor or CB2 [Munro et al, 1993]. Cloning of the cannabinoid receptor led to the hunt for the endogenous ligand(s). The breakthrough came when Devane and coworkers [1992] isolated a porcine brain extract which possessed cannabamimetic properties, the compound was identified as arachidonylethanolamide and called anandamide (see figure 1.9).

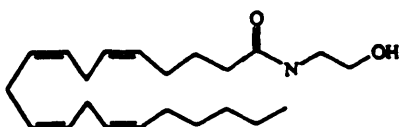


Figure 1.9. Structure of anandamide.

Anandamide is essentially a lipid or more specifically an eicosanoid which is generated from mobilised phospholipid bound arachidonic acid [Burnstein and Hunter, 1995]. Anandamide has been shown to displace radiolabelled cannabinoids from their receptor, inhibiting AC in a pertussis toxin sensitive manner [Vogel et al, 1993] and inhibiting N-type calcium currents [Mackie and Hille, 1992]. Other groups have also shown that cannabinoid receptors can activate voltage sensitive potassium channels in hippocampal cells [Childers et al, 1993] in a cAMP dependent manner [Deadwyler et al, 1995]. The CB1 receptor activation of  $K^+$  currents has been hypothesised to play a role in decreasing presynaptic neurotransmitter release by restoring the resting potential of the neuron following action potential induced depolarisation [Childers et al, 1993].

Studies on cannabinoid receptor pharmacology was hampered by lack of availability of a specific antagonist. However, in 1994 [Rinaldi-Carmona et al], reported the synthesis and pharmacology of the first CB1 selective receptor antagonist, SR141716A (figure 1.10)

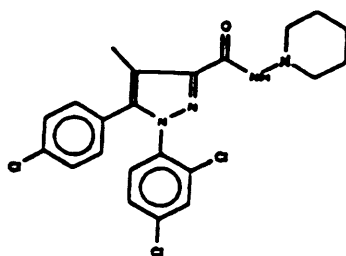


Figure 1.10. Structure of SR141716A.

In a later paper, it was shown that cannabinoid inhibition of cAMP formation was abolished by SR141716A and that oral administration of SR141716A in rats, abolished [ $^3$ H]CP55,940 binding to ex-vivo cerebella membranes [Rinaldi-Carmona et al, 1995]. Using [ $^3$ H]-SR141716A, which binds to the CB1 receptor independently of G-proteins, the same group of workers characterised the rank order binding affinity of cannabinoid ligands, SR141716A > CP55,940 > WIN55-212-2 =  $\Delta^9$ -THC > anandamide [Rinaldi-Carmona et al, 1996].

CB1 receptors are present in the brain at very high concentrations, for example Ney et al [1985] reported 1.2pmol/mg protein in rat brain. Autoradiographic studies have revealed the distribution of CB1 receptors in the brain. CB1 receptors were shown to be present in many brain regions, including olfactory areas, cortex, hippocampus, cerebellum, basal ganglia, whereas the thalamus, hypothalamus and brainstem had very few binding sites [Mailleux and Vanderhaeghen, 1992].

CB1 receptors are also naturally expressed in continuous cell lines including NG108-15 where they cause inhibition of N-type VOCC [Caulfield and Brown, 1992], and in N18TG2 where inhibition of AC has been reported [Howlett, 1984]. More recently, cloned CB1 receptors have been transfected into CHO (Chinese hamster ovary), Ltk (murine fibroblast) and AtT-20 (mouse pituitary) cells all of which do not naturally express the receptor [Felder et al, 1995; Bouaboula et al, 1995; Felder et al, 1992]. CP55, 940 caused an inhibition of AC in CB1 transfected cells only, whereas arachidonic acid release and intracellular  $Ca^{2+}$  release was observed in both CB1 transfects and untransfected cells, this report concluded that cannabinoids stimulate both receptor and non-receptor mediated signal transduction pathways [Felder et al,1992]. In a later study Felder [1995] and coworkers compared the pharmacology of CB1 and CB2 receptors expressed in AtT-20 and CHO cells, they reported that both receptors bound cannabinoid agonists with varying affinity, CP55,940, anandamide and  $\Delta^9$ -THC were equipotent at each receptor, WIN55-212-2 and cannabinal bound with a higher affinity to CB2. Both receptors coupled to an inhibition of AC in a pertussis toxin sensitive manner but only CB1 AC inhibition was reversed by SR141716A. However in AtT-20 cells CB1 but not CB2 coupled to an inhibition of Q-type VOCC and a stimulation of the inwardly rectifying potassium channel. CB1 receptors have also recently been shown to activate mitogen-activated protein kinases in CHO cells expressing CB1 receptors [Bouaboula et al, 1995].

To date, there are no reports in the literature of genetic manipulations of CB1 receptors, and hence regions of the receptor which are responsible for agonist and antagonist binding, G-protein and AC coupling are unexplored at present.

### **1.11. Cell Culture.**

The SH-SY5Y cells used in this study are descended from a parent cell line, SK-N-SH. This parent cell line was established from cell culture of human metastatic neuroblastoma tissue taken from the bone marrow of a Caucasian four-year-old female leukemia patient [Beidler et al, 1973]. The cells were tested for malignancy and fulfilled the criteria that they derived from a tumor. Their neuronal origin was confirmed by the presence of a high activity of dopamine- $\beta$ -hydroxylase, an enzyme which is unique to neuronal tissue.

NG108-15 cells are a hybrid cell line, the cell body consists of rat glioma (C6 BV1) and mouse neuroblastoma (N18TG-2), whose membranes are fused using Sendai virus [Nirenberg, 1988]. Their neuronal status was also confirmed by the high activity of dopamine- $\beta$ -hydroxylase [Nirenberg, 1988]. The cells display neuronal morphology and have been shown to be a good cell line to use for the study of the homogeneously expressed  $\delta$ -opioid receptor [Law et al, 1985].

Chinese Hamster Ovary cells, as the name suggests, are derived from an adult Chinese hamster ovary epithelium. These cells have been widely used as cDNA expression systems due to their ability to freely take up foreign cDNA, the cell will readily incorporate the cDNA into its own genome and express the gene in a stable manner [Puck et al, 1958].

## **1.12. General Aims.**

Understanding the regulation of AC activity by opioids and cannabinoids gives an insight into the mechanisms by which neuronal cells control neurotransmission and hence, mediate the inhibitory pain (and other) pathways. Therefore, further studies are required in order to understand these mechanisms in greater detail.

The central theme of this thesis is the regulation of AC by opioid and cannabinoid receptors, and studies using a variety of preparations will be presented. A large proportion will involve SH-SY5Y human neuroblastoma cells. Initial studies will be performed in order to characterise the isoform(s) of AC in SH-SY5Y human neuroblastoma cells. SH-SY5Y cells express many different G-protein coupled receptors and channels, in addition they respond to a depolarising stimulus by opening L- and N-type VOCC's. Stimulation of the M3 muscarinic receptor by muscarinic agonists or depolarisation by potassium stimulation will cause an increase in intracellular  $Ca^{2+}$  concentration. Experiments to examine whether these rises in  $Ca^{2+}$  can cause a change in AC activity will be performed. If this is the case then a further series of experiments will be carried out in order to elucidate the pools of  $Ca^{2+}$  required for this response. A prediction as to the isoform of AC expressed in these cells can then be made.

In chapter 4, I aim to compare and contrast the changes in AC activity caused by endogenous  $\mu$ - and  $\delta$ -opioid receptors. Using SH-SY5Y (expressing predominantly  $\mu$ -) and NG108-15 cells (expressing  $\delta$ -) the effects of Fentanyl, DAMGO and DPDPE, DADLE will be examined with respect to their binding affinity and functional inhibition of AC. The effect of nociceptin on forskolin stimulated cAMP formation in SH-SY5Y cells will also be examined.

Following this study, using cloned opioid receptors expressed in CHO cells, a pharmacological comparison of  $\mu$ -,  $\delta$ -, and  $\kappa$ -opioid receptor mediated AC inhibition will

be made and compared with endogenous receptors in the previous chapter. In addition, using C-terminal deletion mutants of the  $\delta$ -opioid receptor expressed in CHO cells, I aim to examine the role of the C-terminus in agonist binding and functional AC inhibition.

In chapter 7, the aim will be to develop a method for the measurement of cannabinoid binding to rat cerebella membranes. In addition, I hope to measure cannabinoid induced inhibition of AC activity in SH-SY5Y, NG108-15 and rat cerebella membranes.

Finally, I will attempt to amplify cDNA encoding for the rat CB1 receptor and multiple copies made using ampicillin resistant *E. coli*. If this is successful, I will attempt to transfect the CB1 cDNA into wild type CHO cells and demonstrate cannabinoid binding and inhibition of AC.

**CHAPTER 2: MATERIALS AND METHODS.**

(Additional methodology can be found in specific chapters.)

## **2.1. Sources of chemicals.**

All chemicals and reagents used were of the utmost purity.

### **Sigma chemicals, Poole, Dorset.**

Atropine, Trifluoperazine, IBMX, Forskolin, Carbachol, cAMP, Muscarine, Fura2-AM, Triton-X100, EDTA, EGTA, HEPES, Calmodulin, Creatine Kinase, GTP, Phosphocreatine, ATP, Fentanyl, DPDPE, DADLE, DAMGO, Naloxone, BSA, Sigmacote, DMSO, Tris-HCl, PMSF, Morphine, Acetylcholine, dopamine, Noradrenaline, GABA, Glutamate, Imipramine, Hydrocortizone, Pancuronium, Lignocaine, Bromophenol blue, Agarose, Glycerol, Ethidium bromide, Tryptone, Yeast, MOPS, Rubidium chloride, Lysozyme, Phosphoramidon, Amastatin, Bestatin, Captopryl.

### **Fisons chemicals, Loughborough, Leicestershire.**

Sodium chloride, Potassium chloride, Magnesium chloride, Magnesium sulphate, Sodium hydrogen carbonate, Sodium hydroxide, Hydrochloric acid, Tris-HCl, Calcium carbonate, Ethanol, Methanol, Sucrose, Glucose, Copper sulphate, Potassium dihydrogen phosphate, Nickel chloride, Potassium hydroxide, Activated charcoal.

### **Gibco Life Technologies, Paisley, Scotland.**

Minimum Essential Medium, Dulbeccos Minimum Essential Medium, HAMS F12 medium, Fungizone, Penicillin/Streptomycin, Foetal calf serum, HAT supplement, Genticin, Lipofectin, Trypsin, L-glutamine, Ecor1 and Hind3.

### **Research biochemicals.**

Anandamide, PEI, Cyclodextrin, Naltrindole hydrochloride, WIN55-212-2 mesylate, spiradoline,  $\Delta^9$ -THC,  $\Delta^8$ -THC, Cannabinol.

### Radiochemicals.

[<sup>3</sup>H]cAMP, [<sup>3</sup>H]WIN55-212-2, [<sup>3</sup>H]CP55,940 all greater than 98% pure were obtained from NEN du pont.

[<sup>3</sup>H]NMS, [<sup>3</sup>H]DPN, [<sup>3</sup>H]SR141716A all greater than 98% pure were obtained from Amersham, UK.

### Other chemicals and reagents.

QIAGEN DNA purification kit was obtained from QIAGEN Inc. Chatsworth, CA, USA.

Nabilone was a kind gift from Lilly pharmaceuticals. Nociceptin was a kind gift from Parke-Davis, Cambridge. SR141716A was a kind gift from Sanofi Pharmaceuticals, Montpellier, France. Optiphase Hi-safe3 and optiphase safe liquid scintillation cocktail was from Wallac UK. Plasticware was supplied by Nunc.

### 2.2 Buffer composition.

#### *1. Krebs HEPES. (experiments using whole cells)*

(mM):- Na<sup>+</sup> (143.3), K<sup>+</sup> (4.7), Ca<sup>2+</sup> (2.5), Mg<sup>2+</sup> (1.2), Cl<sup>-</sup> (125.6), H<sub>2</sub>PO<sub>4</sub><sup>2-</sup> (1.2), SO<sub>4</sub><sup>2-</sup> (1.2), Glucose (11.7) and HEPES (10), pH7.4 with 10M NaOH.

#### *2. Mg<sup>2+</sup>-HEPES. ([<sup>3</sup>H]NMS binding experiments)*

(mM):- HEPES (50) and Mg<sup>2+</sup> (3) pH7.4 with 10M NaOH.

#### *3. Tris-HCl. (Membrane receptor binding experiments)*

Tris -HCl (50) pH7.4 with 10M NaOH, (10M KOH, for cannabinoid binding).

#### *4. ATP-Regenerating. (cAMP measurement in membranes).*

(mM)-ATP (0.5), Phosphocreatine (10), GTP (0.1), HEPES (10), Mg<sup>2+</sup> (3), IBMX (0.5) and creatine kinase (30EU/ml), pH7.4 with 10M NaOH.

All other buffers are described in text.

## **2.3 Tissue culture.**

### *1. Un-differentiated SH-SY5Y Human Neuroblastoma cells.*

Confluent monolayers (75cm<sup>2</sup>) of cells (passage 75-90, a kind gift from J. Beidler) were maintained in Minimum Essential Medium supplemented with 10% foetal calf serum, 2mM glutamine, 100iu/ml penicillin, 100iu/ml streptomycin, and 2.5µg/ml fungizone. One flask of confluent cells was split using trypsin (0.5g/l) -EDTA (2g/l, 5ml) solution (0.9g/l NaCl) into 9 other flasks each containing 15ml of supplemented media. After 2 days of incubation (37°C, 5% CO<sub>2</sub> incubator) the media was removed and replaced with 25ml of fresh supplemented media.

### *2. NG108-15 neuroblastoma X glioma hybrid cells.*

As above except, Dulbecco's minimum essential medium was used instead of minimum essential medium. In addition to the supplements as above, 10ml of Hypoxanthine (5mM), Aminopterin (20µM), Thymidine (0.8mM) was added to 500ml of medium. Cells were used from passage number 30-50. Cells were kindly supplied by the European Tissue Culture Bank.

### *3. Chinese Hamster Ovary cell transfects.*

HAMS F12 medium was used containing the supplements as in 1. In addition, 100µg/ml of geneticin was included in separate media. Stock cultures were grown in HAMS F12 medium containing geneticin, whereas experimental cultures were grown in geneticin free medium. All cells were used from passages 5-25 (numbered after transfection) and were kindly supplied to us by L. Devi and D. Grandy. For details of CHO CB1 cell culture the reader is directed to chapter 7.

## **2.4 Harvesting and washing procedure (all cells).**

After approximately 7-10 days of incubation the cells reached confluency and were harvested using 5ml of 50mM HEPES buffered saline (0.9%) containing 3mM EDTA. Cells were used from passage number 68-85, and were 7-10 days old. The cells were detached and then resuspended in 15ml of the appropriate experimental buffer in a 15ml centrifuge tube. The suspension was inverted in order to break up clumps of cells, and sedimented at 1500rpm (1300g) for 2 minutes. This procedure was repeated twice for each 75cm<sup>2</sup> flask of cells.

## **2.5 Membrane preparation.**

In binding and CaM regulation of AC activity experiments a membrane preparation was used. Following washing, the cells (SH-SY5Y and NG108-15) were resuspended in 5ml of buffer in a 50ml high speed centrifuge tube, and homogenised using a tissue tearor or a polytron set on high speed for 5x10 second bursts. The homogenate volume was made up to 40ml and then centrifuged at 13000rpm (10000g) for 10 minutes at 4°C. The resulting pellet was then resuspended in a further 40ml of buffer and re-centrifuged. This procedure was repeated once more prior to experimental protocols. For the preparation of rat cerebella membranes, one cerebellum was homogenised and the membranes were washed as described above.

## **2.6 cAMP experiment and assay.**

cAMP was measured in whole cells and membranes. In whole cells extracellular Krebs/HEPES buffer pH7.4 at 37°C was used. Na<sup>+</sup> concentrations were adjusted to 40mM in order maintain tonicity in K<sup>+</sup> depolarisation experiments.

In membranes ATP regeneration buffer pH7.4 at 37°C was used.

### *1. Whole cells.*

Whole cell suspensions (approx. 200µg) were incubated in 300µl volumes of Krebs/HEPES buffer containing 1mM IBMX, and combinations of other drugs for varying

times at 37°C. Reactions were terminated (cells lysed) by the addition of 20µl of HCl (10M). The pH was equilibrated by the addition of 20µl NaOH (10M) and 180µl of Tris-HCl buffer (1M, pH7.4). Following centrifugation (13000rpm for 2min in a Sarstedt microfuge), cAMP was measured in the supernatant by a radio-receptor (the receptor is unknown but likely to be purified PKA) assay see Brown et al [1971].

## 2. Membranes.

Cell membranes were prepared fresh for each experiment as described above. Following the final wash the membranes were re-suspended in 3-5ml of nominally Ca<sup>2+</sup> free ATP regenerating buffer (as above). Reactions were terminated and cAMP was measured as described in 1 above.

## 3. cAMP assay.

### Assay Principle

The assay relies on the competition between labeled and unlabelled ligand binding to the cAMP binding protein. The soluble binding protein is purified from bovine adrenal glands (see later), and the cAMP dependent protein kinases are probably responsible for binding both labeled and unlabelled cAMP in a ratio proportional to their respective concentrations. There is an inverse relationship as to the amount of unlabelled cAMP and the amount of radioactivity in the samples. When the competing mass of unlabelled ligand is high then there is less labeled cAMP bound to the protein.

The assay was performed on ice. 50µl of supernatant, containing cAMP to be measured, was mixed with 100µl of [<sup>3</sup>H]cAMP (0.925Mbpq stock, 0.5nM approximate final concentration). To this, 150µl of cAMP binding protein (1 in 25 dilution of stock solution, see later) was then added to each tube. The tubes were incubated at 4°C overnight in order for binding to equilibrate. Bound and free radioactivity was separated by addition of 250µl of activated charcoal (250mg/25ml), BSA (100mg/25ml) suspension mixture. This was centrifuged after 1 minute for 1 minute at 13000rpm in a Sarstedt microfuge at room

temperature. 400µl of the supernatant was then mixed with 1ml of Optiphase High Safe 3 liquid scintillation cocktail in order to measure radioactivity.

For each experiment, a set of known cAMP standards (0, 0.25, 0.5, 1, 2, 4, 6, 8, 10pmol/50µl) were run alongside the unknowns, a standard curve was generated (Figure 2.1) and the unknown cAMP amount extrapolated using Riasmart software. Non-specific binding was determined in the presence of 250pmol/50µl cAMP.

#### Assay tests.

The inter- and intra-coefficients of variability of the assay were measured. A 6pmol/50µl sample was measured in 7 independent assays with an inter-assay variation of 8.75%. In addition, 7x6pmol/50µl samples were measured in the same assay yielding an intra-assay variation of 0.76%.

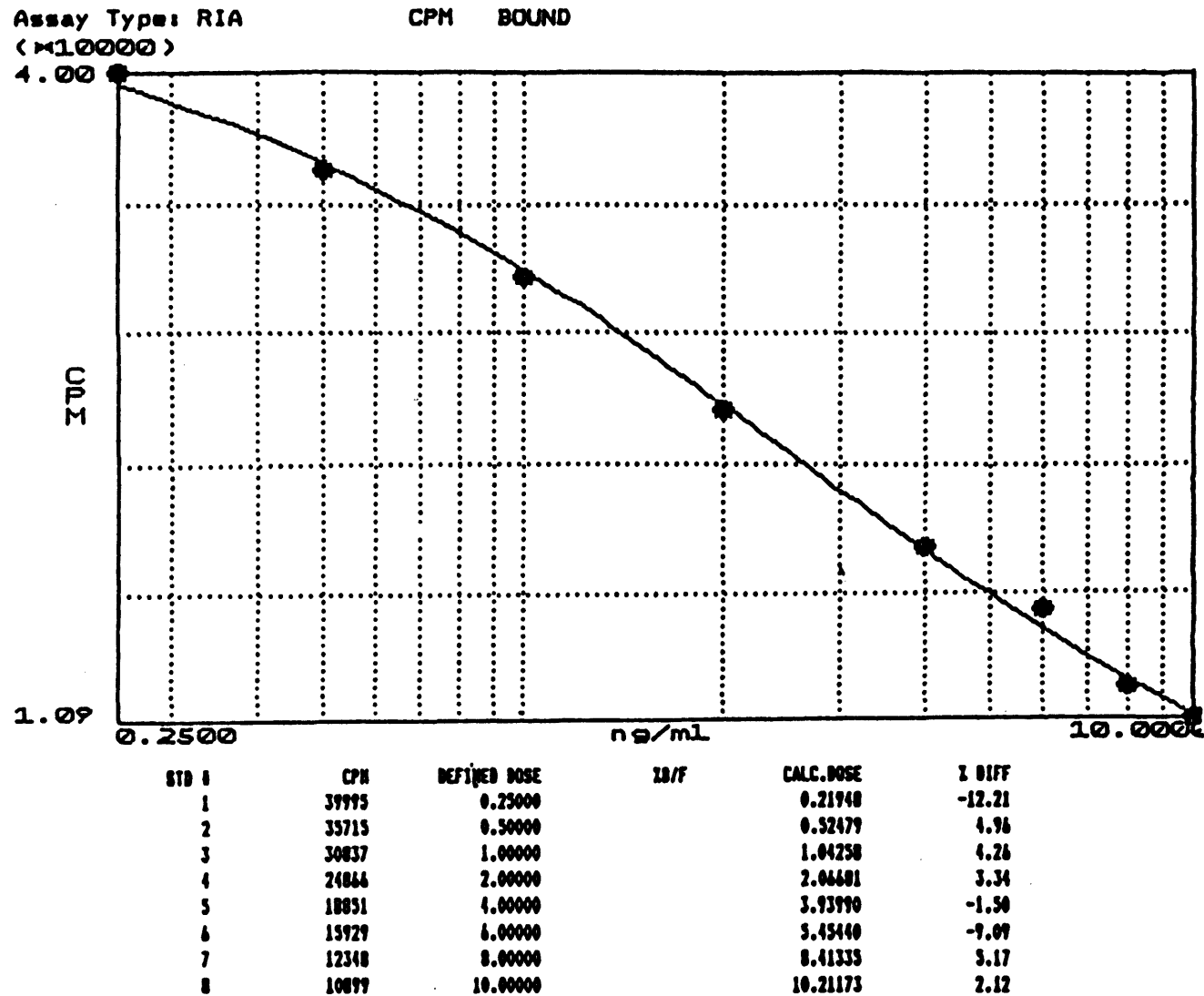


Figure 2.1. A representative cAMP standard curve. Non-linear regression and extrapolation of unknowns was determined using the Packard curve fitting program, Riasmart.

### Calculation of cAMP concentration.

cAMP is expressed as:

- A.  $\text{pmol}/50\mu\text{l} \times 10.4 = \text{pmol}/\text{tube}$  (corrected for dilution).  
 $\text{pmol}/\text{tube} \times \text{Protein (mg)} = \text{cAMP in pmol}/\text{mg protein}$  (corrected for protein).
- B. % inhibition of forskolin stimulated cAMP formation  
$$= 100 - \left[ \frac{\text{cAMP (drug)} - \text{Basal cAMP}}{\text{Forskolin stimulated cAMP} - \text{Basal cAMP}} \right] \times 100$$
- C. % stimulation of basal where basal=100% stimulation.

### Purification of cAMP binding protein.

Bovine adrenal glands (approximately 30 at a time) were dissected, in order to collect the dark purple adrenal cortex tissue taking care as to avoid fat, adrenal medulla and capsule tissue contamination. The adrenal cortex tissue was then homogenised using a tissue tearor (full speed for 20x20 second bursts) in 20ml of Tris-HCl , 3mM EDTA buffer pH7.4 on ice. The 20ml of adrenal cortex slurry was separated into 4x50ml high speed centrifuge tubes and the volume made up to 40ml in each tube. The tubes were mixed well and centrifuged at 13000rpm for 20 minutes at 4°C. The supernatant was removed and re-centrifuged as above. The supernatant (150ml approx.) contained cAMP binding protein at 25 fold higher concentration than that required in the assay.

## 2.7 Measurement of Intra- and Extra-cellular Calcium.

### *1. Intra-cellular $[\text{Ca}^{2+}]$ in SH-SY5Y cells.*

Confluent (6 day old) SH-SY5Y cells were harvested and washed in Krebs/HEPES buffer (3x10ml) as above. Cell suspensions were loaded with 3 $\mu\text{M}$  Fura 2 AcetoxyMethylester (AM) in 3ml for 30minutes at 37°C. Fura 2AM is uncharged and is taken up non-specifically by the cell by virtue of the hydrophobic AM group interacting with membrane lipids. Once inside the cell esterase enzymes cleave the AM group away from Fura 2. Fura 2 free acid is electronegatively charged and is trapped inside the cell where it is free to bind  $\text{Ca}^{2+}$ . The cells were sedimented (1500rpm for 2 minutes) and re-suspended in Krebs/HEPES buffer and incubated a further 15 minutes at room temperature to allow for de-esterification of the Fura 2AM. Intracellular calcium

concentrations were measured at 37°C, using a Perkin-Elmer LS50B fluorimeter. Cell suspensions (2ml) were placed in a cuvette containing a magnetic stirrer and placed in the cuvette holder which is maintained at 37°C with a water jacket. The Fura 2 containing cells were subjected to dual excitation at 340 and 380nm (see figure 2.2), emission was measured at 510nm. The maximum fluorescence ( $R_{\max}$ ) was measured by cell lysis with 0.1% Triton-X100, and the minimum fluorescence ( $R_{\min}$ ) was determined with the addition of 3mM EGTA ( $\text{Ca}^{2+}$  chelating agent). Intracellular  $\text{Ca}^{2+}$  concentration is then calculated according to Grynkiewicz et al [1985].

$$[\text{Ca}^{2+}] = K_d \left[ \frac{R - R_{\min}}{R_{\max} - R} \right] Sfb$$

Where,  $K_d = 225\text{nM}$ ,  $Sfb = 380_{\min} / 380_{\max}$ .

In the experiments,  $R_{\min}$ ,  $R_{\max}$  and Sfb (Ratio of baseline fluorescence (380nm) under  $\text{Ca}^{2+}$  free, EGTA, and bound,  $\text{Ca}^{2+}$ , dye conditions) were  $0.61 \pm 0.01$ ,  $5.1 \pm 0.1$  and  $3.24 \pm 0.07$  (n=24) respectively.

## 2. Extra-cellular $[\text{Ca}^{2+}]$ .

Membrane buffer calcium concentration was also determined fluorimetrically using  $1\mu\text{M}$  Fura 2 free acid,  $R_{\min}$  and  $R_{\max}$  were established by the addition of  $\text{Ca}^{2+}$  (1mM) and EGTA (3mM), respectively.

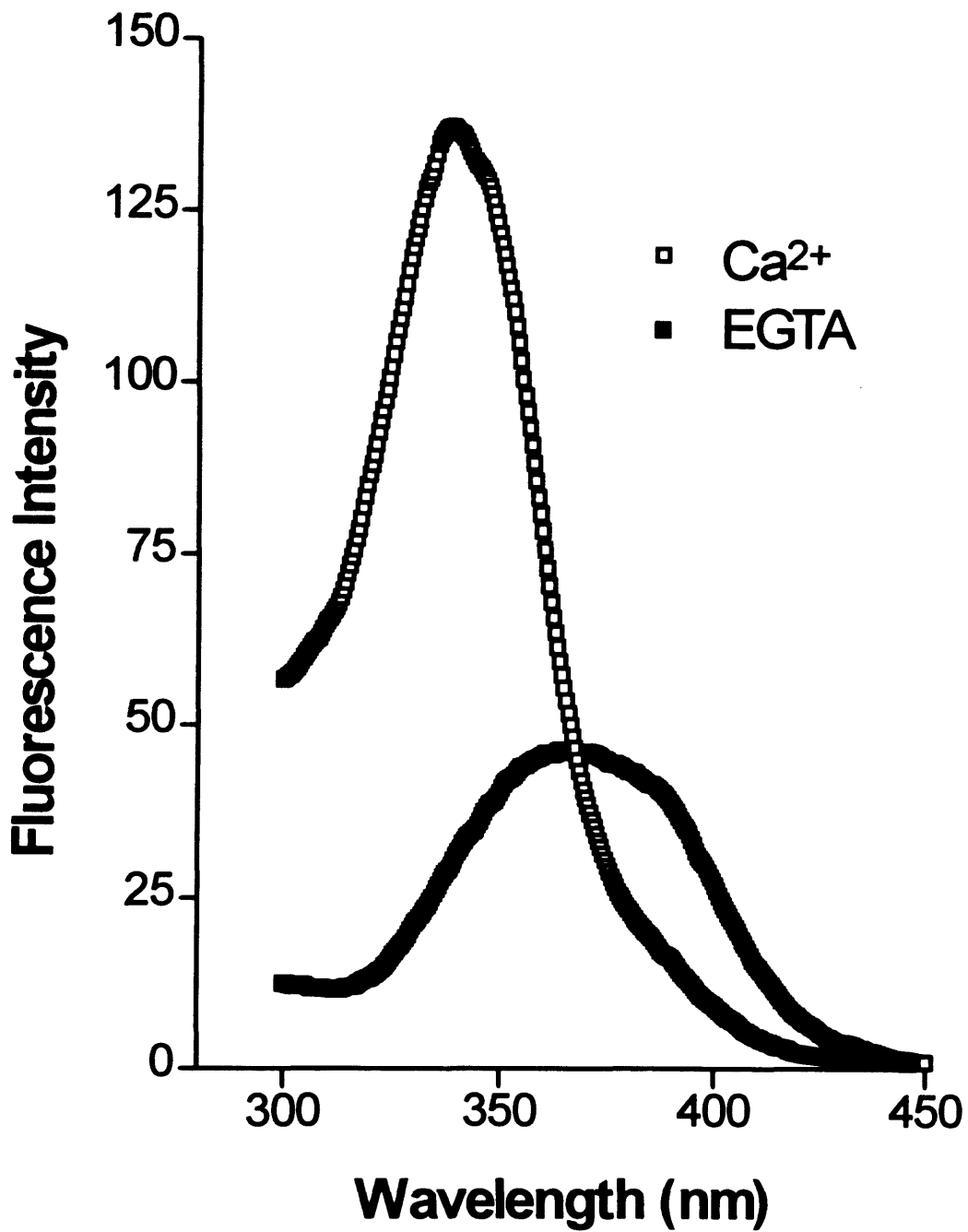


Figure 2.2. Fluorescence spectra of Fura-2 free acid when bound and unbound to  $\text{Ca}^{2+}$ . The isobestic wavelength is where there is no net change in fluorescence.

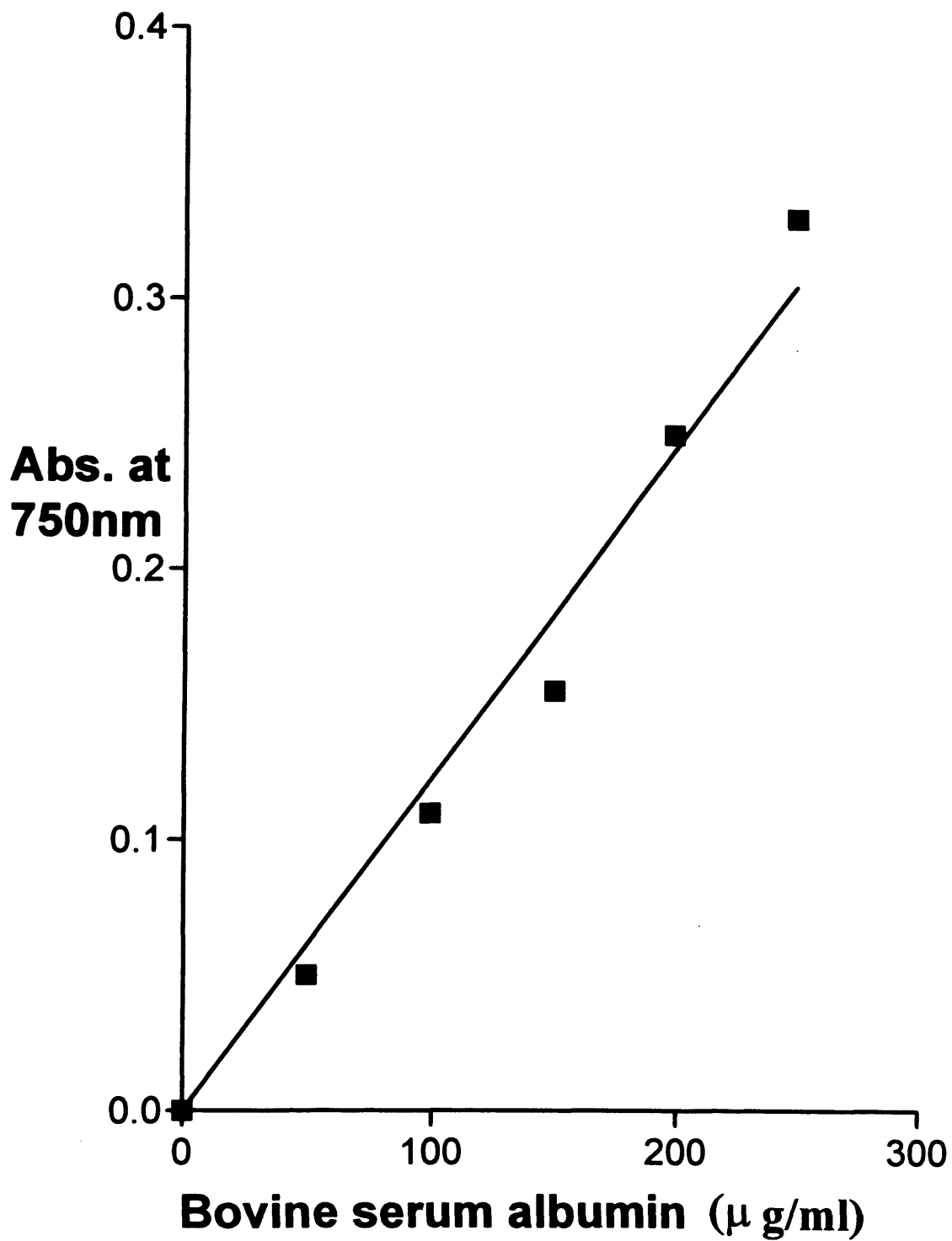


Figure 2.3. A representative protein assay standard curve, where absorbance at 750nm is directly related to the amount of protein. Linear regression ( $R^2=0.98$ ,  $y=mx+c$ ) was fitted using Graphpad prism.

## **2.8 Lowry protein assay.**

The tissue to be assayed was diluted 1:20 (25 $\mu$ l in 475 $\mu$ l) in 0.1M NaOH in order to digest the protein and to fit the unknown protein concentrations on the standard curve. Protein assay reagents were made up as A, B, C where A=2% NaHCO<sub>3</sub> in 0.1M NaOH, B=1% CuSO<sub>4</sub> and C=2% Na<sup>+</sup>K<sup>+</sup> tartrate. The solutions were mixed, 100ml A+1ml B+1ml C. 2.5ml of this mixture was added to each tube containing 0.5ml volumes of protein in 0.1M NaOH and incubated for 10 minutes at room temperature. 250 $\mu$ l of a 1 in 4 dilution (in distilled water) of Folin's phenol reagent was then added to each tube. The tubes were then vortex mixed and incubated for 30 minutes at room temperature in order for the blue colour to develop. Bovine serum albumin protein standards (0, 50, 100, 150, 200 and 250 $\mu$ g/ml) were made up in 0.1M NaOH, and these were measured alongside the unknown samples. The absorbance readings were made in 1ml disposable cuvettes at 750nm in a Corning spectrophotometer. A standard curve (figure 2.3) was generated using Graphpad Prizm (Linear regression fit) and unknown amounts of protein extrapolated from it. Protein concentrations were expressed as  $\mu$ g/ml, therefore the following calculation was made: extrapolated protein in  $\mu$ g/0.5ml X 2 X 1000=extrapolated protein in mg/ml [Lowry et al, 1951].

## **2.9. Binding assay protocols.**

Various binding assay protocols were used throughout. The reader is directed to the results chapters (3, 4, 5, 6 and 7) for details of binding methodology used.

## **2.10. Receptor binding principals.**

One of the most frequently used methods for the study of receptors is ligand/receptor binding. These elegant, yet simple experiments rely on radioactive labeling techniques, in which a particular atom in the ligand was chemically substituted for a radioactive atom. Three types of binding experiments can be performed for the study of ligand/receptor binding these are, saturation, displacement and kinetic.

### 2.11. Saturation studies.

These experiments are performed in order to study the maximum number of binding sites ( $B_{max}$ , fmol/mg protein) and the dissociation constant (concentration of radioligand where 50% of the binding sites are occupied,  $K_d$  in nM) of the radioligand. Increasing concentrations of radiolabel (usually pM-nM) are incubated with the receptor, in the presence and absence of high affinity antagonist. This is in order to determine total and non-specific (+antagonist=NSB) binding. The difference between total and NSB is the specific binding (figure 2.4). The data from these experiments can be treated in three ways.

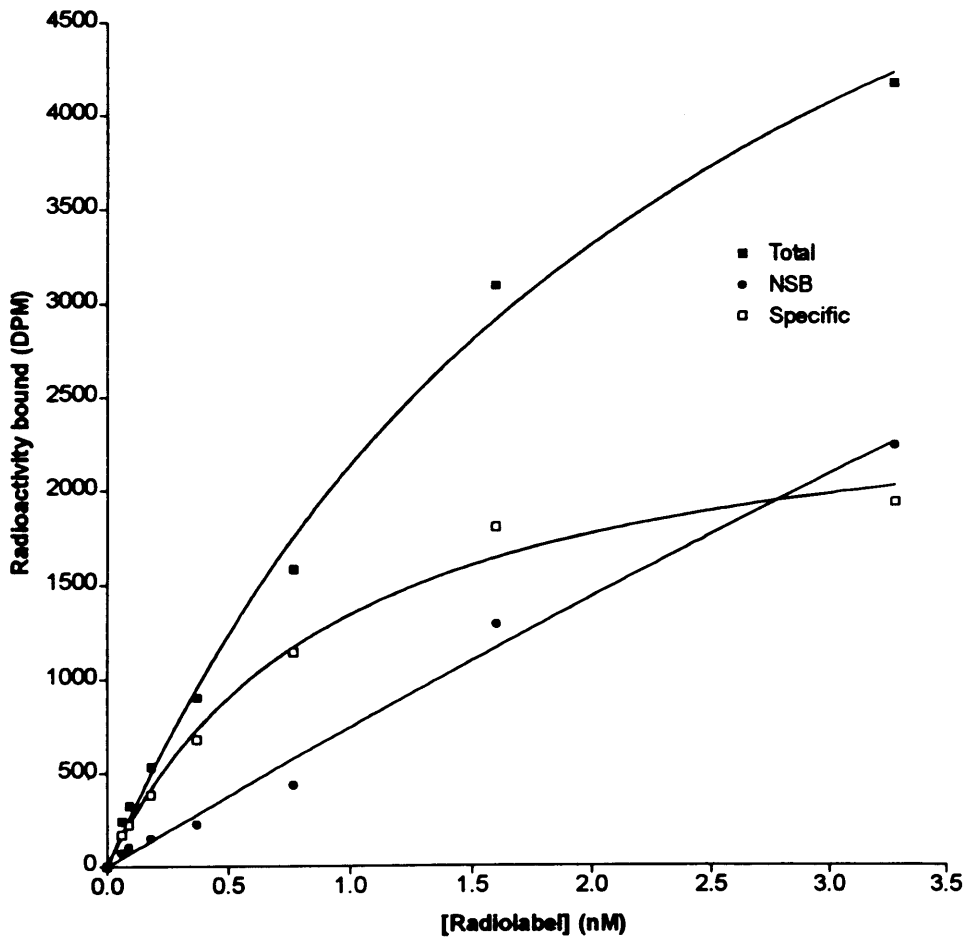


Figure 2.4. Graph which shows dose dependent saturable binding of a radioligand (specific). Where total binding is determined in the absence and non-specific binding in the presence of a high affinity antagonist. Specific binding is total-NSB.

### A. Binding Hyperbola.

Radioactivity bound (Y axis, fmol/mg bound) is plotted directly against concentration (X axis, nM) of radiolabel. The B<sub>max</sub> (fmol/mg protein) is the amount of binding at saturation and the K<sub>d</sub> (nM) is the concentration of radioligand required to occupy 50% of the receptors.

### B. Langmuir-Hill plot.

This plot yields a sigmoidal binding curve. Radioactivity bound (Y axis, fmol/mg bound) is plotted against log Molar concentration (X axis) of radiolabel. The B<sub>max</sub> (fmol/mg protein) is the amount of binding at saturation and the K<sub>d</sub> (nM) is the concentration of radioligand required to occupy 50% of the receptors.

### C. Scatchard Analysis.

This treatment of the saturation data yields a linear relationship and is used throughout this thesis. Bound/Free (Y axis, fmol/mg protein/nM) is plotted against Bound (X axis, fmol/mg protein), where the B<sub>max</sub> is the X axis intercept and the K<sub>d</sub> is -1/slope.

#### 2.11.1 Why use Scatchard analysis?

In 1949, Scatchard [1949] introduced a simple graphical method for the calculation of binding parameters (K<sub>d</sub> and B<sub>max</sub>). Since its introduction, Scatchard analysis has been used to make considerable progress in order to identify the pharmacology of receptors, indeed, since 1949 over 2000 research papers from the literature have used Scatchard analysis. However, since the introduction of computer modeled nonlinear regression curve fitting programs, Scatchard analysis has received some criticism [Burgisser, 1984; Klotz, 1982; Munson, 1983]. These reports all pointed out the problems associated with the analysis, and the main criticisms include:

1. A low range of radioligand concentrations and a clustering of the data points on the x-axis.
2. Dramatically enlarged scatter of the data points following transformation.
3. Difficulty in estimation of saturation of radioligand (B<sub>max</sub>) [Klotz, 1982]

4. Other problems are that background radioactivity is not accounted for, improper subtraction of NSB, receptor heterogeneity, and errors occurring during separation of bound and free radioligand [Burgisser, 1984].

The overall consensus is that the transformed linear regression model is based on too many assumptions and that it is wholly inappropriate to analyse saturation isotherms by Scatchard analysis alone.

However, the presentation of isotherms by linear regression analysis, does have some advantages over binding hyperbolae.

Therefore, to minimise any errors associated with Scatchard analysis, all data were first analysed by rectangular hyperbola to ensure saturation of radioligand. Scatchard analysis was then used to calculate  $K_d$  and  $B_{max}$  values. To demonstrate the small differences in  $K_d$  and  $B_{max}$  values with the use of different graphical representations,  $K_d$  and  $B_{max}$  values were obtained using Scatchard, Langmuir-Hill and Hyperbola analysis for the representative experiments.

It is clear that some problems exist with Scatchard analysis. If however there is little or no difference in  $K_d$  or  $B_{max}$  values following the use of other methods of analysis, then, Scatchard analysis of saturation binding isotherm data is valid.

## **2.12. Displacement studies.**

These experiments are used in order to determine the affinity of an unlabelled ligand which acts at a specific receptor. Displacement of a radioligand bound to a receptor is achieved by increasing concentrations of unlabelled displacing ligand. A sigmoidal displacement curve is obtained where the log concentration of displacer (X axis, molar) is plotted against radiolabelled ligand displacement (Y axis, % inhibition of specific binding). A fixed concentration of radioligand is used. The equilibrium dissociation constant ( $K_i$ ) is an estimate of the  $K_d$  for the unlabelled ligand.  $K_i$  values are the 50% inhibitory concentration ( $IC_{50}$ ) of displacer, corrected for radiolabelled ligand concentration using the Cheng and Prussoff equation (see later)[1972].  $IC_{50}$  values are dependent on radioligand concentration for example, if the concentration of radioligand is increased, a higher concentration of displacer is required in order to achieve the same

amount of displacement. This has the effect of causing the displacement curves to shift. The Cheng and Prussoff equation takes into account both the concentration and the affinity of the radioligand and predicts  $K_i$ .

$$\text{Cheng and Prussoff equation } K_i = \frac{IC_{50}}{1 + \frac{[L]}{K_d}}$$

Where  $IC_{50}$ =half maximal inhibition of binding (nM).

$[L]$ =Radioligand concentration (nM).

$K_d$ =Radioligand affinity (nM).

Agonist displacement of a radiolabelled antagonist display curves which can be fitted assuming the presence of two sites. Using this fit, it is possible to estimate high (G protein coupled) and low (G protein uncoupled) affinity receptor states. Radiolabelled antagonists displaced by an antagonist can display steep curves with a slope factor of unity being indicative of a non-selective antagonist and/or receptor homogeneity. Low slope factors may suggest selectivity and or receptor heterogeneity. Agonists vary in affinity for a receptor depending on their coupling to G-proteins and for this reason, displacement curves by an agonist using a radiolabelled agonist are difficult to interpret.

### **2.13. Kinetic analysis of $K_d$ .**

To estimate the binding affinity ( $K_d$ ) for a radioligand, its association/dissociation rates with the receptor are measured. A fixed concentration of radioligand is incubated for various times with and without a high affinity antagonist in order to determine NSB. When the specific (Total-NSB) binding is at equilibrium, high affinity antagonist is added in excess for various times to 'chase off' the radiolabel. When the NSB is at equilibrium the on and off rates can be determined. The on-rate ( $K_{+1}$ ) is proportional to the radioligand concentration and dependent on the rate of dissociation. Firstly,  $K_{ob}$  is calculated as the observed rate of association.  $K_{+1}$  is calculated by subtracting  $K_{-1}$  from  $K_{ob}$  and dividing this by the radioligand concentration. The  $K_d$  can be determined, using the following equation.

Principle:

$$K_d = \frac{K_{-1}}{K_{+1}}$$

Where,  $K_{+1}$ =on rate,  $K_{-1}$ =off rate,  $K_d$ =affinity constant.

#### **2.14. Data analysis.**

All data, unless otherwise stated, are expressed as mean±Standard Error of the Mean (SEM) of at least 3 independent determinations.  $pIC_{50}$ ,  $pK_i$ ,  $pEC_{50}$  and slope factors were all obtained by computer-assisted curve fitting using Graphpad Prizm.

Both  $pEC_{50}$  and  $pIC_{50}$  values were obtained by fitting a sigmoidal curve with a variable slope.  $pK_i$  values were obtained from displacement curves by modeling the points to a one and a two site fit. The  $pK_i$  values obtained for high and low affinity sites were only performed when the least sum of squares for the two site fit was lower than the one site. Where appropriate statistical comparisons were made using Student's paired or unpaired t-test (following Analysis of variance (ANOVA) where appropriate) and considered significant when  $P < 0.05$ .

**CHAPTER 3. CHARACTERISATION OF ADENYLYL CYCLASE IN SH-SY5Y  
HUMAN NEUROBLASTOMA CELLS.**

### **3.1: Introduction.**

Adenylyl cyclases exist as a family of closely related G-protein linked effector enzymes, all of which convert ATP into cAMP [Iyengar, 1993]. cAMP is an important second messenger responsible for transmitting extracellular signals to modulate a diverse array of cellular responses [Ueda and Tang, 1993]. Eight different isoforms of mammalian adenylyl cyclase have been cloned and comparison of their amino acid sequences has revealed that the overall homology between subtypes is approximately 50% [Iyengar, 1993]. Types 1-8 are all activated by  $G_s$ - $\alpha$  and forskolin, but vary in their sensitivity to different regulatory molecules, these include  $G_i$ - $\alpha$ ,  $G$ - $\beta\gamma$ ,  $Ca^{2+}/CaM$ , PKA and PKC [Iyengar, 1993]. *In situ* hybridization analysis of rat brain has shown that, with the exception of types 4 and 6, all other adenylyl cyclase isoforms are expressed in discrete locations in brain, however some brain regions express more than one isoform [Cooper, et al, 1995]. Type 1, 3 and 8 are all stimulated by  $Ca^{2+}$  [Cooper, et al, 1995] and this represents a mechanism by which  $IP_3$ -induced intra-cellular  $Ca^{2+}$  release and extra-cellular  $Ca^{2+}$  entry can increase the cAMP signal. The reader is directed to the introduction for further information about adenylyl cyclase isoforms.

$Ca^{2+}$  homeostasis in SH-SY5Y human neuroblastoma cells has been extensively studied. Lambert and co-workers have shown that SH-SY5Y cells express a homogeneous population of  $M_3$  muscarinic receptors, which preferentially couple to PLC [1992], probably via  $G_q$  [Smrcka et al, 1991], and cause a biphasic increase in  $[Ca^{2+}]_i$ . This rise in  $[Ca^{2+}]_i$  is due to rapid  $IP_3$ -induced calcium release from an internal store and simultaneous calcium channel opening [Lambert and Nahorski, 1992]. It is not clear which type of  $Ca^{2+}$  channel(s) are opened following muscarinic receptor occupation, two groups have shown that SH-SY5Y cells can utilize both ROCC [Lambert and Nahorski, 1992] and  $I_{crac}$  [Grudt et al, 1995]. Other workers have shown that SH-SY5Y cells also express  $M_1$  and  $M_2$  muscarinic receptors [Adem et al, 1987]. SH-SY5Y cells also possess L- and N-type VOCC's which have been revealed by electrophysiological studies [Seward and Henderson, 1991; Reeve et al, 1994, Kennedy and Henderson, 1992]. These channels can be opened under  $K^+$  depolarizing conditions [Lambert et al, 1990; Vaughan et al, 1995]. The presence of both receptor-dependent

and receptor-independent  $\text{Ca}^{2+}$  signaling pathways on SH-SY5Y cells make them an ideal model for examining the  $\text{Ca}^{2+}$  sensitivity of adenylyl cyclase.

In 1975 it was reported that a crude preparation of purified neuronal adenylyl cyclase was stimulated by  $\text{Ca}^{2+}/\text{CaM}$  whereas the peripheral preparation (bone osteosarcoma) was not [Bronstrom et al, 1975; Cheung et al, 1975]. In 1988 Baumgold and Fishman first demonstrated that muscarinic ( $\text{M}_3$ ) receptor occupation led to an increase in cAMP levels in SK-N-SH cells [Baumgold and Fishman, 1988]. In the same study they reported that this response was not driven by PKC nor resulted from inhibition of cAMP breakdown. Several years later, a neuronal  $\text{Ca}^{2+}/\text{CaM}$  sensitive isoform of adenylyl cyclase was isolated and characterized [Tang et al, 1991], and it was clear that cells expressing this isoform would, as a result of muscarinic receptor mediated rises in  $[\text{Ca}^{2+}]_i$ , increase cAMP formation. However, recent conflicting reports can be found in the literature showing that carbachol can stimulate cAMP formation in SK-N-SH/SH-SY5Y neuronal cells by both  $\text{Ca}^{2+}$ -dependent and  $\text{Ca}^{2+}$ -independent mechanisms [Nakagawa-Yagi, et al, 1991; Jansson et al, 1991; Baumgold and Fishman, 1988]. Moreover, it is still unclear as to whether intra- and/or extra-cellular  $\text{Ca}^{2+}$  causes stimulation of neuronal  $\text{Ca}^{2+}$  sensitive adenylyl cyclase [Cooper et al, 1995].

In this chapter a detailed study into the regulation of adenylyl cyclase by  $[\text{Ca}^{2+}]_i$  and  $[\text{Ca}^{2+}]_e$  will be presented using SH-SY5Y cells. This will be done in order to clarify the controversy as to sources of  $\text{Ca}^{2+}$  which regulate AC and as a prelude to studies of opioid and cannabinoid receptors in these cells.

### **3.2. Methods.**

For details of chemicals, tissue culture, cAMP measurement in whole cells and membranes,  $[Ca^{2+}]_i$  measurement and data analysis the reader is directed to chapter 2.

#### *[<sup>3</sup>H]-NMS binding protocols*

All binding assays were performed in 1ml volumes of whole cells (approx. 200 $\mu$ g) using [<sup>3</sup>H]-NMS at 37°C in various buffer types (see table 3.1). In displacement and saturation experiments bound and free [<sup>3</sup>H]-NMS were separated by rapid vacuum filtration using a 24 place Brandel cell harvester onto Whatman GF/B filters and washed with 2 x 5ml of ice cold buffer. In association kinetic studies bound and free [<sup>3</sup>H]-NMS were separated by rapid vacuum filtration using a Brandel 12 well filter drum onto Whatman GF/C filters and washed with 2 x 5ml of ice cold buffer. In all experiments filters were placed into scintillation vial inserts and covered with 4ml of Optiphase Safe. Radioactivity was extracted overnight. Various incubation times and buffers were used for displacement, saturation and association experiments (see below).

#### *(i) Displacement*

For displacement studies a fixed concentration of [<sup>3</sup>H]-NMS (0.2nM) was used throughout and non-specific binding was determined in the presence of atropine (1 $\mu$ M).

Displacer	Concentration	Incubation time (37°C)	Buffer (pH 7.4)
Atropine	0.1nM-10µM	15 and 60 min	Krebs/HEPES (+Ca <sup>2+</sup> )
		15 min	HBS
Trifluoperazine (TFP)	10nM-1mM	15 and 60 min	Krebs/HEPES (+Ca <sup>2+</sup> )
		15 min	HBS
Nickel	0.05-5mM	15 and 60 min	Krebs/HEPES (+Ca <sup>2+</sup> )
		15 min	HBS
IBMX	10nM-10mM	15 min	Krebs/HEPES (+Ca <sup>2+</sup> )

Table 3.1 Incubation times and buffers used for displacement experiments. HBS= HEPES (10mM) Buffered (pH7.4) Saline (0.9%w/v), IBMX=4-isobutyl-1-methylxanthine.

**(ii) Saturation.**

Various [<sup>3</sup>H]-NMS concentrations (0.1-3nM) were used for saturation experiments. The binding of [<sup>3</sup>H]-NMS was studied for 60 minutes (37°C) in HBS (pH7.4) in the presence and absence of 2.5mM nickel. B<sub>max</sub> and K<sub>d</sub> values were obtained using Sctachard analysis (see chapter 2).

### **3.3. Results.**

Carbachol (1mM) and potassium (100mM) caused a time (approx.  $T_{1/2}$ = 3 and 4 minutes respectively) and dose ( $pEC_{50}$ = $5.27 \pm 0.15$  ( $5.37 \mu\text{M}$ ),  $N=6$  and  $1.47 \pm 0.05$  ( $33.9 \text{mM}$ ),  $N=8$  respectively) related increase in cAMP formation (Figure 3.1A and 3.1B), amounting to an approximate two-fold increase in basal cAMP formation. There was considerable variation in absolute values of cAMP formation, for example, mean basal and 1mM carbachol-stimulated cAMP at 15 minutes were  $9.6 \pm 1.3$ , range 1.3-23.3 and  $20.9 \pm 2.7$ , range 6.6-57.8 pmols/mg protein ( $n=21$ ) respectively. Unless stated otherwise all subsequent values are expressed as % basal.

Carbachol (1mM) and muscarine (1mM) stimulated cAMP formation was reversed by atropine ( $1 \mu\text{M}$ ) (Table 3.2). Carbachol (1mM) stimulated cAMP formation was also inhibited by TFP ( $100 \mu\text{M}$ ). Direct activation of adenylyl cyclase with forskolin ( $10 \mu\text{M}$ ) caused a 33-fold stimulation of cAMP formation. This was increased to 56.9-fold in the presence of carbachol (1mM) with the increase being reversed with atropine ( $1 \mu\text{M}$ ) (Table 3.2). At supramaximal concentrations of carbachol (30mM), cAMP was also increased in an atropine ( $1 \mu\text{M}$ ) and TFP ( $100 \mu\text{M}$ ) reversible manner (Table 3.2).

In the continuous presence of carbachol and potassium, there was a biphasic increase in  $[\text{Ca}^{2+}]_i$  (Figure 3.2). The potassium peak ( $361.6 \pm 40.2$  nM) and plateau (measured at 2 minutes,  $181.5 \pm 19.6$  nM) were lower ( $p < 0.05$ ) than that produced by carbachol (peak= $697.6 \pm 64.0$  nM and plateau= $253.0 \pm 12.7$  nM) (Table 3.3). In the presence of nickel (2.5 mM), carbachol evoked increases in  $[\text{Ca}^{2+}]_i$  were significantly ( $p < 0.05$ ) reduced at basal and peak phases, with the plateau being essentially abolished. However, potassium increases in  $[\text{Ca}^{2+}]_i$  were abolished in the presence of nickel (2.5mM) (Table 3.3 and Figure 3.2), and the lower baseline probably results from  $\text{Ni}^{2+}$  quenching the Fura-2 fluorescence. In addition, the calcium channel subtypes which are blocked by nickel remain to be determined.

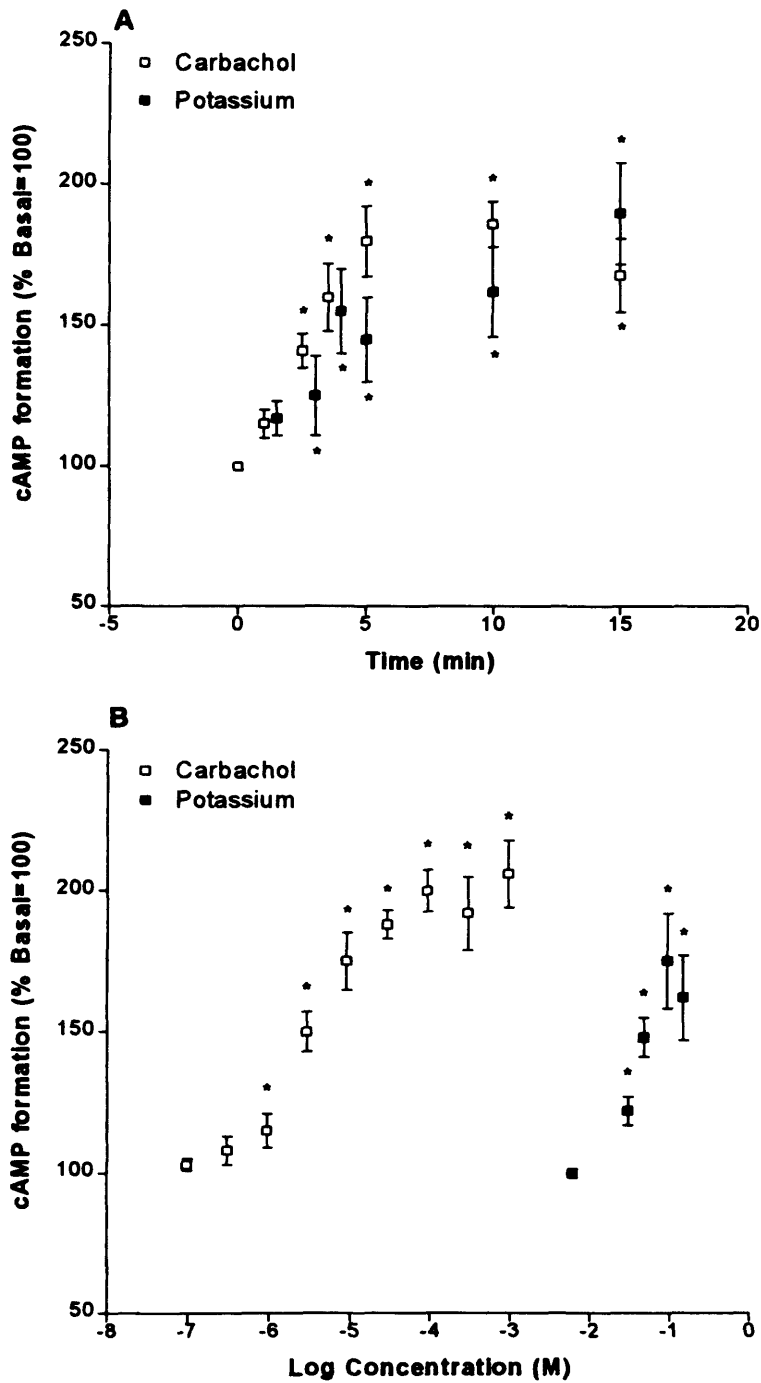


Figure 3.1. (□) Carbachol, and (■) potassium caused (A) a time, and (B) a dose related stimulation of cAMP formation in SH-SY5Y cells. Data are mean±SEM (N= 6-10). Dose response curves and time courses were significant ( $p < 0.05$ ) by ANOVA. \*Significantly ( $p < 0.05$ ) increased compared with basal levels.

Treatment	[cAMP] (% Basal=100)
Muscarine (1mM)	178.9±10.3*
+ Atropine (1µM)	79.8±4.6
Carbachol (1mM)	245.7±18.6*
+ Atropine (1µM)	79.8±5.5
+ TFP (100µM)	96.3±11.0
Forskolin (10µM)	3302.8±138.2*
+ Carbachol (1mM)	5691.4±113.7*#
+ Atropine (1µM)	3658.1±202.3*
Carbachol (30mM)	221.3±14.2*
+ Atropine (1µM)	138.4±14.8
+TFP (100µM)	108.2±11.8

Table 3.2. Muscarinic regulation of SH-SY5Y adenylyl cyclase was reversed by atropine and TFP (mean±SEM, N=3-6). \*Significantly (p<0.05) increased compared with basal. # Significantly (p<0.05) increased compared with forskolin.

In the presence of nickel (2.5mM, 10min) there was no affect on the initial (at 1 minute) carbachol mediated rise in cAMP but there was a significant (p<0.05) reduction in the latter (at 5 and 10 minute) cAMP levels (Figure 3.3). Nickel and TFP also inhibited potassium (100mM, 15 minutes) stimulated cAMP formation by 175±23.2 and 120±25.9% (ie. 75 and 20% below basal), respectively.

Carbachol (1mM) challenge under Ca<sup>2+</sup>-free conditions, stimulated cAMP formation with a significant (p<0.05) increase occurring from 1 minute. This amounted to an approximate 75% enhancement at 3 minutes. Further experiments are required to determine if this rise in cAMP plateaus at 3 minutes. However, subsequent Ca<sup>2+</sup> addition at 3 minutes was followed by a significant elevation in cAMP formation at 3.5

minutes ( $p < 0.05$ ), such that by 6 minutes the increase in cAMP formation was approximately two-fold basal (Figure 3.4).

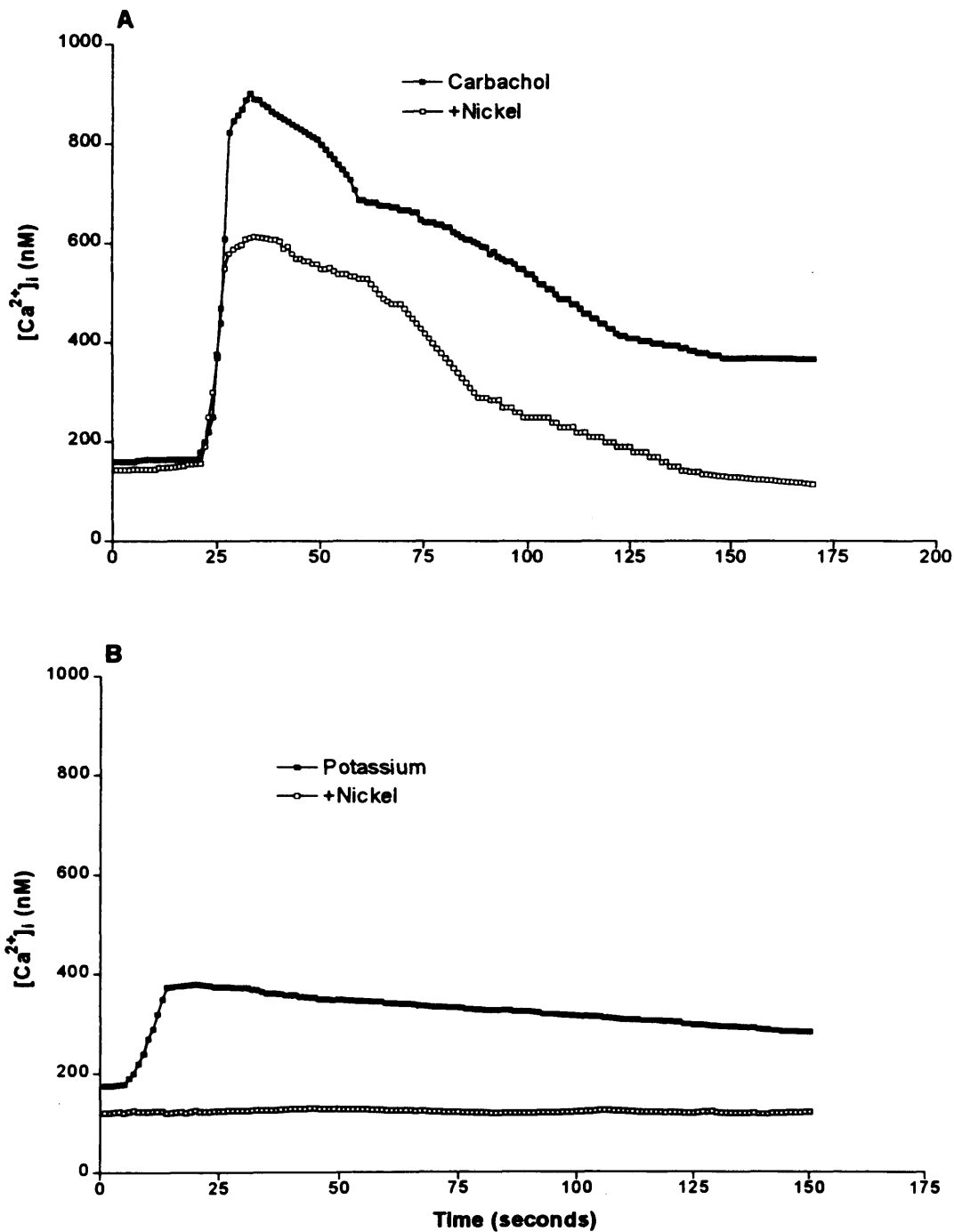


Figure 3.2. In the continued presence of (A, ■) 1mM carbachol, and (B, □) 100mM potassium caused a biphasic rise in  $[Ca^{2+}]_i$ . (□) In the presence of 2.5mM nickel the rise in  $[Ca^{2+}]_i$  was reduced for both stimuli. Data are a single experiment from 6 others.

Intracellular Ca <sup>2+</sup> concentration (nM)			
Treatment	Basal	Peak	Plateau
Carbachol (1mM)	118.4±9.2	697.6±64.0*	253.0±12.7*
+Nickel (2.5mM)	84.8±12.2#	498.0±35.2*#	131.2±12.5*#
Potassium (100mM)	104.0±10.6	351.6±40.2*	181.5±19.6*
+Nickel (2.5mM)	77.6±7.6 <sup>ξ</sup>	99.0±8.1 <sup>ξ</sup>	88.7±9.3 <sup>ξ</sup>

Table 3.3. Carbachol and potassium caused a biphasic increase in [Ca<sup>2+</sup>]<sub>i</sub> (mean±SEM, n=6 or 7). \*Significantly (p<0.05) increased compared with basal. #Significantly (p<0.05) decreased compared with carbachol. <sup>ξ</sup>Significantly (p<0.05) reduced compared with potassium.

In SH-SY5Y membranes, Ca<sup>2+</sup> (1.46μM), CaM (200nM) and forskolin (1μM) applied for 10 minutes caused a significant (p<0.05) stimulation of cAMP formation when compared with EGTA (0.1mM) (Table 3.4). Nominally Ca<sup>2+</sup>-free ATP regenerating buffer contained 1.46±0.02μM (n=4) Ca<sup>2+</sup>. Preincubation (5 minutes) with the PKC inhibitor Ro 318220 [Davis, P. D., et al, 1989] (10<sup>-5</sup>-10<sup>-10</sup>M) failed to significantly inhibit carbachol-stimulated cAMP formation (Figure 3.5). The same compound was successfully used in another study and so confirms the bioactivity of this compound [Smart et al, 1995].

The binding of [<sup>3</sup>H]-NMS was dose-dependent and saturable with K<sub>d</sub> and B<sub>max</sub> values calculated using Scatchard analysis yielding values of 0.3±0.01nM and 74.7±5.2 fmol/mg protein respectively (n=6) (Table 3.5 and figure 3.6). In the presence of nickel (2.5mM, in order to examine it's effects on [<sup>3</sup>H]NMS binding) K<sub>d</sub> and B<sub>max</sub> values were 1.4±0.3 and 64.2±9.2 fmol/mg protein respectively (figure 3.6). Atropine, nickel, TFP and IBMX all caused displacement of 0.2nM [<sup>3</sup>H]NMS, with similar IC<sub>50</sub> and K<sub>i</sub> values

using different incubation times and buffer types (table 3.5, figure 3.7A, B, C). Carbachol (1mM) stimulated cAMP formation experiments were performed in Krebs/HEPES buffer for 15 minutes. However, the concentration of nickel, TFP and IBMX required to inhibit 1mM carbachol stimulated cAMP formation by 50% would be several orders of magnitude above their  $K_i$  values for displacement of 0.2nM [ $^3$ H]NMS.

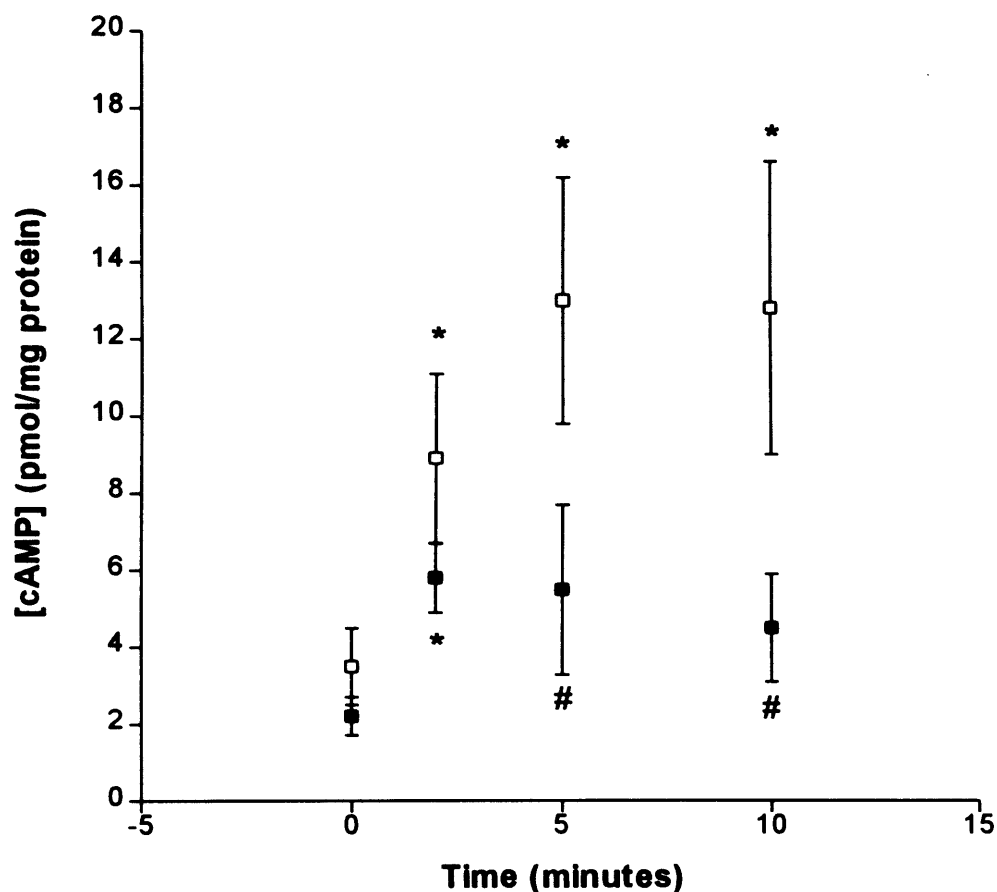


Figure 3.3. Time course for 1mM carbachol stimulated cAMP formation in the presence (■), or absence (□) of 2.5 mM nickel. Data are mean $\pm$ SEM (n=6). \*Significantly ( $p < 0.05$ , paired t-test) increased compared with basal. #Significantly ( $p < 0.05$ , paired t-test) decreased compared with carbachol.

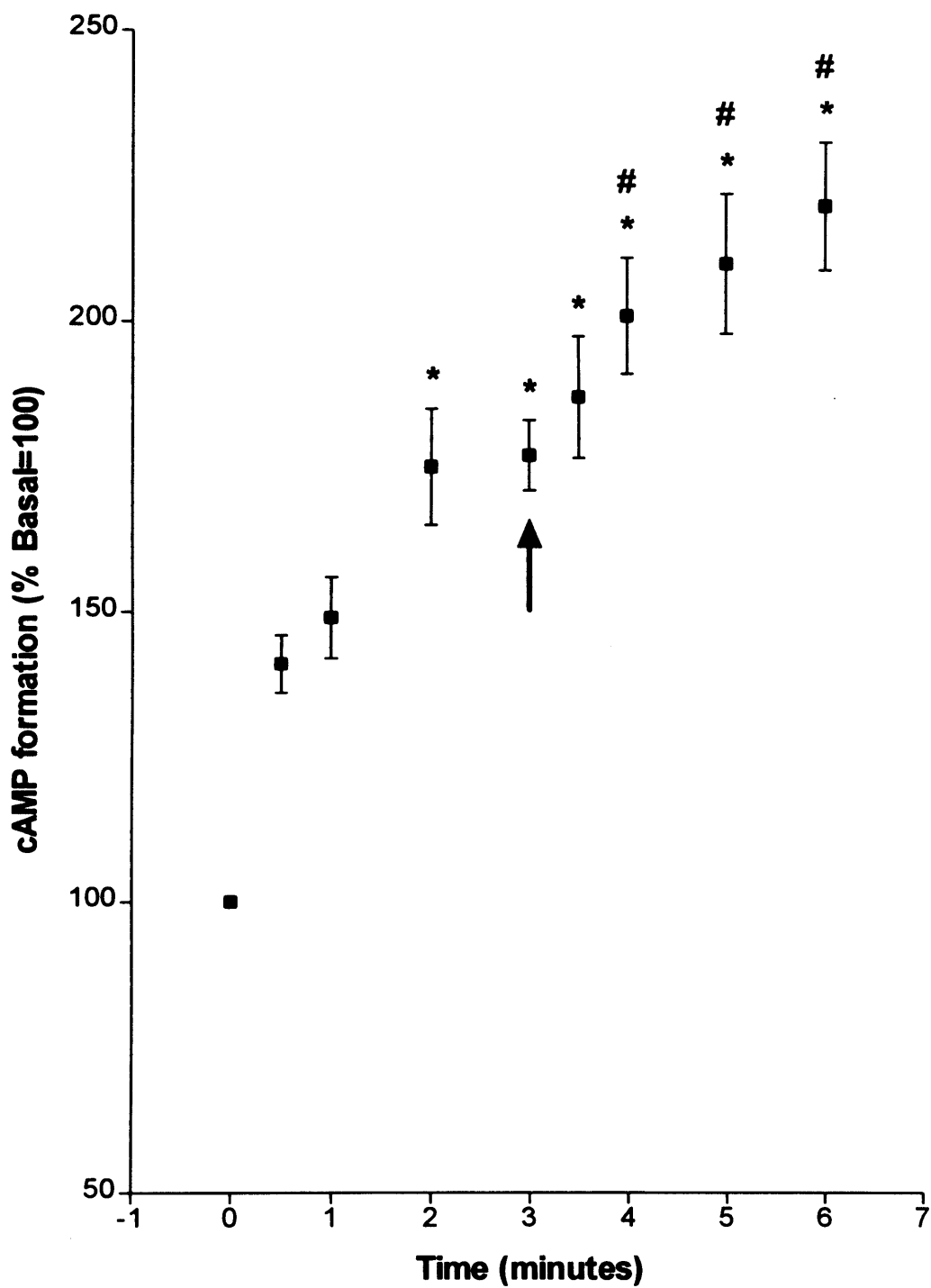


Figure 3.4. 1mM carbachol stimulated cAMP formation in the absence then presence (arrow) of 2.5mM  $\text{Ca}^{2+}$ . \*Significantly ( $p < 0.05$ , paired t-test) increased compared with basal. #Significantly ( $p < 0.05$ , paired t-test) increased compared with 3 minute time point. Data are mean  $\pm$  SEM ( $n=4$ )

Treatment for 10 mins	cAMP (pmol/mg protein)	Stimulation (% basal=100)
EGTA (100μM)	10.4±0.7	100
Ca <sup>2+</sup> (1.4μM)	12.7±0.7*	122.1
Ca <sup>2+</sup> +CaM (200nM)	14.2±0.7*	136.5
Forskolin (1μM)	45.1±4.3*	437.7

Table 3.4. Effects of EGTA, Calmodulin (CaM) and forskolin on adenylyl cyclase activity in SH-SY5Y membranes (mean±SEM, n=10 or 11). \*Significantly (p<0.05) increased compared with EGTA.

Buffer/ Incubation time	Displacer	pK <sub>i</sub>	Hill slope of displacement curves (figure 3.7)
Krebs/HEPES 60 minutes	Atropine	9.16±0.03 (0.7nM)	0.98±0.06
	TFP	5.40±0.22 (3.91µM)	1.56±0.29
	Ni <sup>2+</sup>	ND	ND
Krebs/HEPES 15 minutes	Atropine	9.12±0.02 (0.75nM)	0.94±0.03
	TFP	5.91±0.16 (1.23µM)	1.02±0.10
	Ni <sup>2+</sup>	3.22±0.03 (0.6mM)	1.06±0.08
	IBMX	3.22±0.03 (0.6mM)	0.52±0.03
HBS 15 minutes	Atropine	9.07±0.03 (0.86nM)	0.87±0.09
	TFP	5.59±0.29 (2.53µM)	1.10±0.12
	Ni <sup>2+</sup>	2.95±0.03 (1.11mM)	1.13±0.08

Table 3.5. Equilibrium dissociation constants of atropine, TFP, Ni<sup>2+</sup> and IBMX for the muscarinic receptor on SH-SY5Y cells, using different buffers and incubation times. Data are mean±SEM (n=3-9). ND=No Displacement.

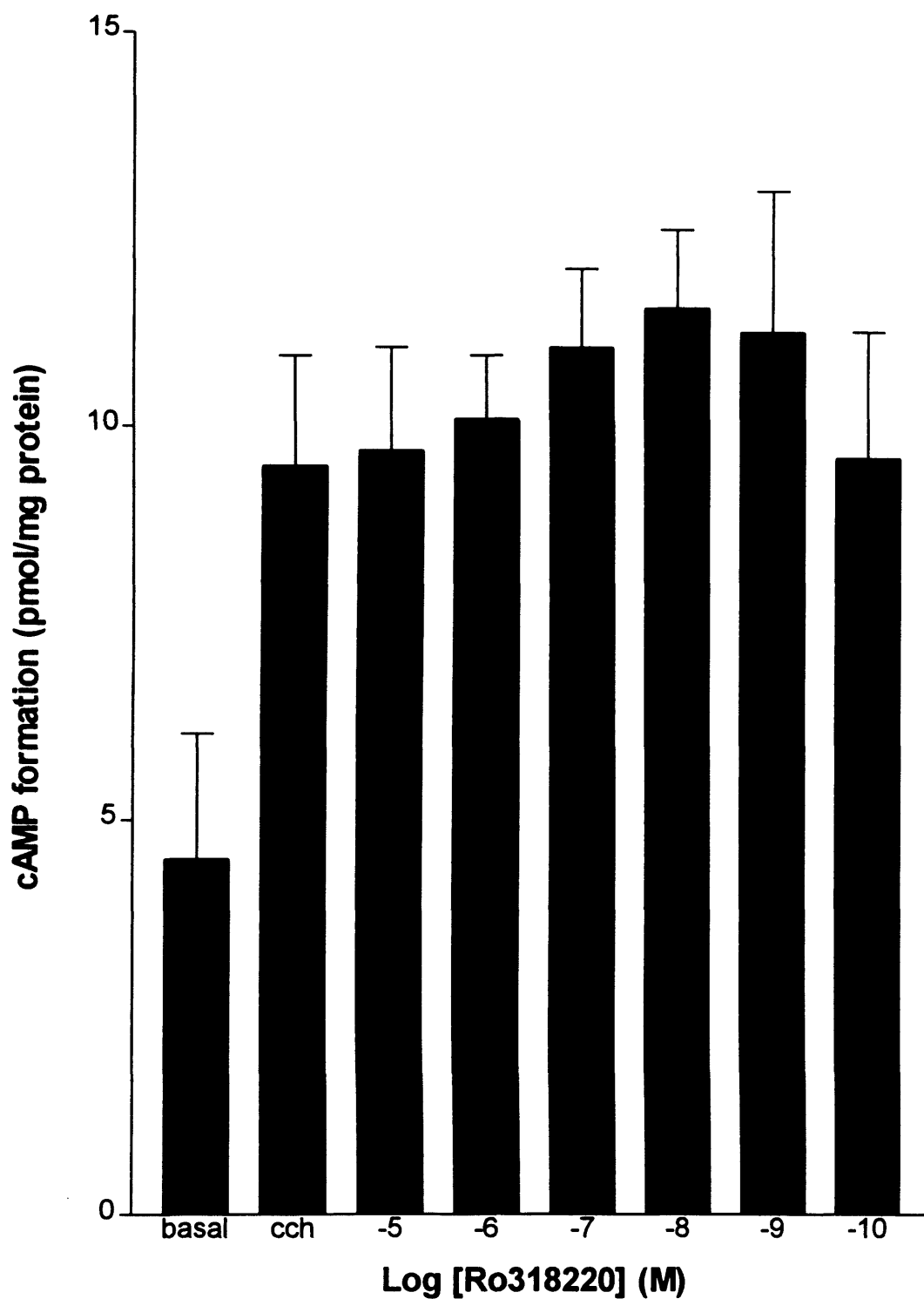


Figure 3.5. Preincubation (15 minutes) with the PKC inhibitor Ro318220 failed to significantly inhibit carbachol (1mM) stimulated cAMP formation. Data are mean $\pm$ SEM of 5 independent experiments. For positive control for the compound see [Smart et al, 1995].

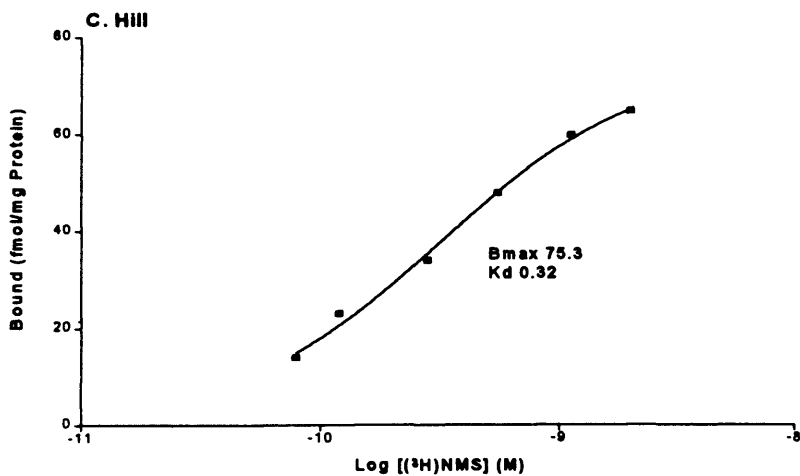
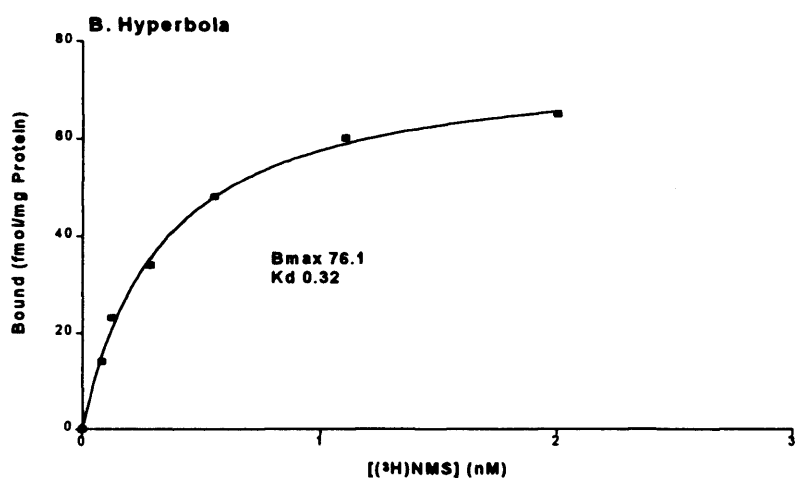
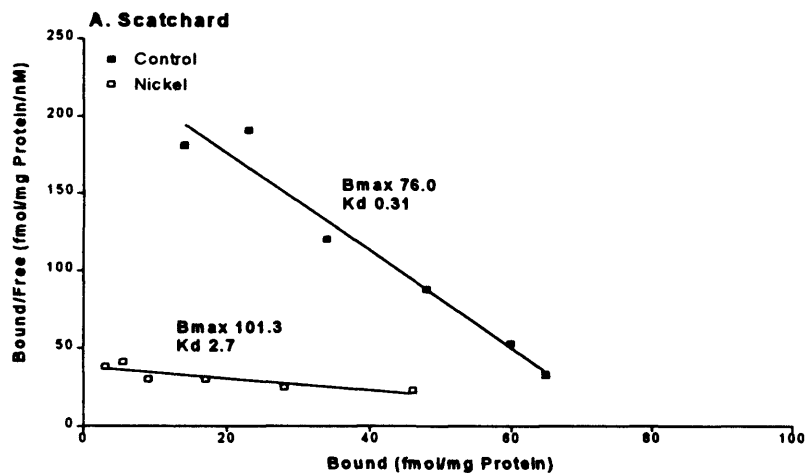


Figure 3.6 Saturation of [<sup>3</sup>H]-NMS binding to SH-SY5Y cells. Control (■) data is shown by Scatchard (A), Hyperbola (B) and Langmuir Hill (C) analyses. In the presence of nickel (□), the Scatchard analysis (A) shows a lower  $K_d$  value than control. Data are a single experiment from 3 others,  $B_{max}$ =fmol/mg Protein,  $K_d$ =nM.

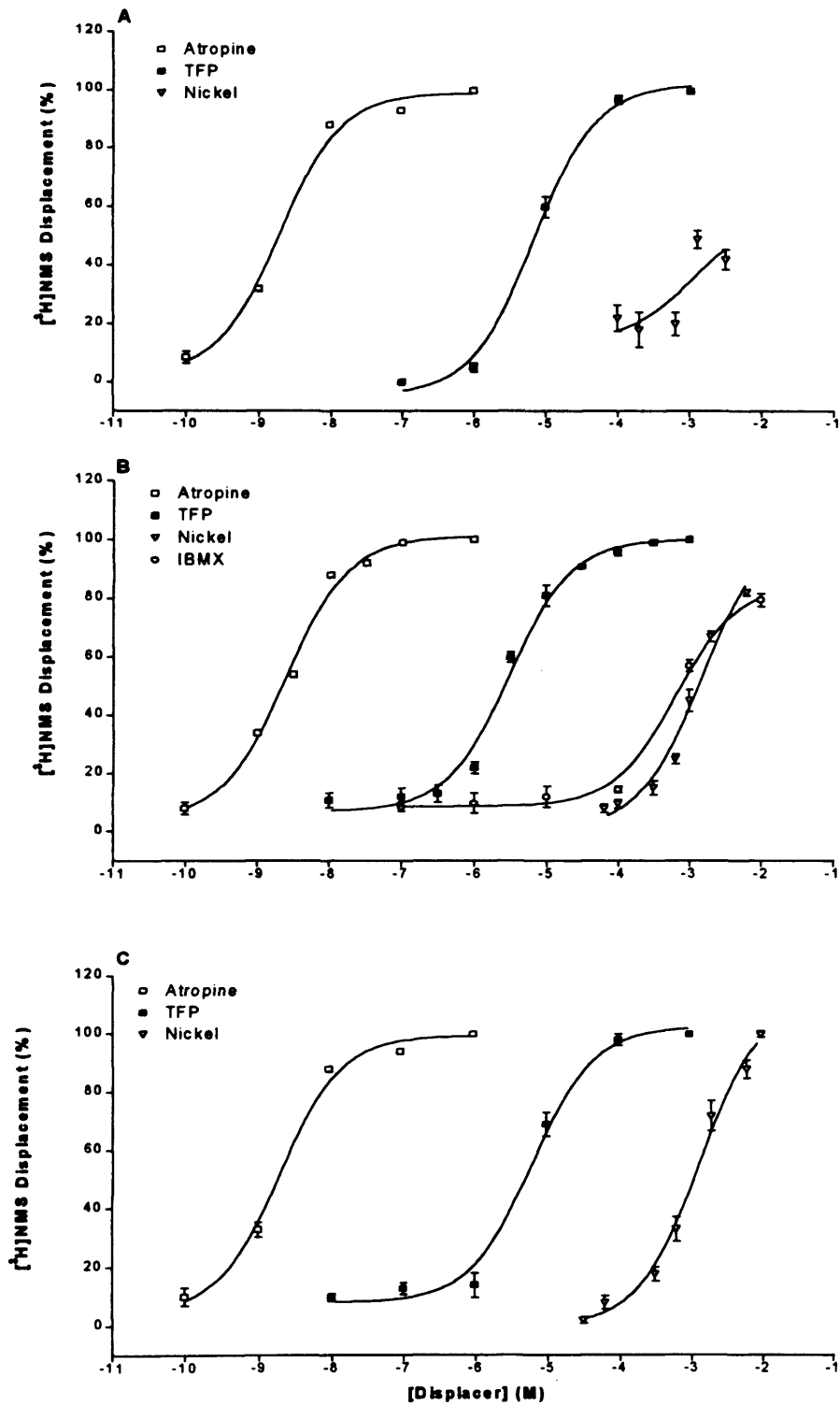


Figure 3.7. Dose related displacement of [ $^3$ H]-NMS (0.2nM) with atropine, TFP, nickel and IBMX in Krebs\HEPES for 60 minutes (A), Krebs\HEPES for 15 minutes (B) and HBS for 15 minutes (C). Data are mean $\pm$ SEM (n=3-8).

### **3.4. Discussion.**

In SH-SY5Y cells, cAMP formation was increased by potassium depolarization and by  $M_3$  muscarinic receptor stimulation, in a time and dose dependent manner. cAMP was increased approximately two fold over basal for both stimuli, with carbachol stimulated levels being consistent with two previous reports [Nakagawa-Yagi et al, 1991; Jansson et al, 1991]. Carbachol stimulated cAMP formation was inhibited by TFP, and appeared to be driven by both intra- and extra-cellular  $Ca^{2+}$ . Potassium stimulated cAMP formation was also reversed by TFP, and was dependent on extracellular  $Ca^{2+}$  alone.

Taken collectively, these data indicate the presence of a  $Ca^{2+}$ /CaM-sensitive isoform of adenylyl cyclase in SH-SY5Y cells, in that both agents (carbachol and potassium) also increased  $[Ca^{2+}]_i$ . Analysis of dose-response curves for carbachol stimulated rises in peak phase  $IP_3$  ( $EC_{50}$ , 9.4 $\mu$ M, [Smart et al, 1994]) and  $[Ca^{2+}]_i$  ( $EC_{50}$ , 7.6 $\mu$ M, [Lambert and Nahorski, 1990]) show close correlation with the  $EC_{50}$  for carbachol stimulated cAMP formation (5.37 $\mu$ M), suggesting a tight coupling of these events. A similar correlation for potassium stimulated cAMP formation ( $EC_{50}$  33.9mM) and potassium stimulated increases in  $[Ca^{2+}]_i$  ( $EC_{50}$ , 34.0mM, [Lambert et al, 1992]) was also observed.

There are conflicting reports on which pools of  $Ca^{2+}$  are required for stimulation of the  $Ca^{2+}$ -sensitive isoforms of adenylyl cyclase [Choi et al, 1992; Jansson et al, 1991; Baumgold et al, 1992; Cooper et al, 1994]. In SH-SY5Y cells, Jansson and co-workers showed that preincubation with the  $[Ca^{2+}]_i$  chelator BAPTA, caused inhibition of carbachol stimulated cAMP formation by approximately 50%, implying that intra and extracellular  $Ca^{2+}$  contributes equally to the muscarinic receptor stimulated cAMP formation [Jansson et al, 1991]. Yet, Baumgold and colleagues reported that carbachol stimulated cAMP formation in the parent SK-N-SH cell line was not affected by BAPTA pretreatment, implicating no role for intracellular  $Ca^{2+}$  in this response [Baumgold et al, 1992]. In addition, when adenylyl cyclase type 1 isoform was transfected into HEK 293, capacitative  $Ca^{2+}$  entry following thapsigargin pretreatment was sufficient to stimulate cAMP formation, indicating a role for  $[Ca^{2+}]_e$  [Cooper et al,

1994]. Yet, Choi et al. reported that BAPTA pretreatment abolished carbachol stimulated cAMP formation in HEK 293 cells transfected with type 1 adenylyl cyclase [Choi et al, 1992]. These later data imply that intracellular  $Ca^{2+}$  release is capable of activating type 1 adenylyl cyclase.

Molecular studies have revealed eight different isoforms of adenylyl cyclase which exist in a variety of different tissues [Iyengar, 1993]. The predominant isoform to be expressed in neuronal tissues is type 1 [Xia et al, 1993], although small amounts of mRNA for types 2, 3, 5, 7, and 8 have also been identified in brain [Cooper et al 1995]. Types 1, 3 and 8 can all be stimulated by  $Ca^{2+}$ /CaM [Bakalyar and Reed, 1990; Yoshimura and Cooper, 1992; Tang and Gilman, 1992.]. The identification of a phosphorylation site on the catalytic subunit of adenylyl cyclase [Yoshimasa et al, 1987] has revealed discrepancy in its regulation by PKC. PKC activation with phorbol esters stimulates cAMP formation in HEK 293 cells transfected with type 1 isoform of adenylyl cyclase [Choi et al, 1993.]. However, in cultured SH-SY5Y cells, Nakagawa-Yagi and colleagues have shown that incubation with the PKC inhibitor Calphostin C had no effect on forskolin stimulated cAMP formation, and that in the same study PKC activation with PMA-enhanced forskolin-stimulated cAMP formation [Nakagawa-Yagi et al, 1991]. However, in another study also using SH-SY5Y cells, PKC inhibition with staurosporine reduced carbachol stimulated cAMP formation by approximately 50% [Jansson et al, 1991]. Yet complete down regulation of PKC expression or PKC activation with PMA, had no overall effect on carbachol stimulated cAMP formation in the parent SK-N-SH cells [Baumgold and Fishman, 1988]. The reasons for these differences are unclear but the finding that PKC inhibition in this study using Ro 318220 had no effect on carbachol stimulated cAMP formation supports the exclusion of PKC.

Carbachol-stimulated cAMP formation in SH-SY5Y cells appeared to be due to  $Ca^{2+}$  release from intracellular stores and  $Ca^{2+}$  entry across the plasma membrane. In the presence of the calcium channel antagonist  $Ni^{2+}$ , the time course for carbachol stimulated cAMP formation was altered such that the later 5 and 10 minute time points were significantly decreased. The 1 minute time point was not changed. As  $Ni^{2+}$  is a

non-specific  $\text{Ca}^{2+}$  channel blocker, no information can be gained regarding which VOCC (L- or N- [Lambert et al, 1990]) is important in the cAMP response. However, the use of nickel clearly indicates a role for extracellular calcium in adenylyl cyclase activation in these cells. Moreover, nickel decreases carbachol stimulated  $\text{Ca}^{2+}$  entry, without affecting  $\text{IP}_3$  induced  $\text{Ca}^{2+}$  release [Lambert et al, 1990.]. These data indicate a role for both  $[\text{Ca}^{2+}]_i$  and  $[\text{Ca}^{2+}]_e$  in carbachol-stimulated cAMP formation. Further evidence for this is that in the absence of extracellular  $\text{Ca}^{2+}$ , carbachol was still able to stimulate cAMP formation, and when  $\text{Ca}^{2+}$  was replaced there was a further significant rise. In the absence of extracellular calcium, carbachol stimulated cAMP formation reached a plateau between 2 and 3 minutes, this was probably caused by a lack of cAMP breakdown resulting from phosphodiesterase inhibition with IBMX. Nevertheless, there remains a discrepancy in the  $\text{Ca}^{2+}$  and cAMP time courses to carbachol in that  $[\text{Ca}^{2+}]_i$  is increased more rapidly than cAMP, but this may reflect a lag required for  $\text{Ca}^{2+}$  and CaM complexes to form, prior to binding and activation of adenylyl cyclase.

When TFP, nickel and IBMX are used alongside muscarinic receptor driven processes there are problems with data interpretation due to their muscarinic antagonistic effects. However, in order to inhibit 1mM carbachol stimulated cAMP formation by 50%, TFP, nickel and IBMX concentrations need to be much higher than the  $K_i$  value obtained by displacement of 0.2nM  $[\text{}^3\text{H}]\text{NMS}$ . By using supramaximal concentrations of carbachol (30mM) the problems associated with significant muscarinic receptor displacement with TFP were overcome, such that 30mM carbachol stimulated cAMP formation was still abolished by 100 $\mu\text{M}$  TFP. In addition, potassium stimulated (receptor independent) cAMP formation was also reversed by 100 $\mu\text{M}$  TFP, giving strong evidence of a role for CaM. Overall the data does not support a role for PKC in carbachol stimulated cAMP formation.

These data strongly suggest that a  $\text{Ca}^{2+}$ /CaM-sensitive isoform of adenylyl cyclase is expressed in SH-SY5Y cells. Indeed, use of well washed SH-SY5Y membranes revealed that basal turnover of cAMP formation was  $\text{Ca}^{2+}$  dependent, in that addition of 100 $\mu\text{M}$  EGTA (to reduce basal  $\text{Ca}^{2+}$  from 1.4 $\mu\text{M}$ ) inhibited cAMP formation. In the

presence of 200nM CaM, cAMP formation was increased, this observation again suggests the presence of a Ca<sup>2+</sup>/CaM-sensitive isoform of adenylyl cyclase. Using western blotting techniques, Gilman and colleagues have shown that SH-SY5Y cells express detectable levels of type 1 adenylyl cyclase only [Tang and Gilman, personal communication, University Department of Pharmacology, Dallas, Texas, USA] in keeping with the neuronal origin of SH-SY5Y cells. In summary, the data show that in SH-SY5Y cells extracellular Ca<sup>2+</sup> entry and intracellular Ca<sup>2+</sup> release are both able to regulate cAMP formation, and indicate the presence of type 1 adenylyl cyclase.

**CHAPTER 4. CHARACTERISATION OF ENDOGENOUS  $\mu$ - AND  $\delta$ -  
OPIOID RECEPTORS IN SH-SY5Y AND NG108-15 CELLS.**

## **4.1 Introduction.**

Pert and Snyder (1973), first demonstrated neuronal opioid binding sites using the opioid antagonist, naloxone. Since then opioid pharmacology has advanced rapidly (see Chapter 1). It is now generally accepted that three major subtypes of opioid receptors ( $\mu$ ,  $\delta$  and  $\kappa$ ) exist, all of which have been cloned [Evans et al, 1992; Chen et al, 1993; Yatsuda et al, 1993]. These receptors can be further classified by the differential effects of agonists and antagonists into subgroups ( $\mu_1, 2$ ;  $\delta_1, 2$ ;  $\kappa_1, 2, 3$ ), however, molecular cloning techniques have been unable to distinguish between the pharmacologically classified opioid receptor subtypes (see Chapter 1). The receptors differ in their tissue distribution, structural homology and function. However all have the ability to produce analgesia, which is achieved at a cellular level by closing of neuronal VOCC's [Seward et al, 1991] and increased potassium conductance [North et al, 1987]. These events lead to a reduction in neurotransmission [Lambert, 1993]. The three subtypes all couple to adenylyl cyclase via  $G_i$ , and recent studies have shown that they also have the ability to couple to  $G_s$  [Crain and Shen, 1990], open calcium channels [Smart et al, 1994], and activate PLC [Smart et al 1995].

The discovery of the endogenous opioid peptide ligands Met- and Leu-enkephalin [Hughes, 1975; Hughes et al, 1975],  $\beta$ -endorphin [Bradbury et al, 1976] and dynorphin [Goldstein et al, 1979] marked an important step in our understanding of opioid pharmacology. The more recent discovery of endomorphin 1 and 2 as the natural ligands of the  $\mu$ -opioid receptor has also contributed to this understanding [Zadina et al, 1997]. The synthesis of agonists and antagonists for specific opioid receptor subtypes has allowed opioid pharmacology to evolve. The most widely used ligands for the subtypes of opioid receptors are shown in chapter 1.

Clonal cell lines have been widely used in the study of opioid receptors and the opioid receptor complement of some commonly used cell lines is illustrated in Table 4.1.

Cell Line	Opioid Receptor		
	$\mu$	$\delta$	$\kappa$
BE(2)-C	$\mu$	$\delta$	$\kappa$
SK-N-SH	$\mu$		
SH-SY5Y	$\mu$	$\delta$	ORL-1/ $\kappa_3$
NG108-15		$\delta$	ORL-1
7315c	$\mu$		
PC12		$\delta$	

Table 4.1. An example of commonly used cell lines for the study of opioid receptor subtypes [see Standifer et al, 1994; Kazmi and Mishra, 1987; Pei et al, 1996; Evans et al, 1992; Cote et al, 1993; Abood and Tao, 1995, Conner and Henderson, 1996; Cheng et al, 1996].

NG108-15 neuroblastoma x glioma hybrid cells express a homogeneous population of  $\delta$ -opioid receptors, and have been proposed as a useful model for the study of  $\delta$ -receptor [Law et al, 1985]. In contrast, SH-SY5Y human neuroblastoma cells have been shown to express predominantly  $\mu$ -opioid receptors [Yu et al, 1986], however low levels of  $\delta$ - and  $\kappa$ -opioid receptor binding sites have also been detected [Yu et al, 1986]. Recent studies have also shown endogenous ORL-1 receptors on SH-SY5Y and NG108-15 cells [Pei et al, 1996].

In this chapter, the SH-SY5Y cell line will be used to study predominantly  $\mu$ -opioid receptor binding and functional inhibition of adenylyl cyclase elicited by fentanyl and DAMGO. In addition, NG108-15 cells will be used to demonstrate  $\delta$ -opioid binding and inhibition of adenylyl cyclase using DPDPE and DADLE. The results of these studies will allow comparison of the predominantly  $\mu$ -(SH-SY5Y) and  $\delta$ -(NG108-15) opioid receptor mediated binding and inhibition of adenylyl cyclase. The effect of nociceptin on AC activity will also be examined using SH-SY5Y cells.

## **4.2 Methods.**

For details of chemicals, tissue culture, membrane preparation, cAMP measurement and data analysis the reader is directed to chapter 2.

### **[<sup>3</sup>H]-DPN binding protocols**

All binding assays were performed in 1ml volumes of well washed (2 x 50ml/10-30mg protein) cell membranes (approx. 200µg/tube) using [<sup>3</sup>H]-DPN at 20°C in Tris-HCl (pH7.4) buffer. In displacement and saturation experiments bound and free [<sup>3</sup>H]-DPN were separated by rapid vacuum filtration using a 24 position Brandel cell harvester onto Whatman GF/B filters and washed with 2 x 5ml of ice cold buffer. In all experiments filters were placed into scintillation vial inserts and covered with 4ml of Optiphase Safe. Radioactivity was extracted overnight.

#### **(i) Saturation.**

Various [<sup>3</sup>H]-DPN concentrations (0.1-3nM) were used for saturation experiments. The binding of [<sup>3</sup>H]-DPN was studied for 60 minutes (20°C) in Tris-HCl (pH7.4).  $B_{max}$  and  $K_d$  values were obtained using Scatchard analysis (see chapter 2).

#### **(ii) Displacement**

For displacement studies a fixed concentration of [<sup>3</sup>H]-DPN (0.2nM) was used throughout and non-specific binding was determined in the presence of Naloxone (1 µM).

## **4.3 Results.**

### **4.3.1. Saturation**

The binding of [<sup>3</sup>H]-DPN was dose dependent and saturable in both SH-SY5Y and NG108-15 cells yielding  $B_{max}$  and  $K_d$  values shown below (table 4.2 for mean data

from Scatchard analysis, figure 4.1 for representative data using all analysis methods).

Cell Type	n	K <sub>d</sub> (nM)	B <sub>max</sub> (fmol/mg Protein)
SH-SY5Y	5	0.16±0.02	98.4±6.5
NG108-15	3	0.20±0.01	280.9±14.4

Table 4.2. Saturation of [<sup>3</sup>H]-DPN in SH-SY5Y and NG108-15 cells. At the radioligand K<sub>d</sub>, specific binding was greater than 90%.

#### 4.3.2. Displacement

The μ-opioid preferring ligands fentanyl and DAMGO and the δ-opioids DPDPE and DADLE displaced [<sup>3</sup>H]-DPN (0.2nM approx) in a dose dependent manner in SH-SY5Y and NG108-15 cell membranes respectively (figure 4.2A and B). The curves were analysed assuming the presence of two sites. This two site model revealed different proportions of low and high affinity

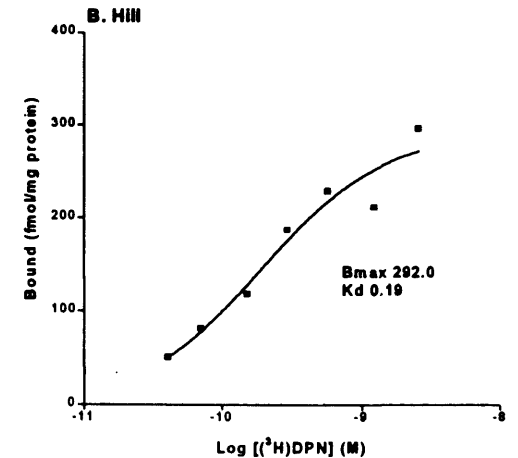
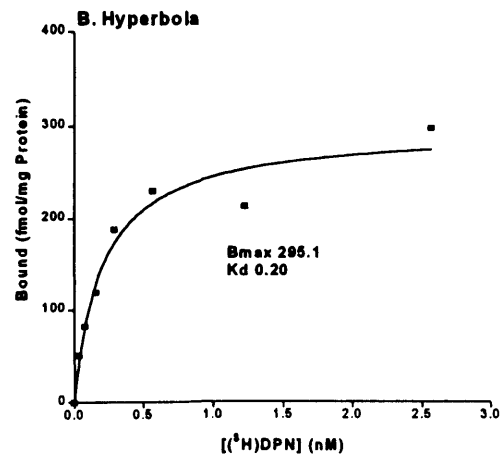
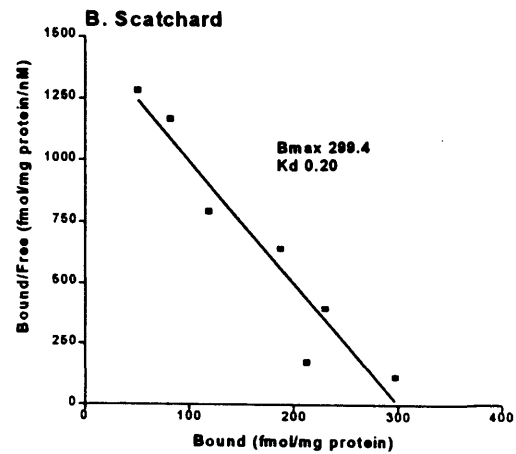
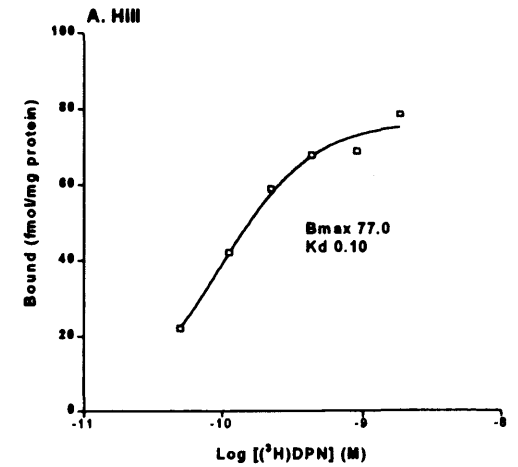
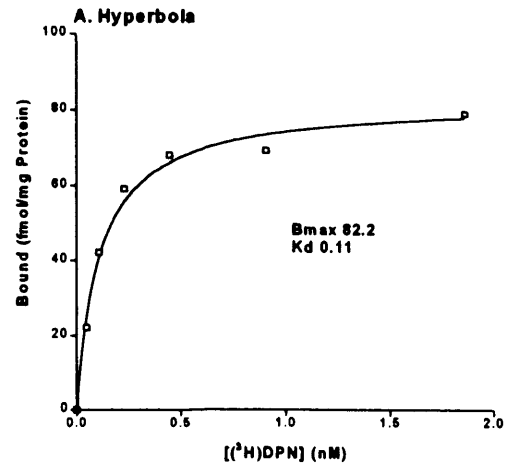
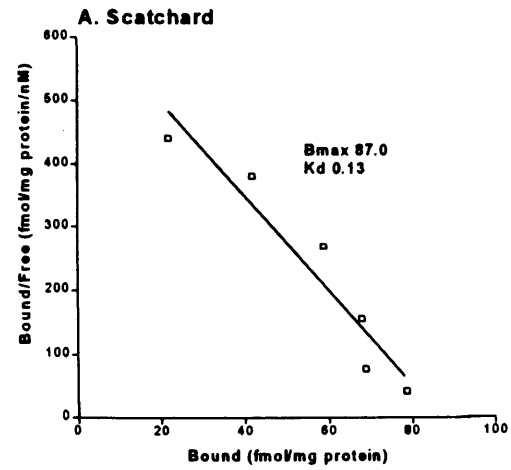


Figure 4.1. Scatchard, Hyperbolae and Langmuir-Hill plots of saturable specific [<sup>3</sup>H]-DPN binding to SH-SY5Y (A) and NG108-15 (B) cell membranes. Data are from a single representative experiment in each cell type of 2 others, Bmax=fmol/mg protein: Kd=nM.

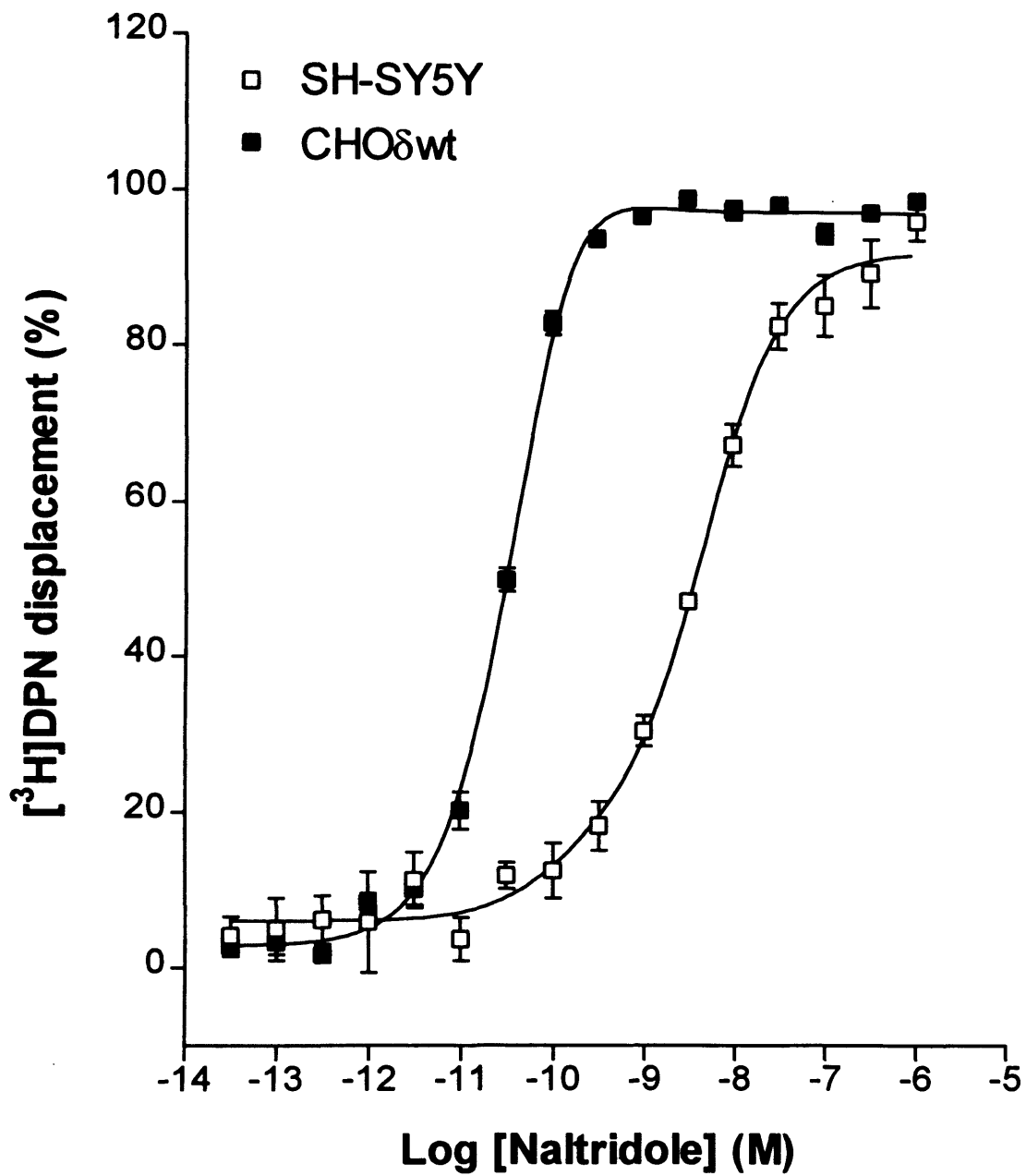


Figure 4.2. Dose dependent inhibition of [<sup>3</sup>H]DPN binding with the highly  $\delta$ -selective antagonist naltridole in SH-SY5Y and CHO $\delta$ wt cells. Data are mean $\pm$ SEM of 3 (CHO) or mean $\pm$ range of 2 (SH-SY5Y) independent experiments.

Cell Type	Opioid	pK <sub>i</sub> H(nM)	pK <sub>i</sub> L(nM)	H(%)	L(%)
SH-SY5Y	Fentanyl	9.99±0.22(0.1)	7.05±0.09(87.7)	25.3±5.6	74.7±5.6
	DAMGO	9.53±0.29(0.29)	6.16±0.1(691)	30.3±2.5	69.7±2.5
	Naltrin.	11.4±1.4(0.003)	8.75±0.12(1.8)	20.9±10.6	79.1±10.6
NG108	DPDPE	9.88±0.13(0.13)	8.91±0.34(1.22)	32.2±10.7	67.8±10.7
	DADLE	9.72±0.27(0.19)	8.03±0.57(9.22)	48.9±10.4	51.1±10.4

Table 4.3. High and low affinity states of the  $\mu$ - and  $\delta$ -opioid receptor revealed by displacement of [<sup>3</sup>H]-DPN using the appropriate opioid agonist (n=3-6, except naltrindole in SH-SY5Y cells where data are mean±range of 2 experiments).

The SH-SY5Y cells used in this study were shown to express 20.9%  $\delta$ -opioid receptors, as revealed by naltrindole displacement of [<sup>3</sup>H]DPN binding (figure 4.2, table 4.3), however this value is slightly misleading (overestimated) as another experiment predicted 0 high affinity sites although the Hill slope was less than 1. In this experiment CHO cells expressing the  $\delta$ -opioid receptor (see Chapter 5) were also examined to determine the K<sub>i</sub> for naltrindole at  $\delta$ -receptors. Naltrindole displaced [<sup>3</sup>H]DPN with a Hill slope of 1.3±0.1 in CHO $\delta$ wt cell membranes compared to 0.7±0.1 in SH-SY5Y cells. The CHO $\delta$ wt displacement curve could only be modeled to a single site which had a pK<sub>i</sub> value of 11.0±0.02, very similar to the high affinity value from SH-SY5Y cells (11.4, table 4.3). These data show that approximately 80% of opioid receptors on SH-SY5Y cells are not- $\delta$ . The predominant subtype expressed on SH-SY5Y cells is the  $\mu$ -opioid receptor [Yu et al, 1986], however the proportion of  $\kappa$ -receptors remains to be determined.

The high affinity G-protein coupled opioid receptors in SH-SY5Y cells displayed a similar affinity for fentanyl and DAMGO (table 4.3, figure 4.3). The  $\delta$ -opioid receptor in NG108-15 cells also displayed a similar high affinity for DPDPE and

DADLE (table 4.3). The low affinity binding sites in SH-SY5Y cells could be  $\delta$ - or  $\kappa$ -opioid receptor sites. Fentanyl was approximately 5.5 fold more potent at revealing low affinity (free) opioid receptors than DAMGO in SH-SY5Y cells. Moreover, when corrected for radioligand concentration, DPDPE was approximately 10 fold more effective than DADLE for demonstrating low affinity receptors in NG108-15 cells. In SH-SY5Y cells, the analysis predicted that approximately 25-30% of the opioid receptors were in the high affinity state in the presence of fentanyl and DAMGO, whereas in NG108-15 cells, the same analysis predicted that there was approximately 32-48% high affinity receptors with DPDPE and DADLE.

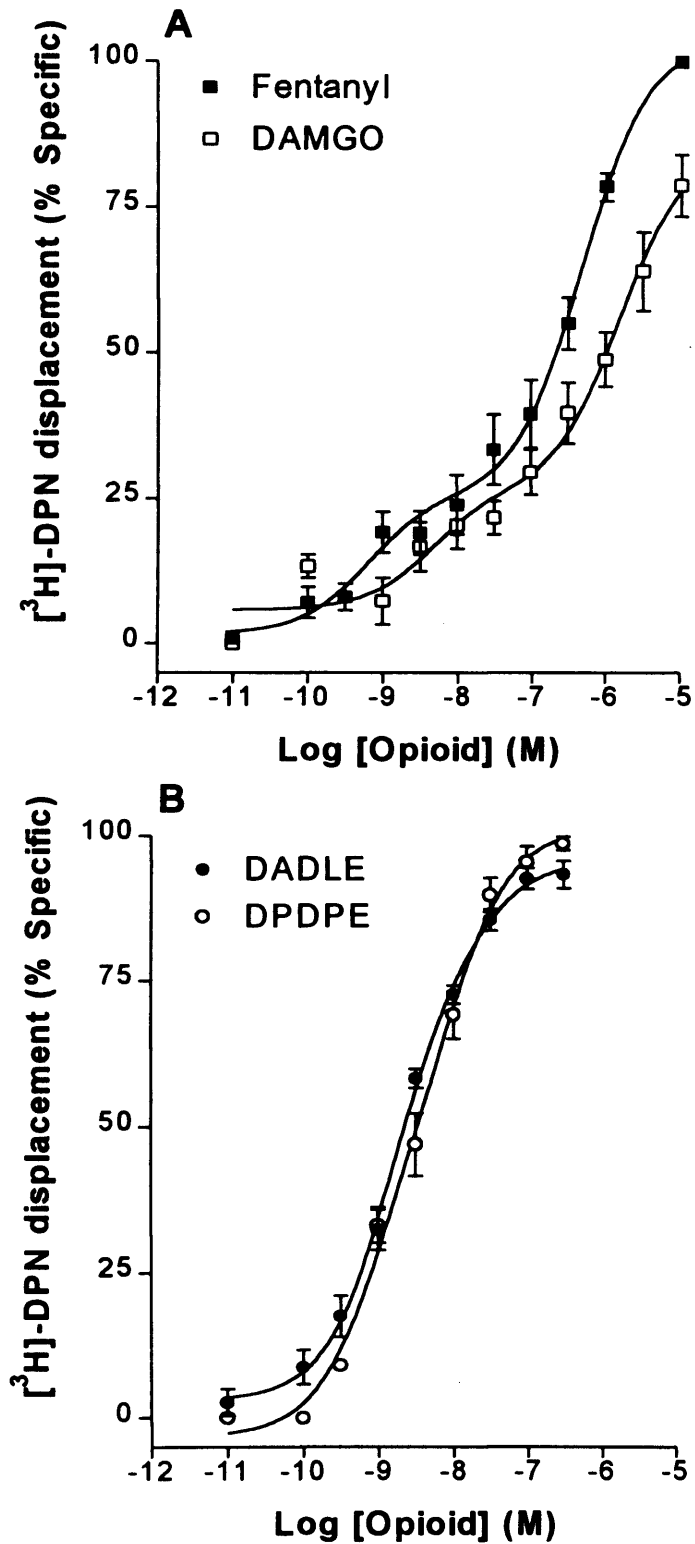


Figure 4.3. Displacement of  $^3\text{H}$ -DPN by Fentanyl, DAMGO (SH-SY5Y, A) and DPDPE, DADLE (NG108-15, B).

### 4.3.3. Inhibition of forskolin stimulated cAMP formation.

Fentanyl, DAMGO (SH-SY5Y) and DPDPE, DADLE (NG108-15) caused a dose dependent inhibition of forskolin stimulated cAMP formation (Table 4.4 and figure 4.4). Nociceptin also caused a dose dependent inhibition of forskolin stimulated cAMP formation in SH-SY5Y cells (Table 4.4 and figure 4.5). In addition, forskolin stimulated cAMP formation was inhibited approximately 60% by all opioids in both cell lines (Table 4.4).

Opioid	SH-SY5Y cells		NG108-15 cells	
	pIC <sub>50</sub> (nM)	I <sub>max</sub> (%)	pIC <sub>50</sub> (nM)	I <sub>max</sub> (%)
Fentanyl	7.75±0.16(17.7)	56.3±5.3		
DAMGO	6.69±0.21(202)	52.9±3.6		
DPDPE			9.11±0.11(0.78)	65.3±2.5
DADLE			9.27±0.06(0.53)	58.7±5.7
Nociceptin	7.14±0.14(72)	47.4±5.8		

Table 4.4. Inhibition of forskolin stimulated cAMP formation by opioids in SH-SY5Y and NG108-15 cells (n=3-8).

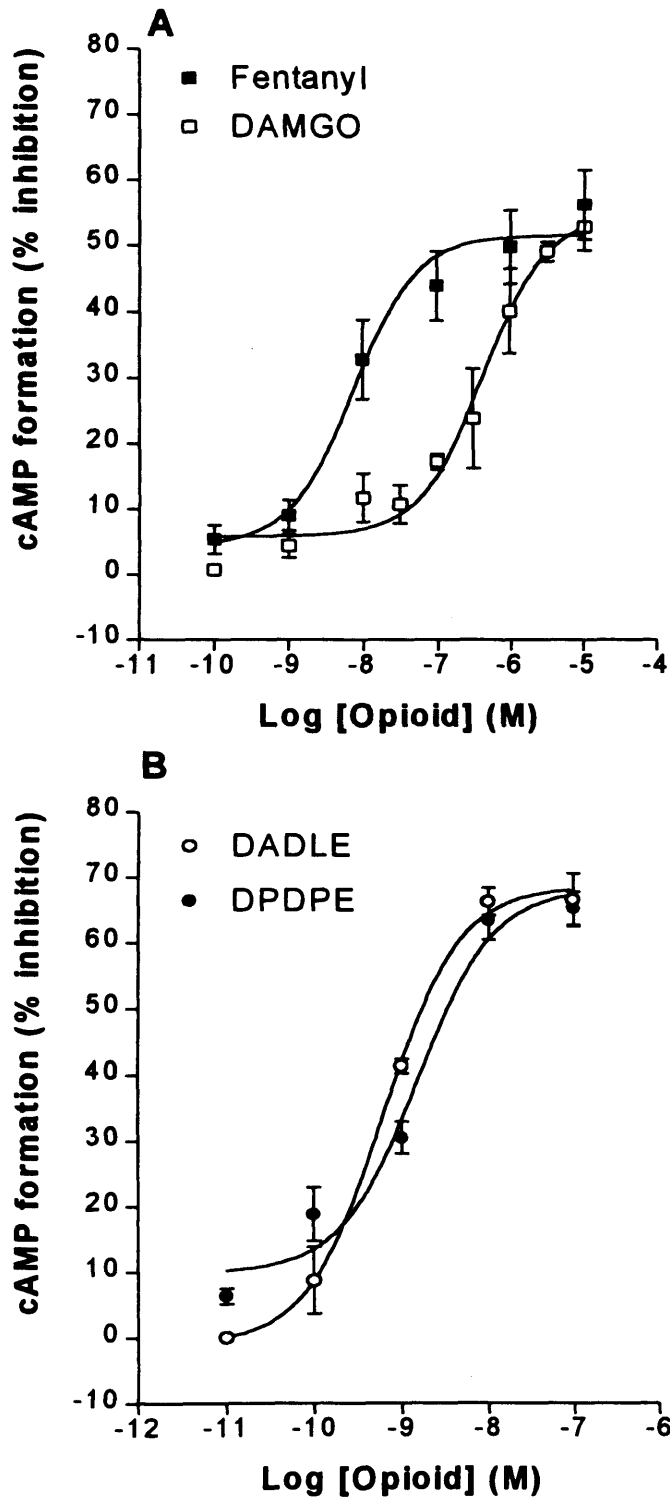


Figure 4.4. Dose dependent inhibition of forskolin stimulated cAMP formation by fentanyl, DAMGO (SH-SY5Y cells, A) and DPDPE, DADLE (NG108-15 cells, B).(n=3-8)

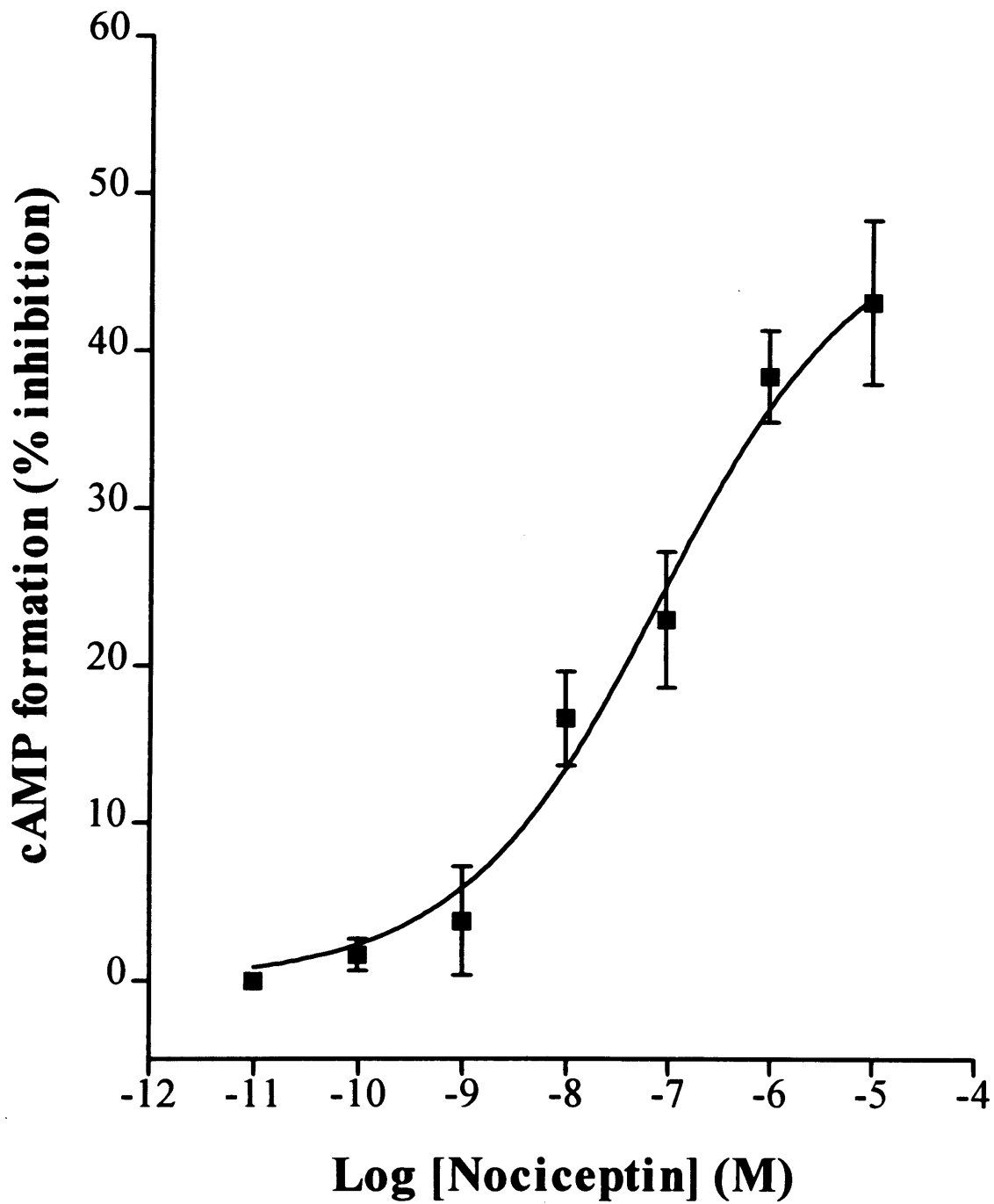


Figure 4.5. Nociceptin caused a dose dependent inhibition of forskolin (1 $\mu$ M) stimulated cAMP formation in SH-SY5Y cells. Data are mean $\pm$ SEM of 8 experiments.

#### **4.4 Discussion**

SH-SY5Y cells express predominantly  $\mu$ -opioid receptors [Yu et al, 1986] whereas NG108-15 cells express a homogeneous population of  $\delta$ -opioid receptors [Chang and Cuatrecasas, 1979]. In SH-SY5Y cells, the proportion of  $\delta$ -opioid receptors was predicted to be less than 20% from naltrindole displacement studies. This value is slightly less than 4 $\mu$ :1 $\delta$  predicted by Yu et al [1986]. It has been reported that in whole SH-SY5Y cells, [<sup>3</sup>H]-DPN bound to opioid receptors with a K<sub>d</sub> value of 0.17nM [Lambert et al, 1993]. In another study [<sup>3</sup>H]-DPN bound to  $\delta$ -opioid receptors in NG108-15 cell membranes with an affinity of 0.73nM [Polastron et al, 1992]. These reports are consistent with [<sup>3</sup>H]-DPN having a slightly higher affinity for  $\mu$ - over  $\delta$ -opioid receptors. However, the results in this study show that [<sup>3</sup>H]-DPN bound with a similar high affinity to both  $\mu$ -opioid (SH-SY5Y) and  $\delta$ -opioid receptors (NG108-15). The reason for these conflicting reports of [<sup>3</sup>H]-DPN affinity for  $\mu$ - and  $\delta$ -opioid receptors are unclear.

There was three fold less [<sup>3</sup>H]-DPN binding sites on SH-SY5Y than on NG108-15 cell membranes. Receptor numbers in a single cloned population of cells can vary quite considerably, this is reflected in the previous reports of B<sub>max</sub> values for SH-SY5Y cells. For example, in our hands we reported that the amount of binding sites in whole SH-SY5Y cells was 167 fmols/mg protein [Lambert et al, 1993], whereas other workers have detected 43 [Yabaluri and Medzihradski, 1995], 350 [Yu et al, 1986] and 60 fmols/mg protein [Toll, 1990]. Using NG108-15 cell membranes under similar assay conditions, Polastron and co-workers (1992) reported that the maximum number of [<sup>3</sup>H]-DPN binding sites was 431 fmol/mg. This is significantly higher than the number reported here. These results suggest that the number, and/or subtype of opioid binding sites may fluctuate between different SH-SY5Y and NG108-15 cell batches. This phenomenon may be as a result of different tissue culture or binding assay conditions between the laboratories.

From displacement studies using SH-SY5Y cell membranes, fentanyl and DAMGO reveal opioid receptors in both high and low affinity states. Both opioids having a similar affinity for the G-protein coupled receptor ( $K_iH$ ). However, fentanyl displays a 5.5 fold greater affinity than DAMGO for the G-protein uncoupled receptor. Both opioid agonists showed that approximately 30% of the opioid receptors in SH-SY5Y cell membranes existed in the high affinity G-protein coupled state, although this may depend on the preparation technique. In NG108-15 cell membranes DADLE and DPDPE both displaced pre-labeled  $\delta$ -opioid receptors with similar affinity for both high and low affinity receptors. This may be due to the fact that the  $\delta$ -opioid receptor in NG108-15 cells is strongly pre-coupled to G-protein [Polastron et al, 1992], or be as a result of  $Na^+$  on opioid receptor binding [Carrol et al, 1984].

In SH-SY5Y cells, fentanyl caused an inhibition of forskolin stimulated cAMP formation which was 4 fold more potent than that caused by DAMGO. The fentanyl displacement curve reveals high affinity ( $K_iH$ ) G-protein coupled receptors at sub-nanomolar concentration of agonist, however the concentration of fentanyl required to inhibit adenylyl cyclase by 50% was one order of magnitude higher. In addition, DAMGO displayed sub-nanomolar affinity for G-protein coupled high affinity opioid receptors, whereas the  $IC_{50}$  for DAMGO mediated inhibition of cAMP formation was 202nM. At a concentration of approximately 10nM fentanyl or DAMGO all the opioid receptors in SH-SY5Y cells are in the high affinity G-protein coupled state which allows  $G_i\text{-}\alpha$  to inhibit adenylyl cyclase, yet only half of the maximal adenylyl cyclase inhibition is achieved. This effect has previously been reported with opioid receptors in brain membranes [Nijssen et al, 1992]. In their study, Nijssen et al concluded that the most likely explanation was that the low affinity sites were able to mediate adenylyl cyclase inhibition. This is supported by observations of electrophysiological experiments on cell firing rates, where micromolar opioid was required in order to achieve a maximal response [Werz and Macdonald, 1983; North et al, 1987; Gross et al, 1990].

In addition, lack of correlation of high affinity opioid receptors and functional potency has also been reported by several other groups [Liu-Chen et al, 1995; Yalbaluri and Medzihradsky, 1997; Carroll et al, 1984; Carroll et al, 1988]. These workers have examined the effects of different incubation conditions on opioid receptor binding, especially  $\text{Na}^+$  and GTP requirement. It was shown that the potency of DAMGO inhibition of forskolin stimulated cAMP formation was reduced by approximately 100mM extracellular  $\text{Na}^+$  [Yalbaluri and Medzihradsky, 1997] and that  $\text{Na}^+$  enhanced the binding of opioid antagonists but reduced that of agonists [Fischel and Medzihradsky, 1981; Liu-Chen et al, 1995]. Carroll et al (1988) concluded that it was indeed the low affinity receptor which is functionally relevant, and that if affinities calculated from binding experiments are to reflect physiological interactions, then such experiments should be performed in the presence of  $\text{Na}^+$  and GTP. Therefore the lack of correlation between agonist binding affinity and functional inhibition of adenylyl cyclase presented here (performed in the presence of 140mM  $\text{Na}^+$ ) could be a result of different assay buffers used in each experiment.

In contrast, DADLE and DPDPE in NG108-15 cells were more potent, both had the ability to cause 50% inhibition of adenylyl cyclase at concentrations of 0.5 and 1nM respectively. In displacement studies, the  $K_i$  for these opioids was only 2-3 fold lower than the  $\text{IC}_{50}$  for the inhibition of adenylyl cyclase. These findings suggest that in NG108-15 cells, the  $\delta$ -opioid induced inhibition of adenylyl cyclase is mainly mediated by the high affinity G-protein coupled receptors that appear to be strongly pre-coupled.

The 140mM  $\text{Na}^+$  included in the cAMP buffer had no effect on agonist binding to  $\delta$ -opioid receptors. Indeed, the effects of  $\text{Na}^+$  on  $\mu$ -,  $\delta$ -, and  $\kappa$ -opioid receptor binding differs for each subtype,  $\text{Na}^+$  having less effect on  $\delta$ - and  $\kappa$ -agonist binding [Werling et al, 1986].

Nociceptin inhibits AC in SH-SY5Y cells with potency similar to the reported inhibition of N-Type VOCC in these cells [Connor et al, 1996] these data strongly suggests the presence of ORL-1 receptors on SH-SY5Y cells.

In summary, these results show that the different opioid receptor subtypes in SH-SY5Y (predominantly  $\mu$ -) and NG108-15 ( $\delta$ -) cells both bind to their selective ligands with multiple affinity states and all couple negatively to adenylyl cyclase. The high affinity G-protein coupled state, mainly responsible for inhibition of adenylyl cyclase, is not sufficient for inhibition of 50% adenylyl cyclase activity by all ligands, in both cells. Results which are in agreement with other studies [Nijssen et al, 1992; Carroll et al, 1984; Carroll et al, 1988; Liu-Chen et al, 1995], suggesting that low affinity opioid receptors may also have a role to play in the functional inhibition of adenylyl cyclase, although the mechanism is difficult to explain.

The results also suggest that the  $\delta$ -opioid receptors in NG108-15 cells are more strongly coupled to G-proteins than the predominantly  $\mu$ -opioid receptors in SH-SY5Y cells. However, in SH-SY5Y cells it is difficult to assess the binding through to functional effects originating from a  $\mu$ -opioid receptor subtype, due to the low levels of  $\delta$ -opioid receptor expression. Cloning of the opioid receptor subtypes has allowed their homogeneous expression in a cell line which has no endogenous opioid receptors. In chapter 5, by using CHO cells expressing a single opioid receptor subtype, an attempt will be made to make a direct comparison of opioid receptor binding and inhibition of adenylyl cyclase for all the opioid receptor subtypes.

**CHAPTER 5. RECOMBINANT  $\mu$ -,  $\delta$ - AND  $\kappa$ -OPIOID RECEPTORS EXPRESSED  
IN CHO CELLS ARE NEGATIVELY COUPLED TO ADENYLYL CYCLASE.**

## **5.1 Introduction**

Recent rapid advances in molecular biological techniques have allowed the identification of many membrane spanning proteins. In 1992, two separate groups working simultaneously, demonstrated cloning and functional expression of the mouse  $\delta$ -opioid receptor from NG108-15 cells [Evans et al, 1992; Keifer et al, 1992]. Soon after, using an oligonucleotide probe directed to the membrane spanning regions of the  $\delta$ -opioid receptor, the rat  $\kappa$ - and rat  $\mu$ - opioid receptors were also cloned and sequenced from the rat cDNA library [Yasuda et al, 1993 and Chen et al, 1993]. When expressed in a continuous cell line which does not express endogenous opioid receptors, the cloned receptors displayed similar pharmacological profiles as the endogenous receptors in their native cellular environment [Evans et al, 1992, Yasuda et al, 1993 and Chen et al, 1993].

The opioid receptor subtypes have a high proportion of homology in their amino acid sequences. All are members of the G-protein coupled receptor family, in that they have seven transmembrane spanning domains, extracellular N-terminus and a bulky intracellular C-terminus. The seven transmembrane spanning domains predominantly consist of hydrophobic amino acids which have the ability to tightly interact with the surrounding membrane phospholipids. Glycosylation sites exist on the extra-cellular N-terminus, whereas the intra-cellular C-terminal tail is rich in serine and threonine residues, which are potential sites for phosphorylation [Evans et al, 1992; Keiffer et al, 1992].

The stable expression of opioid receptor subtypes has allowed extensive pharmacological characterisation of the receptors independent of other subtypes. Cos-1 cells were used as the expression system for the first cloned opioid receptor subtype [Keifer et al, 1992], since then other expression systems have been used, including Chinese hamster ovary (CHO) cells [Fukuda et al, 1993], COS-6 and *Xenopus* oocytes [Wang et al, 1993]. In addition to the intact receptors, chimeric and mutated opioid receptors have been synthesised and transfected into stable cell lines [Kong et al, 1993, Cevjec et al, 1996]. The use of chimeric and mutated opioid receptors have enabled invaluable information to be gained about

which amino acids are important for normal receptor function. It has recently been shown that the C-terminus of the  $\delta$ -opioid receptor prevents receptor desensitisation [Trapaidze et al, 1996]. However, studies performed using the cloned gonadotrophin releasing hormone receptors have shown that this seven transmembrane spanning receptor lacks a C-terminus and yet undergoes normal desensitisation upon occupation [Stojilkovic et al, 1994]. The general role of the C-terminal amino acids in receptor desensitization remains unclear.

A pharmacological comparison of the cloned opioid receptor subtypes will be made in this chapter. CHO cells expressing cloned ( $\mu$ -,  $\delta$ -, and  $\kappa$ -) and mutated ( $\delta$ -) opioid receptors will be used. Moreover, in order to study the role of the C-terminus in ligand binding and functional inhibition of cAMP formation, deletion mutants lacking the final 15 or 37 C-terminal amino acids will be included in the study. In addition, two CHO cell clones expressing  $\delta_{37}$  mutant receptors expressing different numbers of receptors will be utilised (termed  $\delta_{37\text{high}}$  and  $\delta_{37\text{low}}$ ). These cells will be characterised and compared collectively in a single study with respect to their receptor expression levels, agonist competition profiles and adenylyl cyclase coupling.

## **5.2. Methods**

For details of chemicals, tissue culture, membrane preparation, cAMP measurement and data analysis the reader is directed to chapter 2. [<sup>3</sup>H]-DPN binding protocols are identical to those in chapter 4.

## **5.3. Results**

### **5.3.1: Saturation**

The binding of [<sup>3</sup>H]-DPN was dose dependent and saturable in all CHO cells expressing cloned opioid receptors yielding K<sub>d</sub> and B<sub>max</sub> values shown below (table 5.1, fig 5.1A, B and 5.2i A, B and 5.2ii A, B). Analysis of the saturation data by Langmuir Hill analysis yielded K<sub>d</sub> and B<sub>max</sub> values which were not significantly different to Scatchard (data not shown, but in order to show saturation was achieved in the experiments, the Langmuir Hill and hyperbolae data has been graphically represented, Fig 5.1A, B; 5.2iA, B and 5.2iiA, B).

### **5.3.2. Displacement**

The  $\mu$ -Preferring opioids fentanyl and DAMGO displaced [<sup>3</sup>H]-DPN (0.2nM approx.) in a dose dependent manner using CHO cells expressing the cloned  $\mu$ -opioid receptor (figure 5.3A). In CHO cells expressing cloned  $\kappa$ -opioid receptors, spiradoline, a  $\kappa$ -opioid receptor selective agonist, displaced [<sup>3</sup>H]-DPN in a similar dose dependent manner (figure 5.3B). In addition, the  $\delta$ -opioid receptor selective agonists DPDPE and DADLE both displaced [<sup>3</sup>H]-DPN in CHO cells expressing recombinant  $\delta_{wt}$ ,  $\delta_{15}$ ,  $\delta_{37low}$  and  $\delta_{37high}$  receptors (figure 5.4A, B, C, D). All curves were analysed using a one and two site computer fit. The two site fits revealed different proportions of low and high affinity binding sites (table 5.2).

Cell Type	$K_d$ (nM)	$B_{max}$ (fmol/mg protein)
CHO $\mu$	0.18 $\pm$ 0.01	116 $\pm$ 2.4
CHO $\kappa$	0.15 $\pm$ 0.01	231 $\pm$ 24.0
CHO $\delta_{wt}$	0.67 $\pm$ 0.08	452 $\pm$ 45.1
CHO $\delta_{15}$	0.77 $\pm$ 0.03	561 $\pm$ 12.3
CHO $\delta_{37low}$	0.28 $\pm$ 0.03*	35 $\pm$ 5.4*
CHO $\delta_{37high}$	0.18 $\pm$ 0.01*	163 $\pm$ 7.5*

Table 5.1. Saturation of [ $^3$ H]DPN in CHO cells expressing cloned opioid receptors. Data are mean $\pm$ SEM (n=3-5). \*Significantly (p<0.05) decreased compared to  $\delta_{wt}$ .

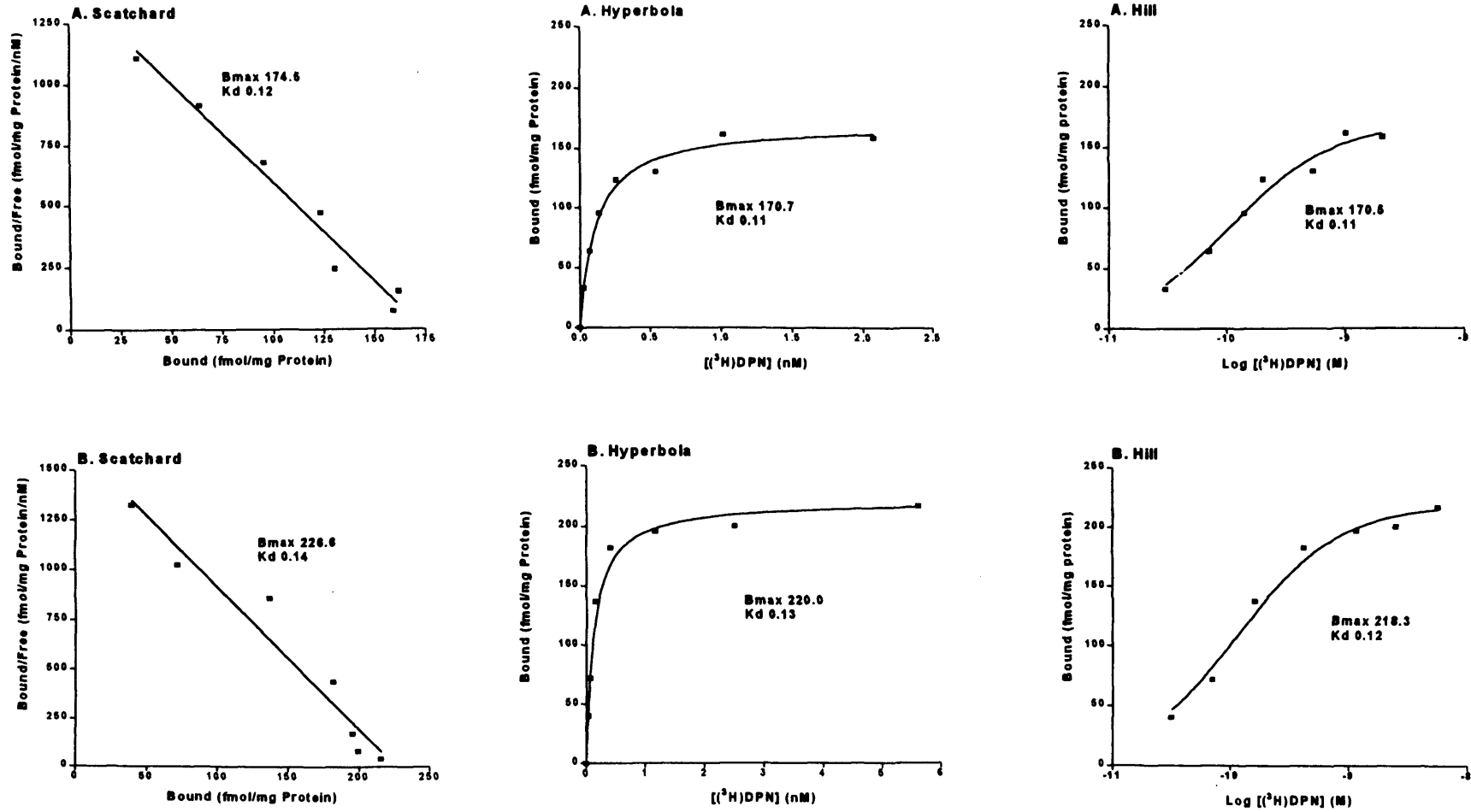


Figure 5.1. Scatchard, Hyperbolae and Langmuir Hill plots showing saturation of [<sup>3</sup>H]DPN binding to CHO cell membranes expressing μ- (A) and κ-opioid receptors (B). Data are from a single representative experiment from 2 others, Bmax=fmol/mg protein; Kd=nM.

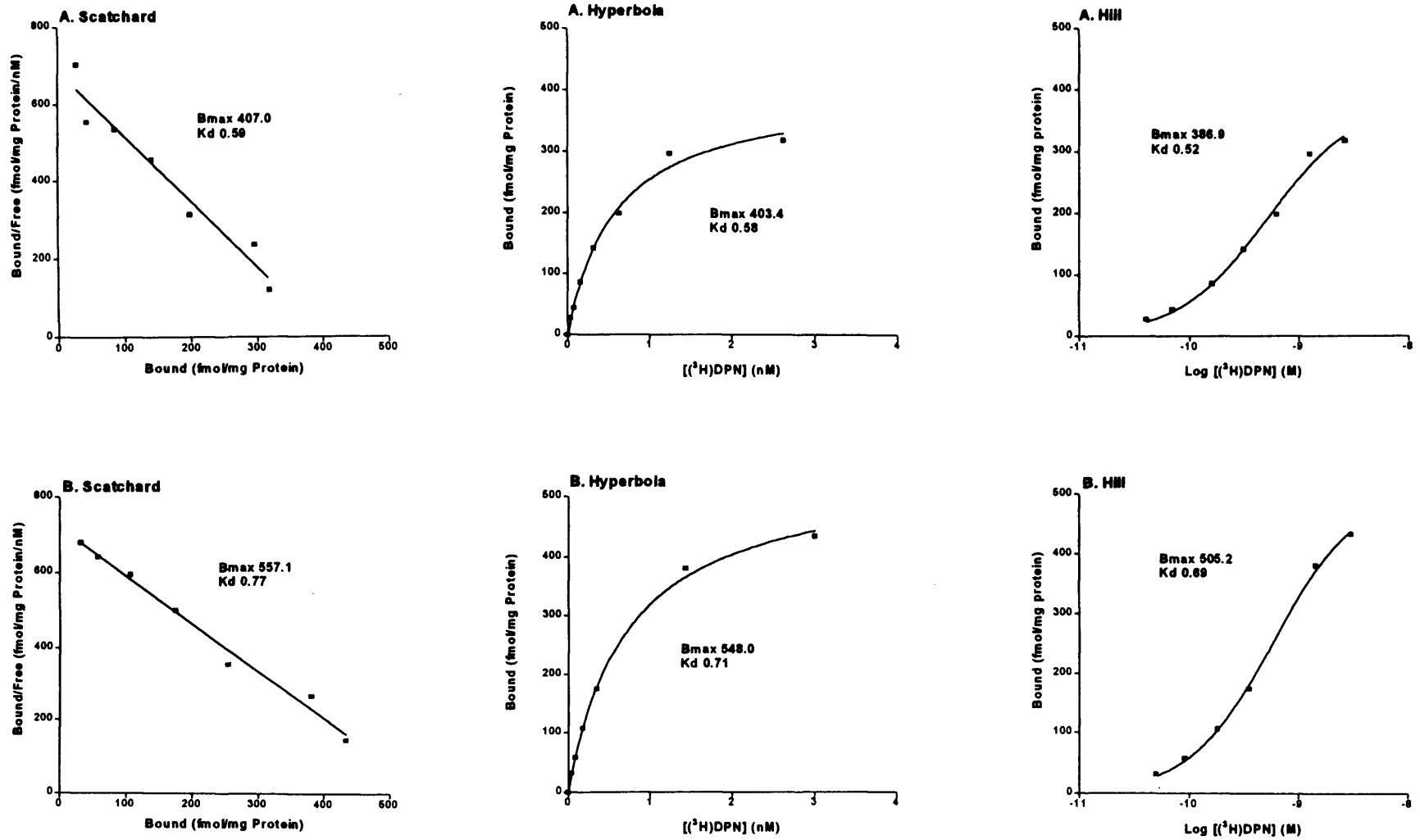


Figure 5.2i. Scatchard and Langmuir Hill plots showing [<sup>3</sup>H]DPN binding to CHO cell membranes expressing  $\delta_{vt}$  (A) and  $\delta_{15}$  (B) opioid receptors. Data are from a single experiment from 2-4 others, Bmax=fmol/mg protein: Kd=nM.

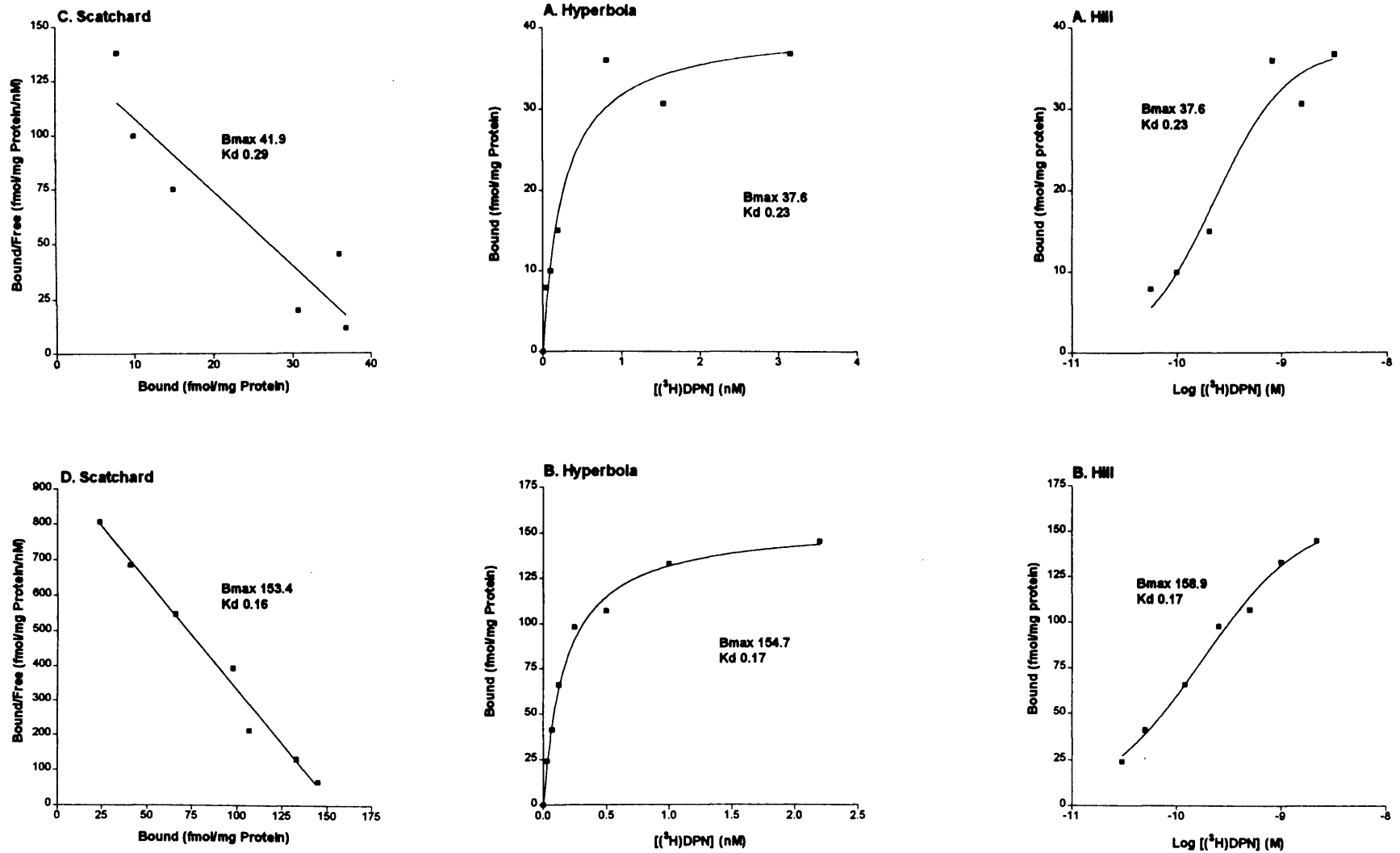


Figure 5.2ii. Scatchard, Hyperbolae and Langmuir Hill plots showing  $[^3\text{H}]\text{DPN}$  binding to CHO cell membranes expressing  $\delta_{37\text{low}}$  (A) and  $\delta_{37\text{high}}$  (B) opioid receptors. Data are from a single experiment from 2-4 others; Bmax=fmol/mg protein: Kd=nM.

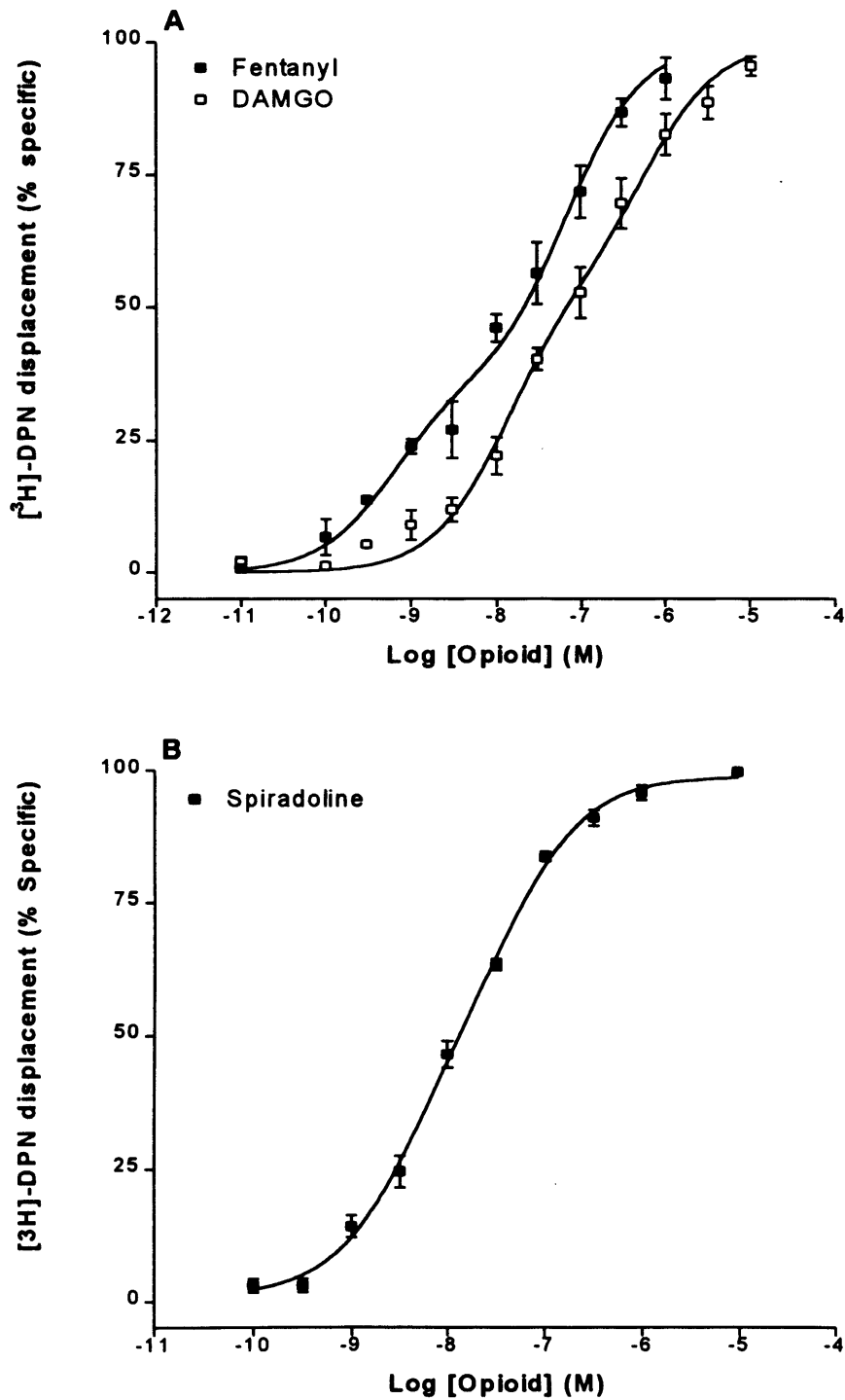


Figure 5.3. Displacement of [<sup>3</sup>H]DPN by fentanyl, DAMGO (CHO $\mu$ , A) and spiradoline (CHO $\kappa$ , B). Data are mean $\pm$ SEM of n=5-7.

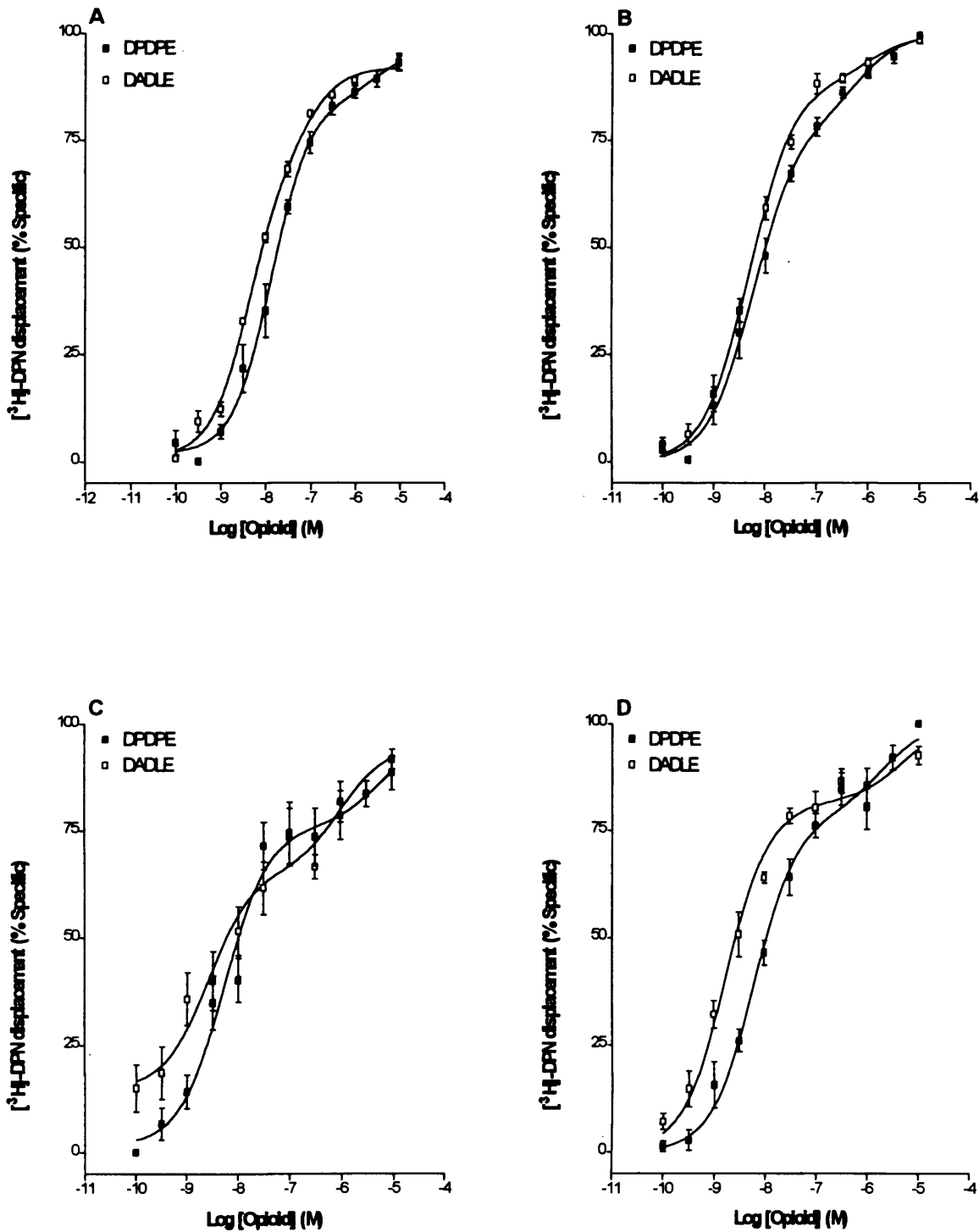


Figure 5.4. Displacement of [<sup>3</sup>H]DPN by DPDPE and DADLE in CHO cell membranes expressing  $\delta_{wt}$  (A),  $\delta_{15}$  (B),  $\delta_{37low}$  (C) and  $\delta_{37high}$  (D) opioid receptors. Data are mean $\pm$ SEM of 3-8 determinations.

Cell	Opioid	pK <sub>i</sub> H (nM)	H (%)	pK <sub>i</sub> L (nM)	L (%)
CHO <sub>μ</sub>	DAMGO	8.27±0.23(5.4)	65.0±6.30	5.78±0.30(1643)	35.0±6.30
	Fentanyl	9.40±0.22(0.4)	27.3±6.60	7.18±0.06(65.5)	72.7±6.60
CHO <sub>κ</sub>	Spiradoline	9.25±0.10(0.6)	47.2±9.60	8.08±0.22(8.35)	52.8±9.60
CHO <sub>δ<sub>wt</sub></sub>	DPDPE	7.93±0.15(9.6)	82.1±3.10	5.34±0.45(4570)	17.9±3.10
	DADLE	8.99±0.04(1.0)	18.6±3.70	6.42±0.36(374)	81.4±3.70
CHO <sub>δ<sub>15</sub></sub>	DPDPE	9.00±0.14(1.0)*	34.1±8.60*	6.89±0.25(128)*	65.9±8.60
	DADLE	8.92±0.18(1.2)	20.1±6.00	6.84±0.29(144)*	79.9±6.00
CHO <sub>δ<sub>37low</sub></sub>	DPDPE	8.81±0.13(1.5)*	18.8±4.10*	6.48±0.19(328)*	81.2±4.10
	DADLE	9.57±0.11(0.3)*	38.9±11.1	6.77±0.51(170)*	61.1±11.1
CHO <sub>δ<sub>37high</sub></sub>	DPDPE	9.06±0.11(0.8)*	66.4±6.10	6.17±0.32(673)*	33.6±6.10
	DADLE	9.86±0.23(0.1)*	53.7±6.50	7.05±0.29(87.3)*	46.3±6.50

Table 5.2. High (H) and low (L) affinity states of the  $\mu$ -,  $\kappa$ -,  $\delta$ -,  $\delta_{15}$  and  $\delta_{37}$  cloned opioid receptors expressed in CHO cells, revealed by displacement of [<sup>3</sup>H]DPN using the appropriate opioid agonist. Data are mean±SEM of 3-8 determinations.\*Significantly decreased compared with  $\delta_{wt}$ .

### 5.3.3 Inhibition of forskolin stimulated cAMP formation

Fentanyl, DAMGO (CHO $\mu$ ), spiradoline (CHO $\kappa$ ), DPDPE and DADLE (CHO $\delta_{wt}$ ,  $\delta_{15}$ ,  $\delta_{37low}$ ,  $\delta_{37high}$ ) caused a dose dependent inhibition of forskolin (1 $\mu$ M) stimulated cAMP formation (figure 5.5 and 5.6, table 5.3).

Cell	Opioid	pIC <sub>50</sub> (nM)	I <sub>max</sub> (%)
CHO $\mu$	DAMGO	7.26 $\pm$ 0.24(54.9)	43.4 $\pm$ 3.2
	Fentanyl	7.94 $\pm$ 0.32(11.4)	37.1 $\pm$ 3.2
CHO $\kappa$	Spiradoline	8.51 $\pm$ 0.15(3.1)	42.2 $\pm$ 3.2
CHO $\delta_{wt}$	DPDPE	8.72 $\pm$ 0.06(1.88)	51.7 $\pm$ 3.2
	DADLE	9.07 $\pm$ 0.12(0.85)	44.3 $\pm$ 3.7
CHO $\delta_{15}$	DPDPE	8.25 $\pm$ 0.11(5.51)*	41.3 $\pm$ 4.8
	DADLE	8.93 $\pm$ 0.14(1.17)	38.4 $\pm$ 1.9
CHO $\delta_{37low}$	DPDPE	7.39 $\pm$ 0.29(40.7)*	42.5 $\pm$ 4.2
	DADLE	8.21 $\pm$ 0.24(6.07)*	42.9 $\pm$ 4.8
CHO $\delta_{37high}$	DPDPE	8.53 $\pm$ 0.38(2.95)	52.1 $\pm$ 4.1
	DADLE	8.7 $\pm$ 0.15(1.98)*	51.3 $\pm$ 4.8

Table 5.3. Inhibition of forskolin (1 $\mu$ M) stimulated cAMP formation by opioids in CHO cells expressing cloned opioid receptors. Data are mean $\pm$ SEM of 3-7 determinations, \*Statistically ( $p < 0.05$ ) increased compared with  $\delta_{wt}$ .

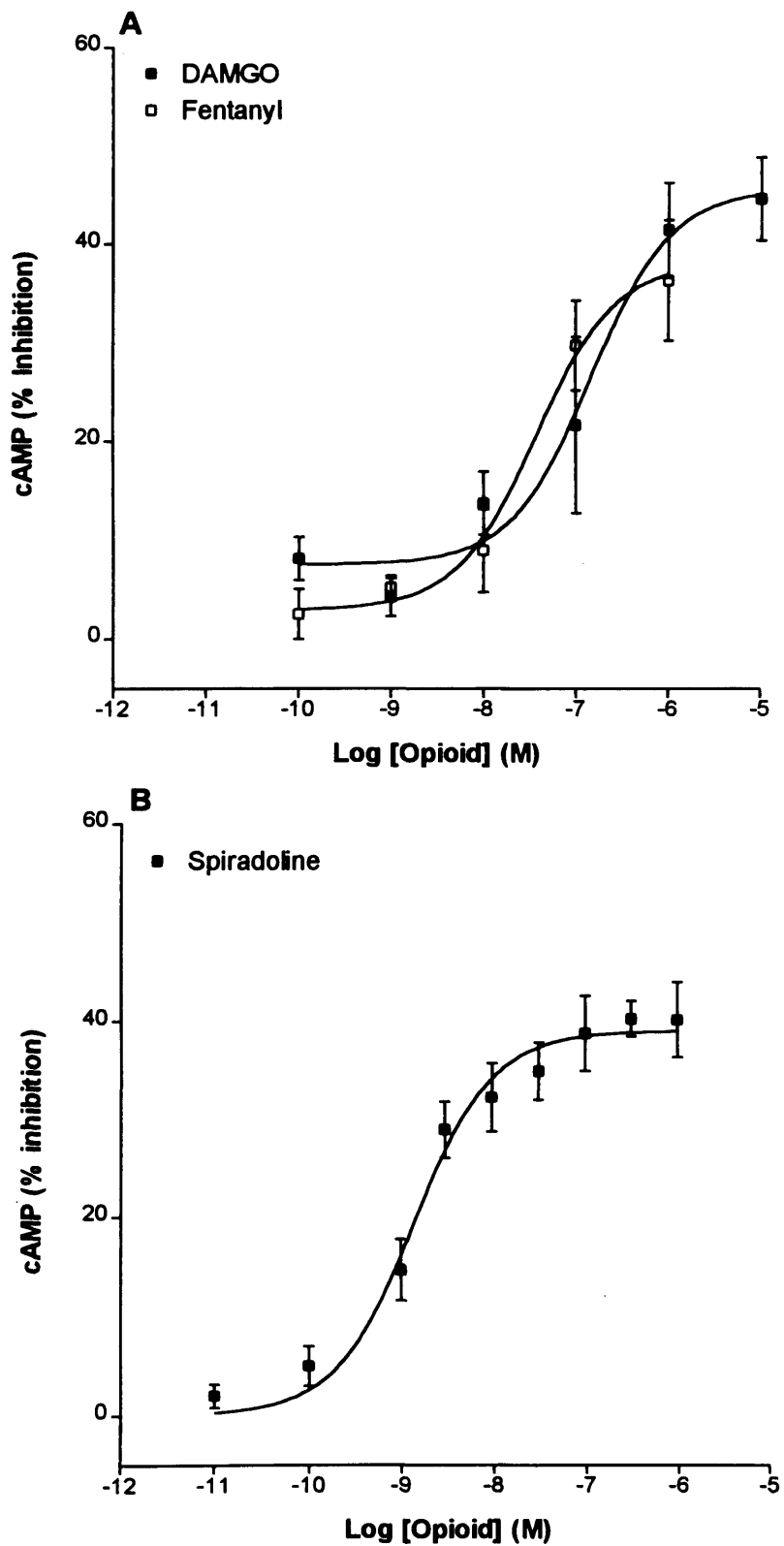


Figure 5.5. Dose dependent inhibition of forskolin stimulated cAMP formation by fentanyl, DAMGO (CHO $\mu$ , A) and spiradoline (CHO $\kappa$ , B). Data are mean $\pm$ SEM (n=7-9).

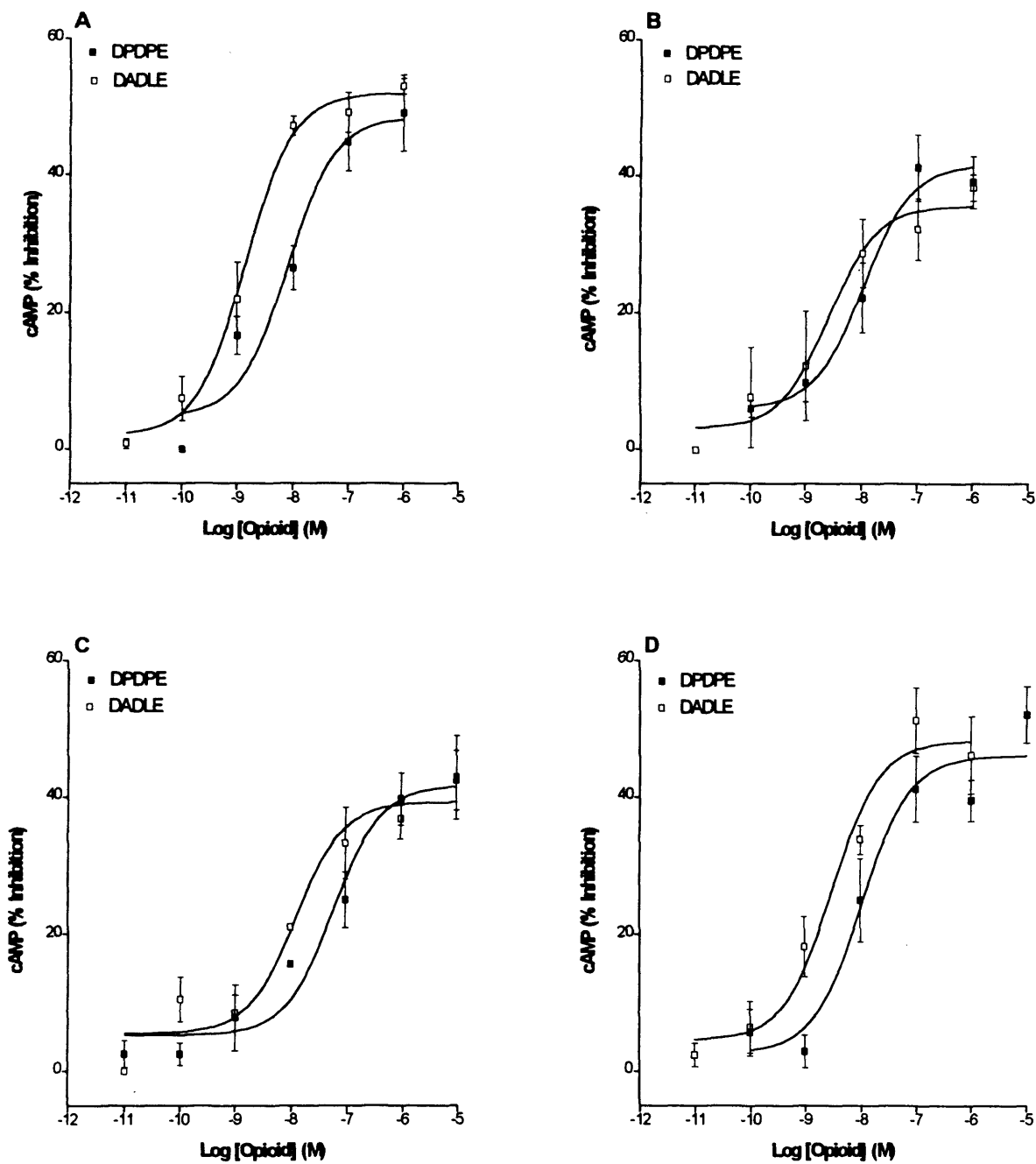


Figure 5.6. Dose dependent inhibition of forskolin stimulated cAMP formation by DPDPE and DADLE in CHO cells expressing  $\delta_{wt}$  (A),  $\delta_{15}$  (B),  $\delta_{37low}$  (C) and  $\delta_{37high}$  (D) opioid receptors. Data are mean $\pm$ SEM (n=3-6).

#### **5.4: Discussion.**

Cloned opioid receptors transfected into cell lines with no endogenous opioid receptor expression, display similar pharmacological profiles as those in their native cellular environment [Evans et al, 1992, Yatsuda et al, 1993 and Chen et al, 1993]. However, the coupling of cloned opioid receptors to adenylyl cyclase has been shown to be both dependent and independent of receptor expression levels [Pranther et al, 1994]. The CHO $\mu$  cells expressed 116 fmol/mg protein [ $^3$ H]DPN binding sites with an affinity of 0.18nM. Both values being very similar to those obtained using SH-SY5Y cells expressing predominantly  $\mu$ - opioid receptors [Yu et al, 1986; Lambert et al, 1994]. The CHO $\delta_{wt}$  and the CHO $\delta_{15}$  cells expressed approximately two fold more, and the CHO $\delta_{37high}$  approximately 50% less receptors than those observed in NG108-15 cells. The Kd values in CHO $\delta_{wt}$  and CHO $\delta_{15}$  for [ $^3$ H]DPN were 0.67 and 0.77nM respectively, demonstrating lower [ $^3$ H]DPN binding affinity for the  $\delta$ -opioid receptor when compared with 0.2nM in NG108-15 cells. However, using CHO $\delta_{37low}$  and CHO $\delta_{37high}$  cells, [ $^3$ H]DPN binding affinity was significantly increased by 2.5-3 fold with the removal of the final 37 C-terminal amino acids in the  $\delta$ -opioid receptor, the changes in Kd being independent of receptor expression levels as the CHO $\delta_{37high}$  cells expressed approximately five fold more [ $^3$ H]DPN binding sites than the CHO $\delta_{37low}$  cells. These data suggest that the C-terminal 16-37 amino acids may convey to the  $\delta$ -opioid receptor the ability to bind [ $^3$ H]DPN more tightly. In order to examine the effect of receptor expression levels on functional agonist binding and coupling to adenylyl cyclase, two cell lines (CHO $\delta_{37low}$  and CHO $\delta_{37high}$ ) were used expressing the same  $\delta_{37}$  mutant receptor with differing expression levels (4.6 fold).

In CHO $\mu$  cells, fentanyl displayed a similar high and low affinity Ki value as those observed using SH-SY5Y cells. However DAMGO was weaker at both high (7.7 fold) and low (2.9 fold) affinity receptors in CHO $\mu$  cells when compared with SH-SY5Y cells. In CHO cells expressing the cloned  $\kappa$ -opioid receptor, spiradoline revealed two affinity states of the receptor. In the CHO cells expressing  $\delta_{wt}$  opioid receptor, DPDPE and DADLE both

displaced [<sup>3</sup>H]DPN in a dose dependent manner revealing both high and low affinity receptor states. Using DPDPE as the displacer, a significant increase in affinity of both high and low affinity receptors was observed with the loss of C-terminal amino acids from the  $\delta$ -opioid receptor, a similar finding to the observed increase in K<sub>d</sub> for [<sup>3</sup>H]DPN binding with the loss of C-terminal amino acids. However, a similar significant increase in affinity was observed using DADLE only in the CHO cells expressing the C-terminal 37 mutant receptor. These results suggest that the C-terminus may play a role in regulating ligand binding affinity, but this has little functional consequence [Smart et al, 1996]. It has been demonstrated that the major role of the C-terminus is to cause receptor desensitisation [Cvejic et al, 1996]. In the CHO $\delta_{37low}$  and CHO $\delta_{37high}$  cells there was only very small differences in K<sub>i</sub> values for the high and low affinity receptors revealed by DPDPE and DADLE displacement, and this may suggest that agonist binding affinity is independent of receptor expression levels.

Inhibition of adenylyl cyclase in CHO $\mu$  cells was dose dependent using fentanyl and DAMGO. As also demonstrated in SH-SY5Y cells, fentanyl was a more potent adenylyl cyclase inhibitor than DAMGO. Cloned  $\mu$ -opioid receptors expressed in CHO cells display a 2 and 4 fold more potent inhibition of forskolin stimulated cAMP formation using both fentanyl and DAMGO respectively when compared with the endogenous  $\mu$ -opioid receptors in SH-SY5Y cells. However, the maximal inhibition was some 10-15% lower in CHO $\mu$  cells than SH-SY5Y cells. This data may suggest that when transfected into CHO cells the cloned  $\mu$ -opioid receptor couples slightly more potently to adenylyl cyclase, however the inhibition of AC is impaired. However, probably due to species G-protein/adenylyl cyclase subtype differences or availability, the maximal inhibition of adenylyl cyclase is impaired. In addition, when the pK<sub>iH</sub> (DAMGO and fentanyl) is compared with the pIC<sub>50</sub> for the inhibition of AC in CHO $\mu$  cells, there is significant inhibition of AC which suggests that high affinity receptors can mediate the functional inhibition of AC. Spiradoline also caused a dose dependent inhibition of forskolin stimulated cAMP formation in CHO $\kappa$  cells, with a pIC<sub>50</sub> slightly higher than the K<sub>iH</sub> for

[<sup>3</sup>H]DPN displacement, suggesting high affinity G-protein coupled receptors are mediating the inhibition of adenylyl cyclase. A similar observation is seen using DPDPE and DADLE in CHO $\delta$  cells, where the cAMP IC<sub>50</sub> values are very similar to the KiH for [<sup>3</sup>H]DPN displacement. Due to the different experimental design in the measurement of binding (membranes) and adenylyl cyclase activity (whole cells), the correlation of high affinity sites with function is difficult, due to changes in affinity of ligands for opioid receptors in the presence of Na<sup>+</sup> [Carrol et al, 1988]. However, in CHO $\delta_{37low}$  cells using DPDPE as the agonist, a higher (40.7nM) IC<sub>50</sub> is observed, the reason for this observation is unknown but may be related to low levels receptor expression or be due to different effects of Na<sup>+</sup> ions on these mutated opioid receptors. The maximal inhibition in the CHO $\delta$  cells is relatively constant, ranging from 38-52%. Therefore, in CHO $\delta_{37low}$  cells, a full agonist inhibition of adenylyl cyclase is achieved, despite the low levels of expression.

The results show that the expression of recombinant opioid receptors into CHO cells allows them to be studied in an expression system independently of other opioid receptor subtypes. Moreover, the construction and expression of opioid receptor mutants can allow important information to be gained in order to reveal which amino acids are important for complete functioning of receptors.

**CHAPTER 6. NEURONAL CANNABINOID RECEPTOR BINDING AND  
INHIBITION OF ADENYLYL CYCLASE IN RAT CEREBELLA, SH-SY5Y AND  
NG108-15 CELL MEMBRANES.**

## **6.1. Introduction.**

Both central (CB1) and peripheral (CB2) cannabinoid receptors have been cloned and sequenced, and possess the predicted seven transmembrane structural motif common to G-protein coupled receptors [Matsuda et al., 1990; Munro et al., 1993]. Central cannabinoid receptors are localised in many parts of the central nervous system (see chapter 1), and are particularly abundant in the cerebellum [Herkenham et al., 1991]. Cannabinoid receptors, via a pertussis toxin sensitive G-protein have been shown to inhibit adenylyl cyclase, close voltage sensitive  $Ca^{2+}$  channels, and induce hyperpolarization via  $K^+$  channel activation [Howlett et al, 1990; Caulfield & Brown., 1992]. In cultured NG108-15 cells, cannabinoids have been shown to close N-type VOCC's [Mackie and Hille, 1992]. Using the neuroblastoma cell line N18TG2 cells, Howlett was the first to demonstrate cannabinoids cause inhibition of cAMP formation via a pertussis sensitive G-protein [Howlett, 1984]. No reports can be found in the literature as to whether central cannabinoid receptors are expressed in SH-SY5Y cells.

Despite rapid advances in our understanding of cannabinoid receptor structure, function and distribution, radioligand binding studies have been hampered by the high lipophilicity of cannabinoid ligands, and the lack of a high affinity *antagonist* to use as a radiolabel. Previous cannabinoid receptor binding studies have used radiolabelled agonists (e.g., [ $^3H$ ]CP55,940, [ $^3H$ ]WIN 55,212-2), under various experimental conditions, however, agonist binding is guanine nucleotide sensitive. In addition, the reported affinities of a range of commonly used unlabelled cannabinoid ligands shows marked variability, probably due to differing binding assay methodologies [Devane et al, 1988; Hillard et al, 1995; Felder et al, 1992; Kuster et al, 1993; Munro et al, 1993]. Rinaldi-Carmona et al [1994; 1995] recently introduced a highly potent CB1 selective cannabinoid receptor antagonist SR141716A ((N-(piperidin-1-yl)-5-(4-chlorophenyl)-1-(2,4-dichlorophenyl)-4-methyl-1H-pyrazole-3-carboxamide hydrochloride) which is now available as a radioligand. The development of a cannabinoid receptor binding assay using [ $^3H$ ]SR141716A will be presented in this chapter. In addition, cannabinoid inhibition of

adenylyl cyclase using rat cerebella membranes (CBM), NG108-15 and SH-SY5Y cells will also be presented. During the preparation of this thesis, Rinaldi-Carmona et al [1996] published a paper detailing the pharmacological characteristics of [<sup>3</sup>H]SR141716A.

## **6.2. Method development.**

### **6.2.1 Cannabinoid binding assay.**

A number of binding assays have been previously described in the literature, all utilised differing methodology and a summary of the main features of each assay are shown in table 6.1. [Ney et al, 1985; Devane et al, 1988; Herkenham et al, 1990; Kaminski et al, 1992; Compton et al, 1993; Felder et al, 1992]. In order to develop a cannabinoid receptor binding assay these reports were used as a reference for assay conditions.

#### **Experiment 1.**

*Method:* Rapid vacuum filtration of a 0.5ml assay volume using a Brandel cell harvester. The filters were washed with 2x4ml of buffer.

*Ligand:* [<sup>3</sup>H]WIN55212-2 (0.925mBq) was purchased from NEN Du Pont was used at (0.25nM).

*Buffer:* 50mM HEPES, 3mM MgCl<sub>2</sub>, 1mg/ml Fatty acid free Bovine serum albumin (BSA), pH7.4 with 10M NaOH.

*Incubation:* 1 hour at 20°C in Sigmacote treated glass tubes.

*Tissue:* Fresh NG108-15, SH-SY5Y and CBM.

*Filters:* Soaked in Sigmacote for 3 hours and dried overnight.

*Displacing ligands:*  $\Delta^9$ -THC (stock 14.4mM in ethanol) and Nabilone (stock 5mM in ethanol) diluted to 10 $\mu$ M in assay buffer.

The results showed no specific binding in the presence of either  $\Delta^9$ -THC (10 $\mu$ M) or Nabilone (10 $\mu$ M) in any of the tissues tested. In addition approximately 50% of the total radioactivity was bound to the filters. The magnesium in the buffer may affect the binding, hence the buffer was changed.

Reference	Method	mM Buffer (pH)	Tissue	Incubation time and temperature.	specific binding enhancement	Specific binding (%)
Ney et al, 1985	Filtration	50 Tris (7.7)	Brain membranes	3 hours at 37°C	Filters (0.3% PEI)	90-95
Devane et al, 1988	Centrifugation	50 Tris, 1 EDTA, 3 Mg <sup>2+</sup> (7.4)	Brain membranes	50 minutes at 30°C	Regisil treated polypropylene tubes	70-80
Herkenham, 1990	Autoradiography	50 Tris, 50mg/ml BSA (7.4)	Brain slices	2 hours at 37°C	50mg/ml BSA	80-90
Kaminski et al, 1992	Filtration	50 Hepes, 100 NaCl, 5mg/ml BSA (7.4)	Spleen cells	1 hour at 30°C	Fliters (PEI), 5mg/ml BSA	45-65
Compton et al, 1993	Filtration	50 Tris, 1 EDTA, 3MgCl <sub>2</sub> , 5mg/ml BSA (7.4)	Brain membranes	1 hour at 30°C	Filters (0.1% PEI), 5mg/ml BSA	90
Felder et al, 1992	Filtration	50 Tris, 5 MgCl <sub>2</sub> , 2.5 EDTA, 5mg/ml BSA, 200 sucrose (7.4)	CHO transfects	1 hour at 30°C	Filters (0.1% PEI), 5mg/ml BSA, ligands in 50mg/ml BSA	90

Table 6.1. Main characteristics of published cannabinoid receptor binding assays. Regisil= sialinising reagent, BSA=Bovine serum albumin, PEI= Polyethyleneimine. [<sup>3</sup>H]CP55,940 was the radioligand used throughout except Ney et al [1985] who used [<sup>3</sup>H]TMA.

### Experiment 2.

All conditions were the same as in *experiment 1* except the buffer was changed to 50mM Tris-HCl, 1mg/ml Fatty acid free Bovine serum albumin (BSA), pH7.4 with 10M NaOH.

### Results.

Tissue	DPM Specific (NSB with $\Delta^9$ -THC 10 $\mu$ M)	DPM Specific (NSB with nabilone 10 $\mu$ M)
NG108-15	240	0
SH-SY5Y	127	132
CBM	1510	1732

Table 6.2: Displacement of [ $^3$ H]WIN55212-2 with  $\Delta^9$ -THC and nabilone. Data are from a single experiment.

Although specific binding was observed, there was no dose related displacement of [ $^3$ H]WIN55212-2 using either agonist. Also, approximately 50% of the total radioactivity added to each tube was on the filters. This may have been due to the radioligand sticking to the filters. The next change in the method involved the pre-treatment of the filters.

### Experiment 3.

The binding assay conditions were as in experiment 2 except that the filters were soaked in Sigmacote overnight, allowed to dry and then soaked again and loaded onto the harvester wet.

This procedure resulted in only approximately 2% of the total radioactivity added to each tube to be retained onto the filters. This was probably a result of sialinisation of the glass fibres which caused the filters to loose their separating ability.

#### *Experiment 4.*

From the previous results it was still not clear as to where the problem was in the methods used. There were a three possible scenarios:

- A. The cannabinoids were very insoluble which may have caused the problems.
- B. The cannabinoids are notoriously sticky and may be lost on the plastic harvester tubes or were still sticking to the filters even after sigmacote treatment.
- C. The instability of [<sup>3</sup>H]WIN55212-22 may be the problem.

As CBM have previously been shown to have picomolar receptor binding sites [Herkenham et al, 1992] these were used alone in subsequent experiments in order to develop the binding assay.

In a method described by Felder et al [1992], who also had cannabinoid solubility problems, the cannabinoid ligands were diluted in Tris-HCl (50mM), MgCl<sub>2</sub> (5mM), EDTA (2.5mM) buffer containing 50mg/ml BSA.

*Method:* Rapid vacuum filtration of a 0.5ml assay volume using a Brandel cell harvester. The filters were washed with 2x4ml of buffer.

*Ligand:* [<sup>3</sup>H]WIN55212-2 (0.925mBq) was purchased from NEN Du Pont was used at (0.25nM).

*Buffer:* Tris-HCl (50mM), MgCl<sub>2</sub> (5mM), EDTA (2.5mM), pH7.4 with 10M NaOH.

*Incubation:* 1 hour at 20°C in Sigmacote treated glass tubes.

*Tissue:* Fresh rat CBM (50µg/tube)

*Filters:* Soaked in Sigmacote for 3 hours and dried overnight.

*Displacing ligands:* <sup>Δ9</sup>-THC (stock 14.4mM in ethanol) and Nabilone (stock 5mM in ethanol) diluted to 10µM in buffer containing 50mg/ml BSA.

The results were very inconclusive, approximately 80% of NSB tubes filtered contained more radioactivity than the totals in the presence of no displacing ligands.

### *Experiment 5.*

The stability of [<sup>3</sup>H]WIN55212-2 was questioned due to the lack of its use in previous reports. In addition, [<sup>3</sup>H]CP55940 was newly available from NEN Du Pont and this was used instead of [<sup>3</sup>H]WIN55212-2. The method was the same as in experiment 4 except magnesium and EDTA was removed from the buffer, as these may have been inhibiting displacement in some way. This experiment was performed in the presence of different concentrations of BSA. Two totals and two NSB tubes were set up for 0, 5, 10, 15 and 20mg/ml BSA.

### *Results.*

In the tubes containing 0mg/ml BSA there was 9800dpm specific counts compared with only 4620dpm specific in the presence of 20mg/ml BSA. This suggested that BSA was not required in the experimental tubes. Also there remained a high proportion (~60%) of the total radioactivity added to the tubes sticking to the filters.

### *Experiment 6.*

In order to attempt to decrease the filtration problems the filters were then soaked in 0.3% PEI instead of Sigmacote [Nye et al, 1985]. Cyclodextrin (2mg/ml) was also added to the Tris-HCl experimental buffer in order to enhance the solubility of the cannabinoids. No BSA was added to the Sigmacote treated experimental tubes, however BSA (0.5mg/ml) was included in the wash buffer and the filters were washed with 4x4ml of buffer. The incubation was performed at 37°C for 60 minutes.

The results showed that only 1% of total radioactivity added to each tube was retained on the filters.

### *Experiment 7.*

The pharmacological characterisation of the cloned peripheral cannabinoid receptor [Munro et al, 1995] was performed using a centrifugation assay. After consultation with Dr Munro, MRC Laboratory of Molecular Biology, Hills Road, Cambridge, who also had problems developing the filtration assay, his method was adopted, which, in his hands, consistently resulted in 50% specific binding.

*Separation method.* High speed centrifugation (12000rpm for 5 minutes) of a 0.5ml assay volume in 1.5 ml eppendorf tubes. The supernatant, pellet and the empty tube were analysed for radioactivity.

*Ligand:* [<sup>3</sup>H]CP55940 (0.925mBq) was purchased from NEN Du Pont and was used at (0.25nM).

*Buffer:* Tris-HCl (50mM), pH7.4 with 10M KOH instead of 10M NaOH (In Dr Munro's experiments, Na<sup>+</sup> ions inhibited CB2 receptor binding).

*Incubation:* 1 hour at 37°C

*Tissue:* Fresh rat CBM (50µg/tube)

*Displacing ligands:* WIN55212-2 (stock 5mM in DMSO) and Nabilone (stock 5mM in DMSO) diluted to 10µM in buffer.

### Results.

	Total (dpm)	NSB +Nabilone 10µM(dpm)	Specific (dpm)
Pellet	1349±38	1145±66	204
Supernatant	2878±69	2825±45	53
Tube	1657±66	1893±87	0

Table 6.3: Displacement of [<sup>3</sup>H]CP55940 binding with nabilone (10µM). Data are mean±SEM of 4 independent experiments.

The results show that the pellet fraction only has 204dpm specific binding, and there is more radioactivity on the tube than on the CBM. The extraction of radioactivity from the pellet was incomplete and methanol (300µl for 3 hours prior to counting) was used in subsequent experiments.

*Experiment 8.*

The method used was as in experiment 7 except more protein (200µg/tube) was added and the radioactivity was extracted from the pellet using methanol.

Results.

	Total (dpm)	Nabilone (dpm)	Total (dpm)	WIN (dpm)
Pellet	16220	8409	16598	9073
Tube	9312	4980	10242	7669
Supernatant	27179	36809	27461	36929

Table 6.4: Displacement of [<sup>3</sup>H]CP55,940 (0.5nM) with Nabilone (10µM) and WIN55212-2 (10µM). Data are mean of a single experiment performed in triplicate.

The results show that both displacing ligands produced 45-50% specific binding, and this method was then used in order to identify cannabinoid binding sites on SH-SY5Y human neuroblastoma cells.

### *Experiment 9.*

In SH-SY5Y cells a dose dependent displacement of [<sup>3</sup>H]CP55940 (0.2nM) was observed using increasing concentrations of nabilone (Table 6.5).

[Nabilone] $\mu$ M	[ <sup>3</sup> H]CP55940 displacement (%)
0.01	16.7
0.1	22.5
1	77.2
10	98.9

Table 6.5. Dose dependent displacement of [<sup>3</sup>H]CP55940 with Nabilone in SH-SY5Y cell membranes. Data are mean of a single experiment performed in duplicate.

The results showed that there was very low levels of cannabinoid receptor binding sites on SH-SY5Y cells (total tubes=9341dpm specific and NSB=7712dpm specific). The approximate resulting  $K_i$  value for nabilone was 500nM, which was much higher than the values of 22.3nM found in the literature [Compton et al, 1993]. In addition these results could not be repeated in subsequent experiments using identical assay conditions.

The kinetics of cannabinoid binding showed rapid on and off rates [Devane et al, 1988] and the pellet was cut off the eppendorf tube by eye and led to the possibility of investigator errors. As a result of these considerations it was then decided that the filtration method would be attempted once more with the changes in experimental conditions shown below.

### *Experiment 10.*

*Method:* Rapid vacuum filtration of a 0.5ml assay volume using a Brandel cell harvester. The filters were washed with 2x4ml of buffer.

*Ligand:* [<sup>3</sup>H]CP55940 (0.925mBq) was purchased from NEN Du Pont was used at (0.25nM).

*Experimental Buffer:* Tris-HCl (50mM), pH7.4 with 10M KOH instead of 10M NaOH.

*Wash Buffer.* Tris-HCl (50mM) containing BSA (1mg/ml), pH7.4 with 10M KOH

*Incubation:* 1 hour at 30°C in Sigmacote treated glass tubes.

*Tissue:* Fresh rat CBM (50µg/tube)

*Filters:* Soaked in 0.2% PEI for 3 hours and loaded onto the harvester wet.

*Displacing ligands:* Nabilone (stock 5mM in DMSO) diluted to 10µM in experimental buffer.

The saturation of [<sup>3</sup>H]CP55940 binding was measured in fresh CBM (50µg) using 10µM nabilone in order to determine NSB (figure 6.1).

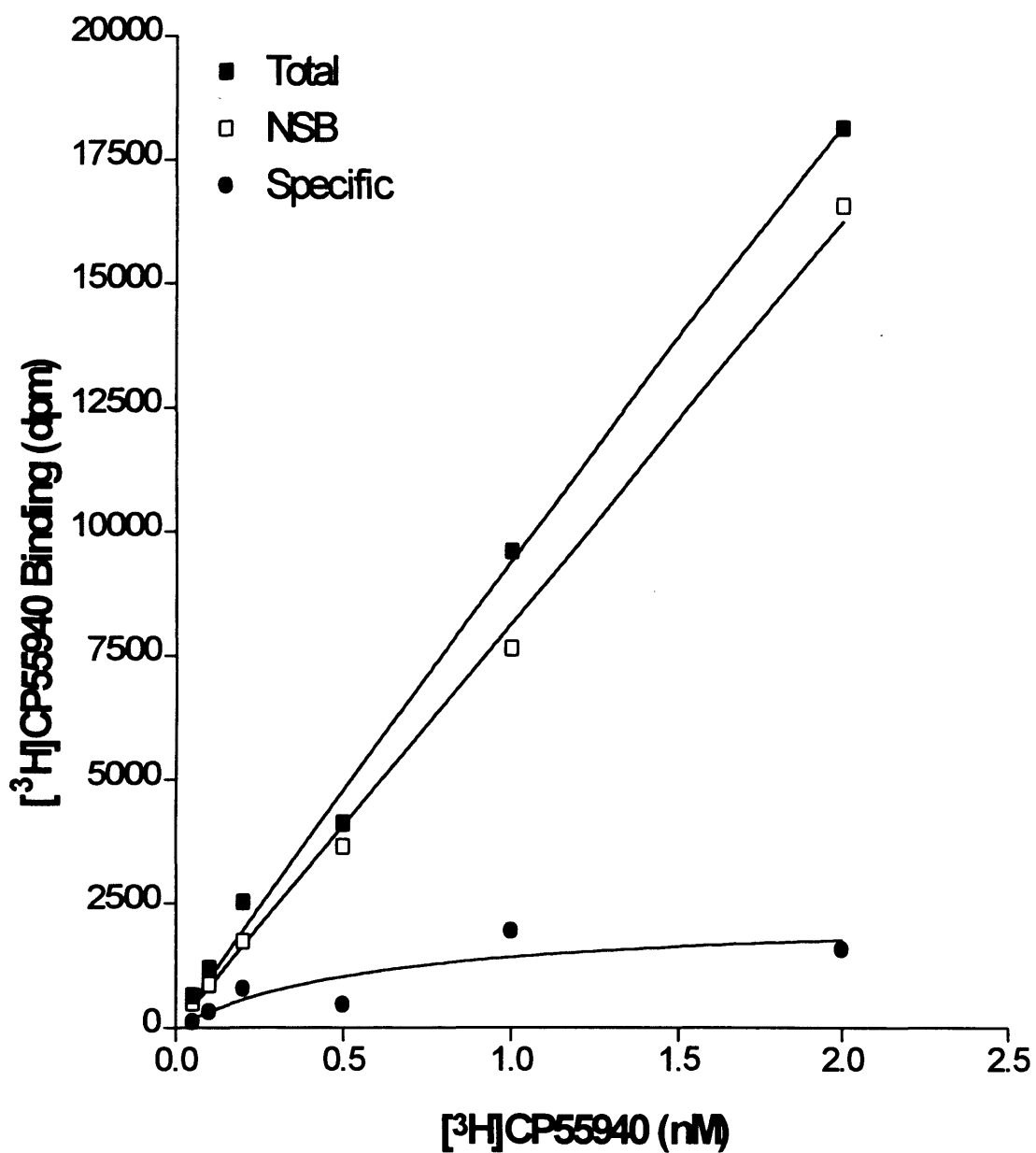


Figure 6.1: Saturation of  $[^3\text{H}]\text{CP55940}$  binding in rat CBM. Data are from a single experiment. The results show dose dependent and saturable binding of  $[^3\text{H}]\text{CP55940}$  to rat CBM. However there was still an unacceptably high proportion of NSB.

### *Experiment 11.*

The first report of a neuronal cannabinoid antagonist enhanced the study of cannabinoid pharmacology [Rinaldi-Carmona et al, 1995]. Consultation with Madam Rinaldi-Carmona yielded a supply of the new ligand, SR141716A. Radiolabelled [<sup>3</sup>H]SR141716A was supplied by Amersham, and the final experimental conditions were as described in detail below.

### **6.3 Final Method.**

For further details of chemicals, tissue culture, and cAMP measurement the reader is directed to chapter 2. For membrane preparation see the previous section in this chapter.

#### **6.3.1 Binding assay.**

All experiments were performed at 30°C [Devane et al., 1988] in 500µl volumes of Tris. HCl (50mM), pH 7.4 for 60mins using approximately 50-100µg of membrane protein measured according to Lowry et al. [1951]. All binding studies were performed in disposable glass tubes (Fisons, Loughborough UK) pretreated with Sigmacote® (Sigma Chemical Co. Ltd, Poole, UK), and allowed to dry.

#### **6.3.2 Saturation**

In saturation studies increasing concentrations (0.01-5.3nM) of [<sup>3</sup>H]SR141716A (Specific activity 40Ci/mmol, Radiochemical purity 98.6%, Amersham International, Bucks, UK) were used.

### 6.3.3 Displacement.

In competition studies a fixed concentration of approximately 0.4nM was used. Non-specific binding was defined in the presence of 1 $\mu$ M (from a 5mM stock in DMSO) unlabelled SR141716A. Stock concentrations of anandamide,  $\Delta^9$ -tetrahydrocannabinol,  $\Delta^8$ -tetrahydrocannabinol were supplied (Semat, St Albans, UK) in ethanol at 10mg/ml; WIN 55,212-2 mesylate was supplied (Semat, St Albans, UK) as a powder and made in DMSO at 5mM. Nabilone (Lot 94H047) was a kind gift from Eli Lilly (Basingstoke UK) and prepared as a 5mM stock in DMSO. DMSO and ethanol concentrations in the assay never exceeded 0.02% and 0.2% respectively and were always included in the appropriate controls. In addition, the effects of PMSF (Phenylmethylsulfonyl Fluoride; 1mM, a serine protease inhibitor) on the binding of anandamide and methanandamide were examined. Due to instability in aqueous media, PMSF was added directly from an isopropanol stock solution prior to incubation. Bound and free radioligand were separated by rapid vacuum filtration using a Brandel cell harvester. The wash buffer was Tris.HCl (50mM, pH7.4), containing bovine serum albumin (2g/l) in order to reduce NSB to Brandel cell harvester tubes. In addition, harvester papers (Whatman GF/B) were soaked in polyethyleneimine (0.5%) and loaded onto the harvester *wet*. Filters were extracted with Optiphase Safe (Whatman, UK) overnight prior to assessing bound radioligand.

### 6.3.4 Data analysis.

See chapter 2.

## **6.4. Results.**

### 6.4.1 Association

The  $K_d$  has been determined kinetically by calculating the rates of specific (70%) binding association and dissociation using a fixed concentration ( $\sim$ 0.2nM) of [ $^3$ H]SR141716A.  $K_{+1}$  is calculated by subtracting  $K_{-1}$  from  $K_{ob}$  and dividing this by the radioligand concentration (see chapter 1). Curves were fitted using Graphpad Prizm and  $K_{-1}$  and  $K_{+1}$ , were expressed

as a ratio which resulted in a calculated  $K_d$  of 0.72nM ( $K_{-1}=1.57 \text{ min}^{-1} / K_{+1}=2.17 \text{ nM}^{-1} \text{ min}^{-1}$ ) (Figure 6.2).

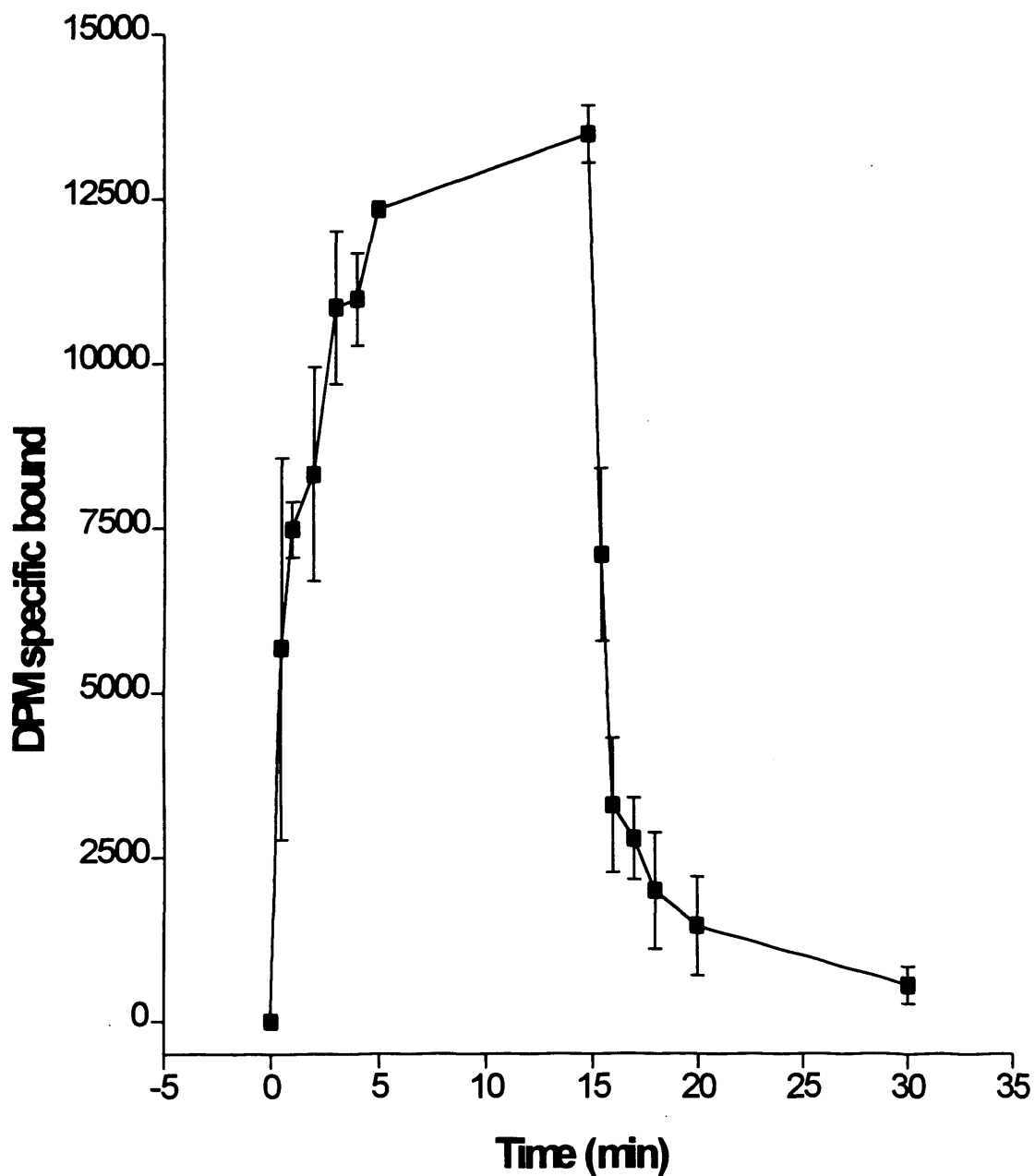


Figure 6.2. Association (0-15 minutes) and dissociation (15-30 minutes, in the presence of unlabeled SR141716A) time course for specific binding of [ $^3\text{H}$ ]SR141716A (0.4nM). Data are mean $\pm$ SEM (n=3).

#### 6.4.2. Saturation

The binding of [<sup>3</sup>H]SR141716A (approximately 0.4nM) to rat cerebella membranes was dose-dependent and saturable (Figure 6.3), Calculation of the saturation data by Scatchard yielded a  $K_d$  and  $B_{max}$  of  $0.61 \pm 0.12$ nM and  $1752 \pm 294$ fmol/mg protein respectively (n=7), (Figure 6.3). At approximately 0.4nM [<sup>3</sup>H]SR141716A the specific binding amounted to  $71.1 \pm 1.5\%$  (n=11) of the total binding.

In SH-SY5Y and NG108-15 cell membranes the determination of  $B_{max}$  and  $K_d$  by saturable binding of [<sup>3</sup>H]SR141716A proved unsuccessful. This is likely to be due to low levels of receptor expression in these cells (data not shown).

#### 6.4.3 Displacement.

A range of cannabinoid ligands produced a dose-dependent displacement of [<sup>3</sup>H]SR141716A binding, (Figures 6.4A and B), with  $K_i$  values and slope factors in rat CBM, as shown in Table 6.6. It should be noted that for some compounds 100% displacement was not achieved due to low solubility. Where 100% displacement was not achieved the one site computer fit was based on a theoretical maximum of 100%. The rank order potency was SR141716A  $\geq$  nabilone  $>$  WIN 55,212-2  $\geq$   $\Delta^9$ -tetrahydrocannabinol  $\geq$   $\Delta^8$ -tetrahydrocannabinol  $>$  anandamide. The affinity for anandamide was increased by co-incubation with PMSF (1mM), a protease inhibitor (Hillard et al., 1995), (Table 6.6).

Displacer	n	pK <sub>i</sub> (nM)	Slope factor
SR141716A	12	8.37±0.07(4.24)	1.15±0.13
Nabilone	3	8.29±0.08(5.0)	0.67±0.06
WIN 55212-2	5	7.75±0.15(17.7)	0.78±0.06
<sup>Δ9</sup> -tetrahydrocannabinol	6	7.29±0.21(51.2)	0.92±0.12
<sup>Δ8</sup> -tetrahydrocannabinol	4	6.53±0.09(291)	0.82±0.16
Anandamide	4	5.92±0.04(1181)	1.15±0.17
+PMSF(1mM)	3	6.26±0.13(545)*	0.74±0.27

Table 6.6. K<sub>i</sub> and slope factors for a range of natural and synthetic cannabinoids. Data are Mean±SEM and are derived from the curves in Figure 6.4A and B, excluding PMSF data which is derived from curves not shown. \*=Significantly (p<0.05) different compared with anandamide. Due to low solubility and hence less than 100% displacement two site fits were not attempted.

In SH-SY5Y cell membranes (287µg protein) Nabilone (10µM) displaced [<sup>3</sup>H]SR141716A (0.5nM) with 2532±232 dpm specific binding, no dose related displacement was observed. In NG108-15 cell membranes (120µg protein) Nabilone (10µM) displaced [<sup>3</sup>H]SR141716A (0.5nM) with 2324±455 dpm specific binding and again no dose related displacement was observed. Data for SH-SY5Y and NG108-15 cell membranes are mean±SEM of 4 experiments.

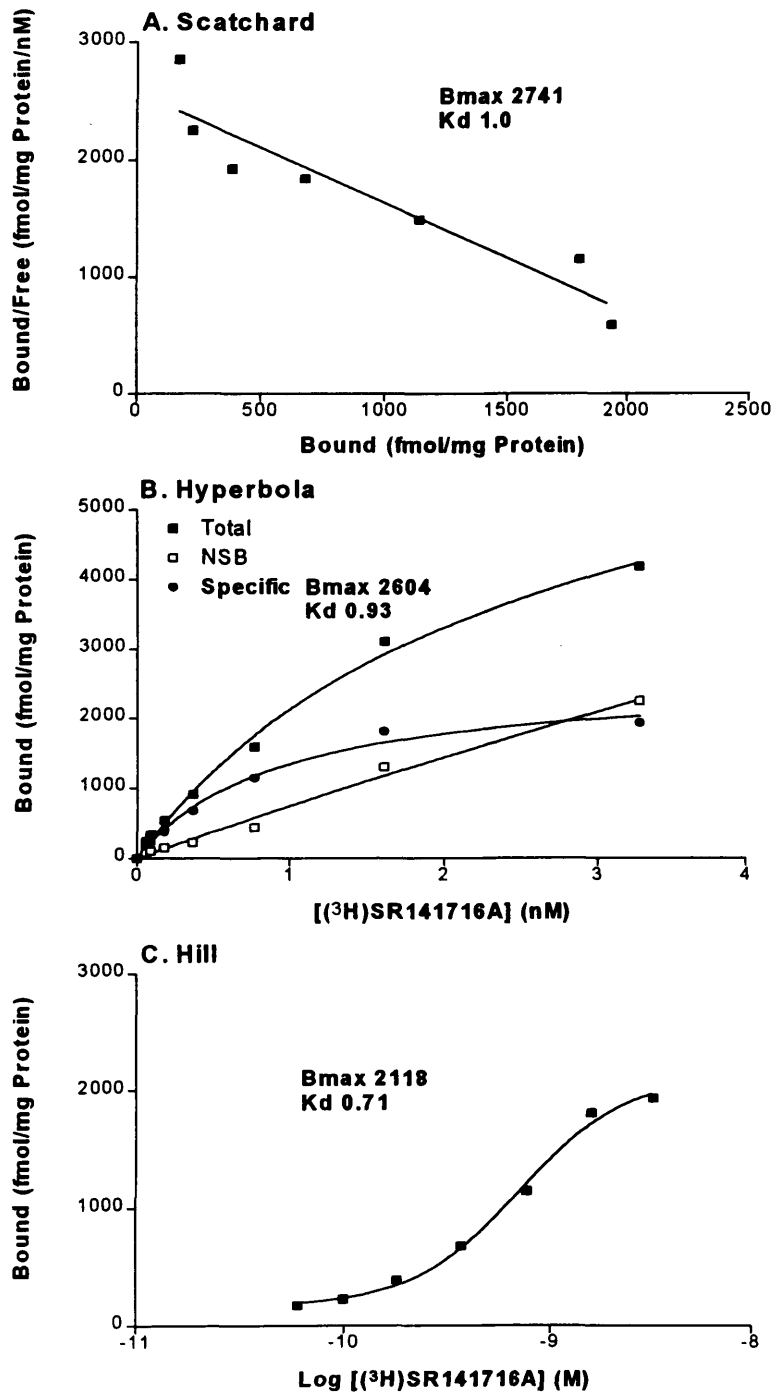


Figure 6.3: Dose dependent and saturable binding of  $[^3H]SR141716A$  to rat cerebella membranes (B, Hyperbola showing Total NSB and specific). Scatchard (A) and Langmuir Hill (C) analysis of specific binding is also shown. Data are from a single experiment from 6 others.  $B_{max}$ =fmol/mg protein:  $K_d$ =nM.

A range of 13 commonly used ligands included at 100 $\mu$ M concentrations caused no more than 39.5% displacement of [ $^3$ H]SR141716A in rat CBM, (Table 6.7).

Ligand	$\mu$ M	% inhibition of specific binding
SR141716A	1	100 $\pm$ 0
Morphine	100	39.5 $\pm$ 15.2
Naloxone	100	13.0 $\pm$ 7.5
Acetylcholine	100	21.9 $\pm$ 12.9
Dopamine	100	21.7 $\pm$ 10.7
Noradrenaline	100	15.7 $\pm$ 9.9
GABA	100	7.4 $\pm$ 3.1
Glutamate	100	2.9 $\pm$ 2.9
ATP	100	1.3 $\pm$ 0.6
Imipramine	100	30.7 $\pm$ 7.2
Hydrocortisone	100	8.8 $\pm$ 4.9
Pancuronium	100	7.6 $\pm$ 6.1
Lignocaine	100	5.5 $\pm$ 5.3
Atropine	100	3.8 $\pm$ 3.3

Table 6.7. Effects of a range of ligands on the binding of [ $^3$ H]SR141716A in rat CBM. Data are Mean $\pm$ SEM (n=3).

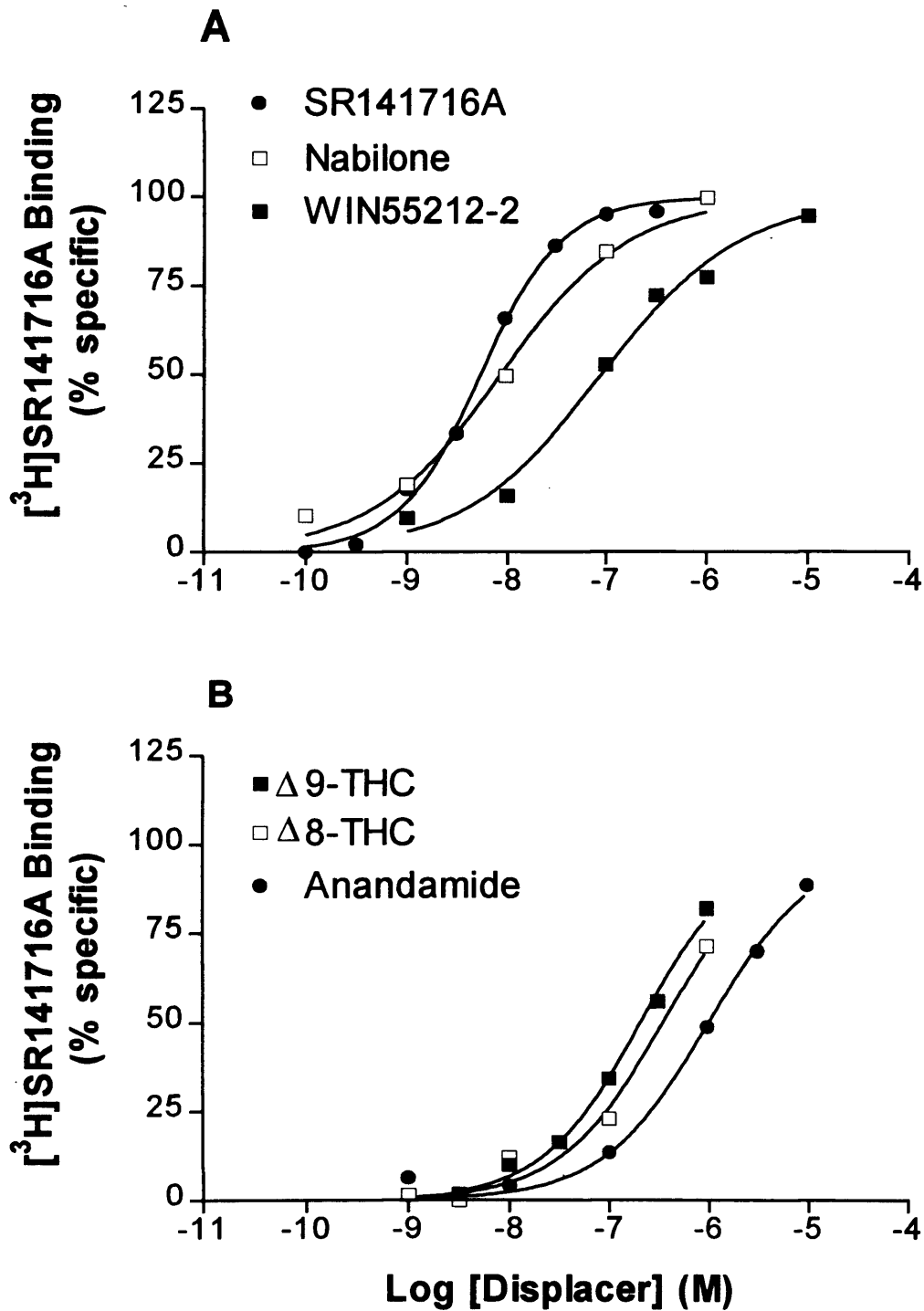


Figure 6.4A: One site competition curves, showing dose related displacement of [<sup>3</sup>H]SR141716A (0.4nM) with SR141716A (●), Nabilone (□), and WIN 55-212-2 (■), and 6.4B, Δ<sup>9</sup>-THC (■), Δ<sup>8</sup>-THC (□) and Anandamide (●). Error bars have been omitted for clarity but an estimate of error is shown in table 6.6.

#### 6.3.4 cAMP inhibition.

In whole SH-SY5Y and NG108-15 cells, nabilone caused a dose dependent inhibition of forskolin ( $1\mu\text{M}$ ) stimulated cAMP formation with respective  $\text{pIC}_{50}$  (nM) and  $I_{\text{max}}$  (%) values of  $7.72\pm 0.26(18.9)$ ,  $7.92\pm 0.16(11.9)$  and  $36.4\pm 4.3$ ,  $30.1\pm 2.9$  (Figure 6.5A). Dose dependent inhibition of basal cAMP formation in rat cerebella membranes was observed using WIN 55,212-2 (figure 6.5B) which yielded a  $\text{pIC}_{50}$  of  $7.61\pm 0.12$  (24nM), the response was abolished by co-incubation with SR141716A ( $1\mu\text{M}$ ,  $3.2\pm 3.2\%$ , figure 6.5B). In addition, carbachol (as a positive control,  $10\mu\text{M}$ ), also inhibited basal cAMP formation in rat cerebella membranes by  $53.8\pm 10.1\%$  and this response was reversed ( $3.4\pm 3.3\%$ ) by co-incubation with atropine ( $1\mu\text{M}$ ) respectively. Due to the timing of the experiments and the availability of SR141716A, experiments to show reversal of nabilone inhibition of forskolin stimulated cAMP formation in NG108-15 and SH-SY5Y cells with SR141716A were not performed.

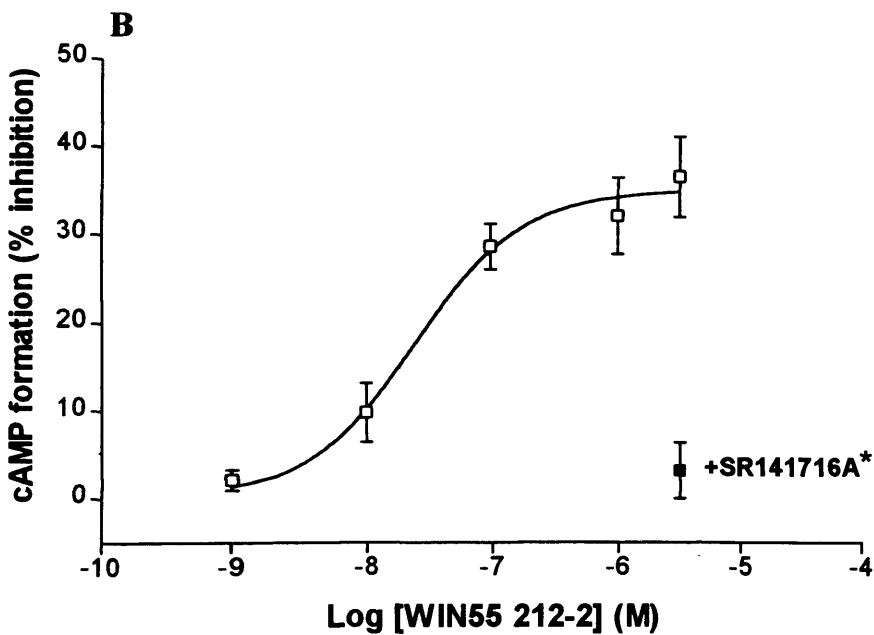
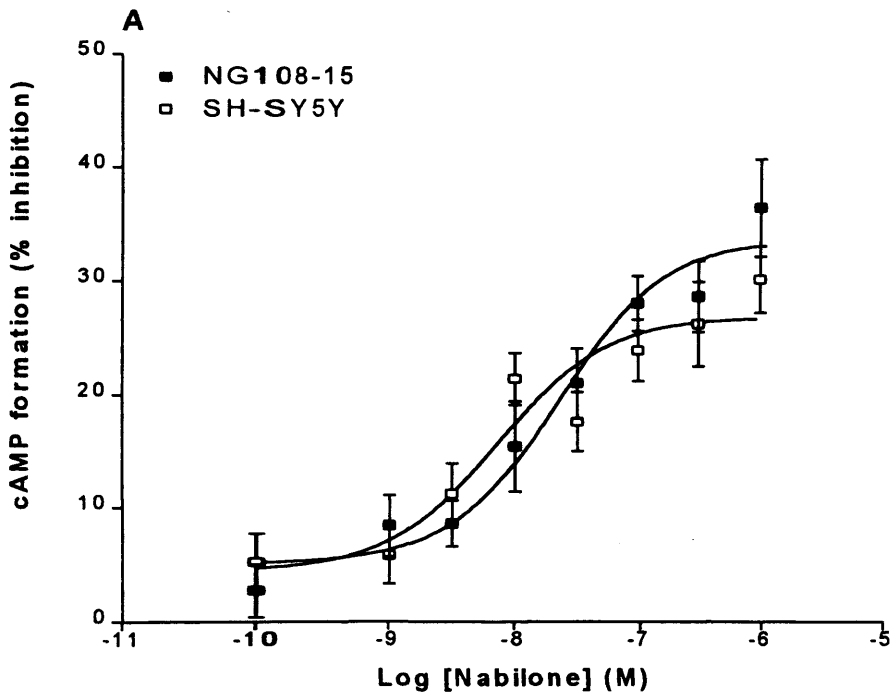


Figure 6.5A. Dose dependent inhibition of forskolin ( $1\mu\text{M}$ ) stimulated cAMP formation in SH-SY5Y and NG108-15 cells with nabilone. Data are mean $\pm$ SEM of 6-8 independent experiments. 6.5B. Inhibition of basal cAMP formation with WIN55212-2 in rat cerebella membranes. Data are mean $\pm$ SEM of 4-6 independent experiments. \*Statistically ( $p<0.05$ ) reduced compared with WIN55-212 ( $3\mu\text{M}$ ).

## **6.5. Discussion.**

The results show the successful development of a cannabinoid binding assay, and report the use, in cerebella, SH-SY5Y and NG108-15 membranes, of the newly available CB1 selective cannabinoid receptor antagonist SR141716A in both radiolabelled and unlabelled form. In rat CBM, the binding of [<sup>3</sup>H]SR141716A is time- and dose-dependent, saturable, and displays relatively high affinity. The K<sub>d</sub> of 0.4-2.0nM compares favorably with the figure of 1.98nM (K<sub>i</sub>) in rat brain and 5.6nM (K<sub>i</sub>) in CHO cells expressing CB1 receptors quoted by Rinaldi-Carmona et al (1994, 1995) in displacement studies using [<sup>3</sup>H]CP55,940 as the radioligand. In addition, Rinaldi-Carmona and colleagues [1996] reported an affinity of 0.61nM for [<sup>3</sup>H]SR141716A in rat forebrain membranes. In rat CBM, B<sub>max</sub> (1.8pmol/mg protein) values for [<sup>3</sup>H]SR141716A are relatively large but compare favorably with 0.76pmol/mg protein (mean at 4 different temperatures) for [<sup>3</sup>H]CP55,940 in rat forebrain [Hillard et al., 1995], 1.2pmol/mg protein for [<sup>3</sup>H]WIN 55212-2 in cerebellum [Kuster et al., 1993], 2.5pmol/mg protein for [<sup>3</sup>H]CP55,940 in cerebellum [Felder et al., 1992] and 1.9pmol/mg protein for [<sup>3</sup>H]CP55,940 in rat cortical membranes [Devane et al., 1988]. In SH-SY5Y and NG108-15 cell membranes, binding experiments (saturation or displacement) failed to show cannabinoid receptors on either cell type. The specificity of [<sup>3</sup>H]SR141716A for the cannabinoid receptor is confirmed by the inability of a range of non-cannabinoid ligands included at high concentrations to displace [<sup>3</sup>H]SR141716A binding in rat CBM. Moreover, as [<sup>3</sup>H]SR141716A is an antagonist [Rinaldi-Carmona et al, 1994, 1995; Bouaboula et al., 1995; Collins et al., 1995] the binding characteristics will not be influenced by guanine nucleotides.

The cannabinoid receptor binding profiles of a range of unlabelled compounds that interact with the cannabis receptor can be found in the literature but there is considerable variation in the absolute affinities reported and the rank order potencies. For example, K<sub>i</sub> values for  $\Delta^9$ -tetrahydrocannabinol of 1.6nM [Devane et al., 1988], 43nM [Hillard et al., 1995] and 53nM[-isomer], 920nM[+isomer] [Felder et al., 1992] have been reported using

[<sup>3</sup>H]CP55,940, and a value of 10nM has been reported using [<sup>3</sup>H]WIN 55,212-2 [Kuster et al., 1993]. These differences may arise from the use of differing radiolabelled cannabinoid agonists or differing assay systems. In this chapter the radiolabelled agonists ([<sup>3</sup>H]WIN 55,212-2 and [<sup>3</sup>H]CP55,940) showed promising results in binding experiments, however due to solubility and availability problems they were replaced by [<sup>3</sup>H]SR141716A. In SH-SY5Y and NG108-15 cell membranes, a dose related displacement of [<sup>3</sup>H]SR141716A (0.5nM) with nabilone was not observed. However, nabilone included at 10μM consistently displaced [<sup>3</sup>H]SR141716A revealing approximately 2000dpm specific binding in both cells tested. Whether this displacement is at the level of a central cannabinoid receptor remains to be determined.

In both SH-SY5Y and NG108-15 cells, nabilone caused a dose dependent inhibition of forskolin stimulated cAMP formation, with IC<sub>50</sub> values which approximate to the K<sub>i</sub> value for nabilone displacement of [<sup>3</sup>H]SR141716A in rat CBM. These data suggest that there are very few cannabinoid receptor binding sites on SH-SY5Y and NG108-15 cells, however they can still functionally couple to an inhibition of adenylyl cyclase. In rat CBM, the cannabinoid agonist WIN55212-2 also caused a dose dependent inhibition of forskolin stimulated cAMP formation, a response which was reversed by SR141716A (1μM). In conclusion, high levels of cannabinoid receptors exist in rat CBM, whereas SH-SY5Y and NG108-15 cell membranes express very low levels. Moreover, the low levels of receptor on SH-SY5Y and NG108-15 cell membranes couple strongly to the inhibition of adenylyl cyclase. Cannabinoid induced inhibition of adenylyl cyclase can be demonstrated using rat cerebella membranes, and this effect can be reversed by SR141716A. The new antagonist SR141716A will prove to be a useful tool for the study of CB1 receptor pharmacology.

**CHAPTER 7. FUNCTIONAL EXPRESSION OF THE RECOMBINANT CENTRAL  
CANNABINOID RECEPTOR.**

## **7.1. Introduction.**

The pharmacologically active constituent of *cannabis sativa* is  $\Delta^9$ -THC which has been shown to cause CNS depression, analgesia, anti-inflammation and immunosuppression [reviewed by Martin, 1986]. The hydrophobic nature of cannabinoids led to the notion that these compounds exerted their effects in a similar fashion to anaesthetic agents, that is they disrupt cell membranes in a non-specific manner [Lawrence and Gill, 1975]. However, the hypothesis was that some of the effects of cannabinoids were due to interactions with specific binding sites [Martin, 1986]. The introduction of the potent non-classical cannabinoid, [ $^3\text{H}$ ]CP55,940 led to its use in radioligand binding experiments using brain membrane preparations [Devane et al, 1989] and in brain radio-imaging [Herkenham et al, 1990]. The discovery of specific cannabinoid binding sites were interpreted as evidence for a new putative cannabinoid receptor.

The cloning of cannabinoid receptors from brain (CB1) [Matsuda et al, 1990] and peripheral (spleen, CB2) tissue [Munro et al, 1993] has revitalised the interest in cannabinoid pharmacology. The cloned receptors demonstrate a prototypical G-protein linked structure, with seven hydrophobic membrane spanning domains and several potential glycosylation sites. Translation of the CB1 cDNA resulted in a protein product consisting of 473 amino acids. The central cannabinoid receptor and the peripheral receptor share only approximately 44% overall homology, with 68% homology in the membrane spanning regions [Munro et al, 1993]. Both the CB1 and CB2 receptors are coupled to a pertussis toxin sensitive G-protein which when activated results in agonist inhibition of adenylyl cyclase [Matsuda et al, 1990; Felder et al, 1995]. The CB1 receptor also produces an inhibition of VOCC (N-type [Mackie and Hille, 1992]), blockade of long term potentiation [Collins et al, 1995], modulation of potassium-A currents [Deadwyler et al, 1995], inhibition of  $\text{Na}^+\text{K}^+$ - and  $\text{Mg}^{2+}\text{Ca}^{2+}$ -ATPase [Bloom et al, 1978] and an activation of mitogen-activated protein kinase [Bouaboula et al, 1995]. Recently, the presence of a truncated and modified isoform of the central cannabinoid receptor was discovered [Shire et al, 1995], and termed CB1a. The pharmacology of CB1a was almost identical to CB1

except that agonist binding affinity to CB1a was slightly reduced when compared with CB1 [Rinaldi-Carmona, 1996].

The identification of specific cannabinoid receptors in the CNS led to the search for an endogenous ligand(s). A brain constituent was soon isolated from porcine tissue which bound to the CB1 receptor with a high affinity. This compound was arachidonylethanolamide, an arachidonic acid derivative which was named anandamide [Devane et al, 1992]. The progress of cannabinoid pharmacology was aided further by the synthesis of a CB1 specific antagonist, SR141716A [Rinaldi-Carmona et al, 1994; see chapter 6].

The cloned CB1 receptor has been functionally expressed in CHO [Matsuda et al, 1990], AtT-20 [Felder et al, 1995] and murine Ltk- cells [Felder et al, 1992]. Here, an attempt will be made to amplify CB1 cDNA, and functionally express cloned central cannabinoid receptors in CHO cells. The resulting CB1 transfects will then be used in order to study receptor binding profiles and agonist inhibition of adenylyl cyclase and the data will be compared with rat cerebella (chapter 6).

met-lys-ser-ile-leu-asn-gly-leu-ala-asp-thr-thr-phe-arg-thr-ile-thr-thr-asp-leu-leu-tyr-val-gly-ser-asn-asp-ile-gln-tyr-glu-asp-ile-lys-gly-asp-met-ala-ser-lys-leu-gly-tyr-phe-pro-gln-lys-phe-pro-leu-thr-ser-phe-arg-gly-ser-pro-phe-gln-glu-lys-met-thr-ala-gly-asp-asn-ser-pro-leu-val-pro-ala-gly-asp-thr-thr-

1. asn-ile-thr-glu-phe-tyr-*asn*-lys-ser-leu-ser-ser-phe-lys-glu-asn-glu-glu-asn-ile-gln-cys-gly-glu-*asn*-phe

-met-asp-met-glu-cys-phe-met-ile-leu-*asn*-pro-ser-

2. gln-gln-leu-ala-ile-ala-val-leu-ser-leu-thr-leu-gly-thr-phe-thr-val-leu-glu-*asn*-leu-leu-val-leu-cys-val-ile-leu-his-ser-arg-ser-leu-

3. arg-cys-arg-pro-ser-tyr-his-*phe*-ile-gly-ser-leu-ala-val-ala-asp-leu-leu-gly-ser-val-ile-*phe*-val-tyr-

ser-phe-val-asp-phe-his-val-phe-his-arg-lys-asp-ser-pro-asn-val-phe-leu-phe-lys-

4. leu-gly-gly-val-thr-ala-ser-phe-thr-ala-ser-val-gly-ser-leu-*phe*-leu-thr-ala-ile-asp-arg-tyr-

ile-ser-ile-his-arg-pro-leu-ala-tyr-lys-arg-ile-val-thr-arg-pro-lys-ala-val-

5. val-ala-*phe*-cys-leu-met-trp-thr-ile-ala-ile-val-ile-ala-val-leu-*pro*-leu-leu-gly-trp-*asn*-cys-lys-lys-

leu-gln-ser-val-cys-ser-asp-ile-phe-pro-leu-ile-asp-glu-thr-tyr-lue-met-phe-trp-ile-gly-val-thr-ser-

val-leu-leu-leu-*phe*-ile-val-tyr-ala-tyr-met-tyr-ile-leu-trp-lys-ala-his-ser-his-

6. ala-val-arg-met-ile-gln-arg-gly-thr-gln-lys-ser-*ilr*-ile-ile-his-thr-ser-glu-asp-gly-

lys-val-gln-val-thr-arg-pro-asp-gln-ala-arg-met-

7. asp-ile-arg-leu-ala-lys-thr-leu-val-leu-ile-leu-val-val-leu-ile-ile-cys-trp-gly-*pro*-leu-

leu-ala-ile-met-val-tyr-asp-val-phe-gly-lys-met-*asn*-lys-leu-ile-lys-thr-val-phe-ala-phe-cys-ser-met-

leu-cys-leu-leu-*asn*-ser-thr-val-*asn*-*pro*-ile-ile-tyr-ala-leu-arg-ser-lys-asp-leu-arg-his-ala-*phe*-arg-

ser-met-phe-pro-ser-cys-gly-gly-thr-ala-gln-pro-leu-asp-*asn*-ser-met-gly-asp-ser-asp-cys-leu-his-lys-

his-ala-*asn*-*asn*-thr-ala-ser-met-his-arg-ala-ala-glu-ser-cys-ile-lys-ser-thr-val-lys-ile-ala-lys-val-thr-

met-ser-val-ser-thr-asp-thr-ser-ala-glu-ala-leu

Figure 7.1. The translated primary structure of the cloned CB1 receptor. The predicted hydrophobic domains are shown (1-7), bold amino acids are those that are highly conserved among other G-protein coupled receptors. Italic, bold, underlined asparagine residues are potential N-glycosylation sites. [Taken from Matsuda et al, 1990].

## **7.2 Methods.**

For details of chemicals, tissue culture, membrane preparation, cAMP measurement and data analysis the reader is directed to chapter 2.

### **7.2.1 CB1 cDNA Amplification.**

A small aliquot (approx. 10 $\mu$ l) of cloned CB1 receptor DNA inserted into pGEM mammalian expression plasmid was a kind gift from Dr D. K. Grandy, Vollum Institute, Portland, Oregon. In order to obtain enough cDNA for transfection into CHO cells, multiple copies of the plasmid were made using E. coli.

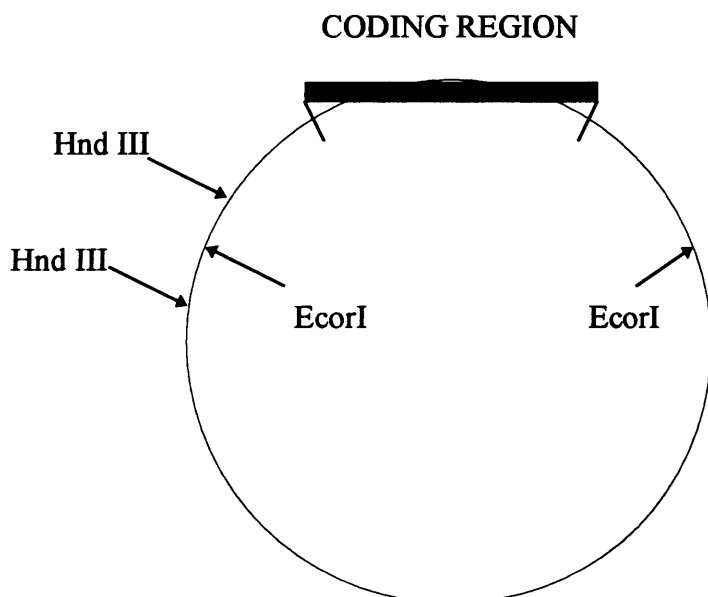


Figure 7.2. Schematic diagram of pGEM expression plasmid, the coding region is the position of CB1 cDNA along with ampicillin and geneticin resistance. The restriction endonuclease (EcorI and HndIII) sites are also indicated (arrows). The plasmid consists of approximately 2700 base pairs.

(i) *In order to make E.coli bacterial cells competent for cDNA uptake.*

5ml of an overnight culture was mixed into 200ml of pre-warmed nutrient agar media. The cells were grown to an optical density(600nm) of 0.5-1. The cells were sedimented at 5000rpm for 4 mins. The cells were then re-suspended in 5mls of ice cold buffer A (10mM MOPS 10mM RbCl, pH7.0). 2.5ml of the suspension was made up to 25ml with buffer A. The suspension was centrifuged at 5000rpm for 5minutes. The cells were then re-suspended in 2.5ml of buffer B (10mM MOPS, 50mM CaCl<sub>2</sub> and 10mM RbCl at pH6.5), the volume was increased to 30mls using buffer B. The suspension was left on ice for 30minutes. The cells were then pelleted at 5000rpm for 5 minutes and the cells resuspended in 6ml of buffer B containing 15%v/v glycerol. The resulting competent cells were aliquoted into 0.5ml volumes and snap frozen at -70°C.

(ii) *Transformation of plasmid DNA into competent E.coli.*

S.O.B media was made (Tryptone 2%, yeast 0.5%, 0.5g/l NaCl, 25mM KCl, pH7.0 made up to 1 litre with water). This was then autoclaved to sterilise the media. Prior to use of media, 5ml of 2M MgCl<sub>2</sub> was added per litre. 100 ml of S.O.C media (S.O.B without MgCl<sub>2</sub> containing 20mM sterile glucose) was made. The competent bacteria were thawed out and 100µl of the cell suspension was inoculated with 5µl of the plasmid DNA. The cells were then incubated on ice for 30 minutes. The cells were then heat shocked by incubation at 60°C for 1 minute. 0.9ml of S.O.C was then added at room temperature, and the cells were plated out (1µl, 10µl and 100µl) on nutrient agar plates containing 100µg/ml ampicillin. The plates were incubated at 37°C overnight and the resulting ampicillin resistant colonies containing the plasmid DNA were visible. Several colonies were selected and used to inoculate 2 litres of nutrient agar broth. The bacteria were then incubated overnight.

*(ii) DNA purification using QIAGEN plamid purification kit.*

The bacterial cells were harvested at 4°C for 15 minutes at 5000rpm. The supernatant was then removed and 4ml of buffer 1 (100µg/ml RNase A, 50mM Tris-HCl, 10mM EDTA at pH8.0) was added to the pellet and the bacteria were thoroughly re-suspended. 4ml of buffer 2 (200mM NaOH, 1% SDS) was added in order to cause complete cell lysis. The lysate was incubated at room temperature for 5 minutes. 4ml of chilled buffer 3 (3.0 M potassium acetate, pH5.5) was added and mixed. The mixture was centrifuged at 4°C for 30min at 15000rpm and the supernatant removed promptly. The QIAGEN columns were equilibrated by applying 4ml of QBT buffer (750mM NaCl, 50mM MOPS, 15% ethanol, 0.15% triton-X100, pH7.0). The supernatant containing the plasmid was then placed onto the QIAGEN columns which was allowed to enter the resin by gravity. The resin was then washed with 2X10ml of buffer QC (1M NaCl, 50mM MOPS, 15% ethanol, pH7.0). The DNA was eluted with 5ml of buffer QF (1.25M NaCl, 50mM Tris-HCl, 15% ethanol at pH8.5). The resulting DNA was precipitated with 0.7 volumes of isopropanol at room temperature. The precipitate was centrifuged at 15000rpm for 30minutes and the supernatant was carefully removed. The DNA pellet was then washed with 5ml of 70% ethanol and the DNA pellet was resuspended in 300µl of sterile water. The yield was roughly determined using a UV spectrophotometer set at 260nm, where absorption is directly proportional to the amount of DNA.

*(iii) Analysis of plasmid purity by DNA digestion.*

2x2µl of the purified plasmid DNA along with 2x2µl of D. K. Grandy's plasmid DNA was digested with 2 restriction enzymes (Ecor1 and Hind3). 1µl of each enzyme was added to 10µl of DNA and 5µl of sterile water. The mixture was incubated for 1 hour at 37°C. A 1% agarose gel was made by dissolving the agarose in TAE buffer (40mM Tris-acetate, 1mM EDTA, pH8.0) containing 10mg/ml ethidium bromide. The solution was microwaved in an NEC microwave oven set on full power for 30 seconds and allowed to cool before pouring. When the gel was set 50ml of TAE was used as the running buffer, the wells were then loaded with a mixture of digested DNA, 1µl of bromophenol blue and 5µl glycerol. The

gel was run at 30mv for 1 hour before photography of the digestion products under UV light.

### 7.2.2. Transfection of Plasmid DNA into CHO cells.

Wild type CHO cells were cultured to approximately 70% confluency prior to transfection. Lipofectin reagent (1:1w/w liposome formulation of the cationic lipid N-[1-(2,3-dioleoyloxy)propyl]-n,n,n-trimethylammonium chloride and dioleoyl

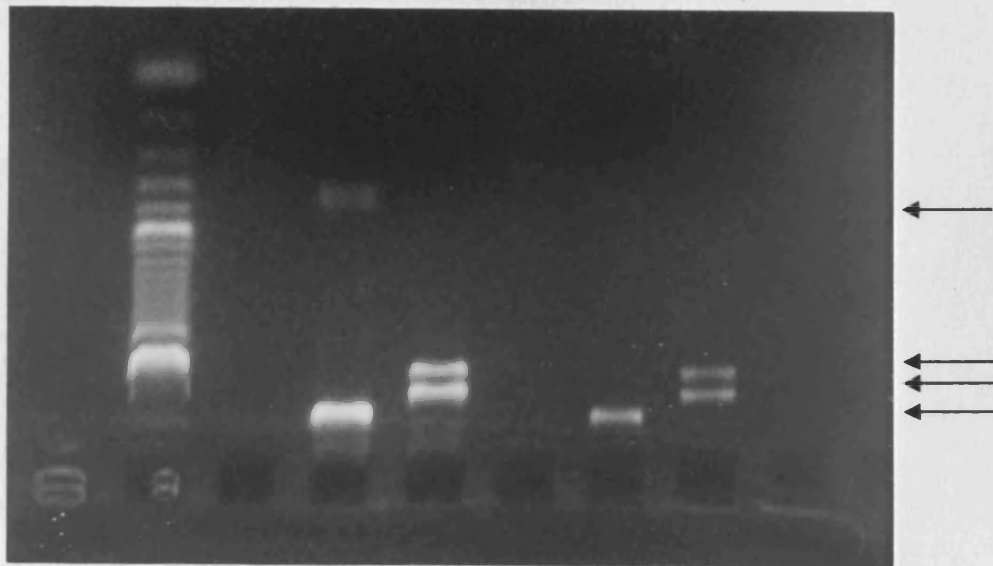
phosphatidylethanolamine in membrane filtered water) was used in order to aid DNA uptake. 5x15µl of the purified cDNA was mixed with 5x100µl of serum free Hams F12 media. In order to optimise the lipofectin concentration, 2, 5, 10, 15 and 20µl of lipofectin was added to 5x100µl of serum free Hams F-12 medium. This was allowed to stand at room temperature for 15 minutes. The DNA and lipofectin were then mixed together and this was allowed to stand at room temperature for 30 minutes. 5x70% confluent monolayers of CHO cells in 20cm<sup>2</sup> flasks were washed with 2ml each of serum free Hams F-12 medium. 0.8ml of serum free Hams F-12 medium was then added to each flask, to this the DNA/lipofectin mixtures were also added. The solution was transferred over the cell monolayer, and the cells incubated a further 12 hours at 37°C in a CO<sub>2</sub> incubator. The cells were then given 5ml of serum containing Hams F-12 medium supplemented with 200µg/ml gentamicin. The gentamicin resistant CHO cells were observed after 5 days, subcultured at 10 days to confluency (21 days) and frozen under liquid nitrogen (see methods, chapter 2). CHO cells transfected using Lipofectin 20µl were used in order to characterise cannabinoid binding and inhibition of adenylyl cyclase. Data presented are from primary transfections as no clonal cell colonies have yet been isolated.

### 7.3 Results.

#### 1. plasmid purity.

The plasmid pGEM containing CB1 cDNA was amplified using *E. coli* and purified using a QIAGEN kit, its purity was confirmed by *Eco*r1 and *Hind*3 digestion products (see figure 7.1 for restriction sites and 7.3 for electrophoretic gel results).

[H]-SR141716A displacement (% specific)



Lane number	1	2	3	4	5
Plasmid		A		B	

Figure 7.3. Agarose (1%) gel electrophoresis of purified (A) and D. K. Grandy's (B) pGEM plasmid both digested with *Eco*r1 (lanes 3 and 5) and *Hind*3 (lanes 2 and 4). Lane 1 shows molecular mass marker. Arrows represent DNA fragments.

## 2. Displacement.

In CHO cell membranes expressing the cloned central cannabinoid receptor, a fixed concentration of [<sup>3</sup>H]SR141716A was displaced in a dose dependent manner by increasing concentrations of SR141716A yielding a pK<sub>i</sub> value of 8.66±0.26 (2.17nM) (figure 7.4).

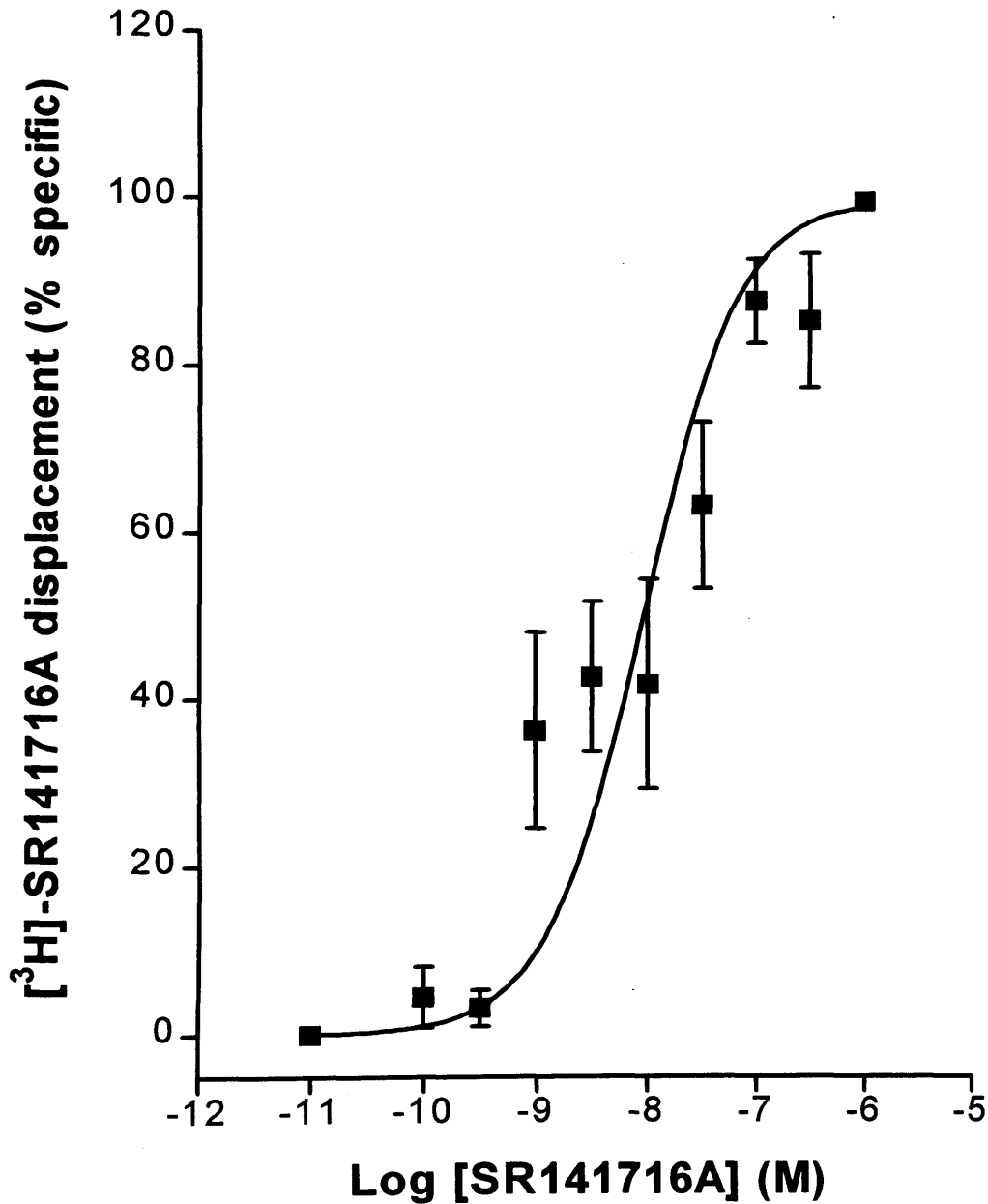


Figure 7.4. Displacement of [<sup>3</sup>H] SR141716A with SR141716A in CHO CB1 cell membranes. Data are mean±SEM of 6 independent experiments. The specific binding ranged from 15-20% in each experiment.

### 3. Inhibition of forskolin stimulated cAMP formation.

Nabilone caused a dose dependent inhibition of forskolin stimulated cAMP formation in whole CHO<sub>CB1</sub> cells with  $pIC_{50}$  and  $I_{max}$  values of  $8.47 \pm 0.53$  (3.4nM) and  $25.5 \pm 4.0$  respectively (figure 7.5).

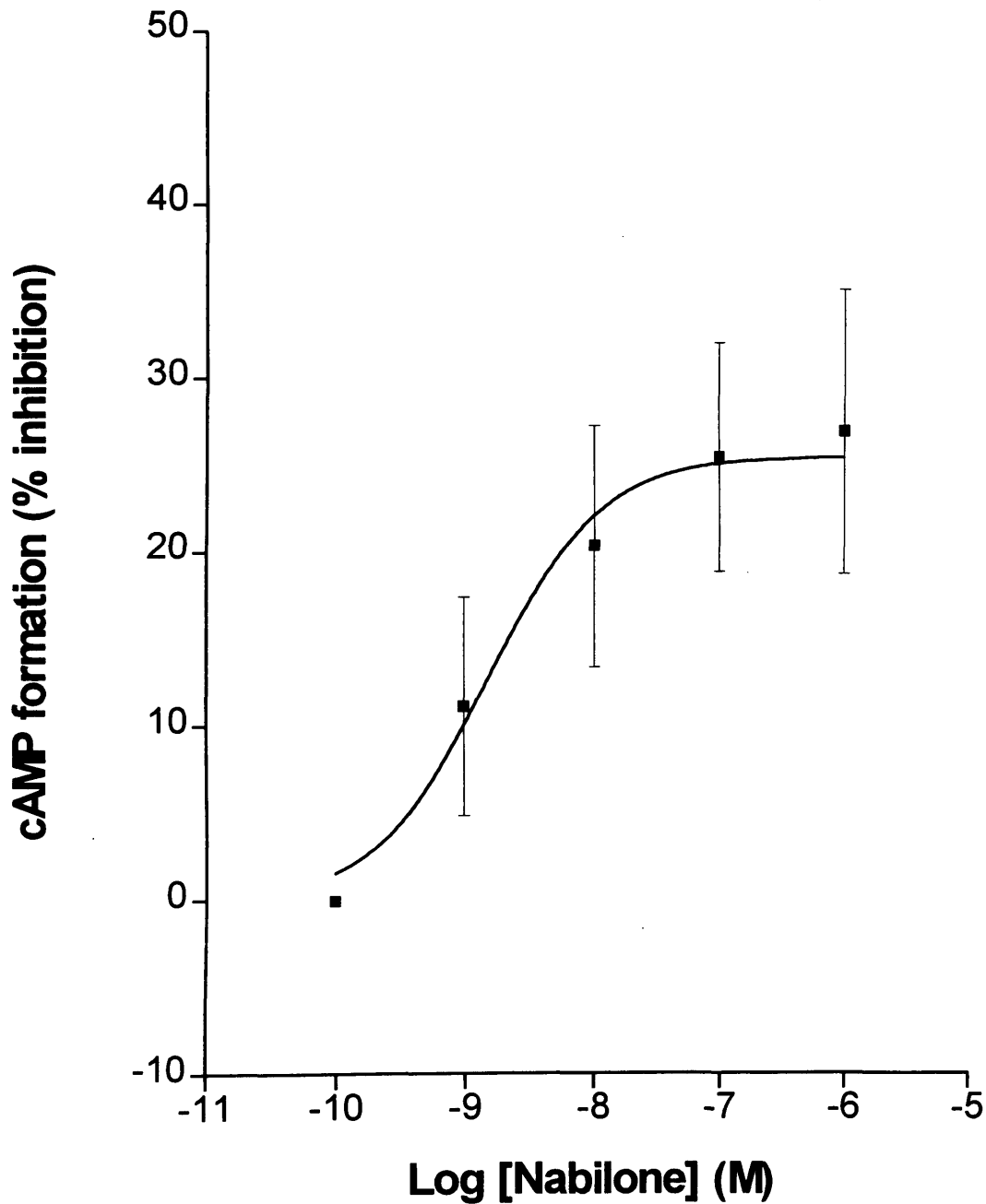


Figure 7.5. Dose dependent inhibition of forskolin (1 $\mu$ M) stimulated cAMP formation by nabilone. Data are mean $\pm$ SEM of 4 independent experiments.

#### **7.4. Discussion.**

Molecular biological techniques have led to the cloning of the central cannabinoid receptor [Matsuda et al, 1990]. This has allowed it to be studied in mammalian expression systems independently of other cannabinoid receptor subtypes and native signal transduction machinery. In transformation experiments, confirmation of plasmid purity was shown using restriction nuclease digestion. These experiments were performed to show that purification of the plasmid was successful, and no quantitative information can be obtained from the gel due to poor discrimination of molecular mass markers.

When CHO cells (lipofectin 20 $\mu$ l, uncloned population) were transfected with cDNA, both a displacement of [<sup>3</sup>H]SR141716A and an inhibition of adenylyl cyclase was observed. CHO CB1 cells showed a similar K<sub>i</sub> value (2.17nM) for [<sup>3</sup>H]SR141716A displacement using SR141716A with that observed in rat cerebella membranes (4.2nM, see chapter 6). In addition, when the CB1 receptor is transfected in murine L cells, SR141716A displaces [<sup>3</sup>H]CP55,940 with a slightly higher K<sub>i</sub> value of 11.8nM [Felder et al, 1995]. The slight difference in K<sub>i</sub> value presented here and that by Felder et al [1995] may result from using a radiolabelled agonist in their study, or be as a result of different levels of expression. Felder reported a B<sub>max</sub> of 7pmol/mg protein on murine L cells [1992], however the density of CB1 receptors on the CHO cells was not measured in this study because the cells first require sub-cloning.

Nabilone, a non-classical cannabinoid agonist, caused a dose dependent inhibition of forskolin stimulated cAMP formation in CHO CB1 cells. The IC<sub>50</sub> and the I<sub>max</sub> values of 3.4nM and 25.5% were similar to those observed using rat cerebella membranes (see Chapter 6). Moreover, a similar IC<sub>50</sub> value of 3.1nM has been reported for nabilone inhibition of cAMP accumulation in murine L cells expressing the CB1 receptor [Felder et al, 1992]. The coupling of the cloned CB1 receptor to adenylyl cyclase has been shown to be mediated via a pertussis toxin sensitive G-protein (Gi/G0) [Felder et al, 1995]. Overall, the results show that cloned CB1 cDNA can be functionally expressed in CHO cells.

However more work is required in order to subclone a population of CHO CB1 cells which express a high density of receptors in a stable fashion.

**CHAPTER 8. DISCUSSION AND SUMMARY**

The relay of information across the plasma membrane requires a multitude of proteins which act in concert to mediate cellular responses. Opioid and cannabinoid receptor mediated signal transduction are good examples of pathways whereby excitable cells can respond to external stimuli to alter the levels of cAMP and phosphorylation which in turn causes changes in cell responsiveness.

### **8.1. Summary of results.**

In SH-SY5Y human neuroblastoma cells, muscarinic receptor occupation and potassium depolarisation both increase intracellular  $\text{Ca}^{2+}$  concentration in a biphasic manner. The free  $\text{Ca}^{2+}$  then binds to calmodulin and activates a  $\text{Ca}^{2+}$ /CaM sensitive isoform of AC. This produced a two-fold increase in basal levels of cAMP. The pools of  $\text{Ca}^{2+}$  which drive this response may originate from extra- or intracellular sources.

SH-SY5Y cells express opioid receptors which bind [ $^3\text{H}$ ]DPN. The  $\mu$ -opioid receptor agonists, fentanyl and DAMGO both displace [ $^3\text{H}$ ]DPN with high affinity in SH-SY5Y cells. Both agonists also caused approximately 50% inhibition of forskolin stimulated cAMP formation, with fentanyl being more potent than DAMGO. In addition, nociceptin, the ligand for the ORL-1 receptor, produced a dose dependent inhibition of forskolin stimulated cAMP formation in SH-SY5Y cells, suggesting the existence of ORL-1 receptors on these cells.

NG108-15 cells also express opioid receptors which bind [ $^3\text{H}$ ]DPN. The  $\delta$ -opioid agonists DPDPE and DADLE both displace [ $^3\text{H}$ ]DPN in cell membranes with a high affinity. In addition, both agonists caused a dose dependent inhibition of forskolin stimulated cAMP formation amounting to approximately 50%.

Fentanyl and DAMGO using CHO $\mu$ , DPDPE and DADLE using CHO $\delta$ , and spiradoline using CHO $\kappa$  cells produced both a displacement of [ $^3\text{H}$ ]DPN and an inhibition of forskolin stimulated cAMP formation.

Removal of the final 37 C-terminal amino acids from the  $\delta$ -opioid receptor had the effect of increasing [ $^3$ H]DPN binding affinity some 2.5-3 fold when compared with intact or truncated (removal of the final 15 C-terminal amino acid)  $\delta$ -opioid receptors. When DPDPE was used to displace [ $^3$ H]DPN in CHO cells expressing C-terminal truncation (C-37 and C-15) mutants of the  $\delta$ -opioid receptor, its binding affinity was increased with the removal of the final 15 or 37 C-terminal amino acids. These data suggests that the C-terminus of the  $\delta$ -opioid receptor may convey to the receptor the ability to bind ligands. However, the functional coupling of these truncated (C-37 and C-15)  $\delta$ -opioid receptors to adenylyl cyclase remains unaffected, as both DPDPE and DADLE caused a maximal inhibition (40-50%) of forskolin stimulated cAMP formation which was comparable with CHO cells expressing the intact  $\delta$ -opioid receptor. The pIC<sub>50</sub> values for adenylyl cyclase inhibition by DPDPE and DADLE was decreased slightly in CHO cells expressing truncated (C-15 and C-37)  $\delta$ -opioid receptors, this is likely to have little functional significance.

The effect of receptor expression levels on ligand binding and inhibition of adenylyl cyclase was addressed using CHO $\delta_{low}$  and CHO $\delta_{high}$  (4.6 fold more receptors than CHO $\delta_{low}$ ) cells. The K<sub>d</sub> for [ $^3$ H]DPN binding and the K<sub>i</sub>H for DPDPE and DADLE displacement were not significantly different in the two populations. In addition, both high and low expressing cells produced a similar (40-50%) maximal inhibition of adenylyl cyclase. However, the IC<sub>50</sub> value for DPDPE inhibition of adenylyl cyclase in CHO $\delta_{low}$  was approximately 20 fold higher than that in CHO $\delta_{high}$ , the reason for this is unclear, but may relate to Na<sup>+</sup> sensitive opioid receptor binding and function.

The successful development of a cannabinoid binding assay, revealed that the CB1 selective antagonist SR141716A in both labeled and unlabeled form bound to its receptor in rat CBM with relatively high (0.4-2nM) affinity. A range of commonly used non-cannabinoid ligand failed to displace [ $^3$ H]SR141716A, demonstrating its cannabinoid selectivity. The CB1 binding profiles of a range of unlabeled compounds that interact with

the cannabinoid receptor, revealed rank order potency of SR141716A > nabilone > WIN55212-2 >  $\Delta^9$ -THC >  $\Delta^8$ -THC > anandamide. Moreover, the binding affinity of anandamide was doubled in the presence of the serine protease inhibitor, PMSF. In NG108-15 and SH-SY5Y cells, nabilone caused a dose dependent inhibition of forskolin stimulated cAMP formation. Binding experiments using these cells revealed very low levels of CB1 expression, however functional inhibition of adenylyl cyclase was readily measured, which suggests that the few receptors present are functionally coupled. In rat CBM, WIN55212-2 also caused a dose dependent inhibition of AC, this effect was reversed by co-incubation with SR141716A.

Using CHO<sub>CB1</sub> cells, [<sup>3</sup>H]SR141716A was displaced in a dose dependent manner by unlabelled SR141716A, and nabilone inhibited forskolin stimulated cAMP formation in these cells, both effects demonstrating successful transfection and expression of CB1 receptors.

## **8.2. Regulation of AC in SH-SY5Y cells by muscarinic and depolarisation induced increases in $[Ca^{2+}]_i$ .**

There have been a number of reports in the literature which show that muscarinic phospholipase C coupled receptors can activate adenylyl cyclase [Baumgold et al, 1992; Jansson et al, 1991; Nakagawa-Yagi et al, 1991; Baumgold et al, 1992<sup>a</sup>; Suh and Kim, 1995; Felder et al, 1989]. Collectively, these studies have shown inconsistent results as to the role of  $Ca^{2+}$  and other regulatory molecules (CM, PKC, PKA,  $\beta\gamma$ ) in the response. Felder and Nakagawa-Yagi both suggested that increases in  $[Ca^{2+}]_i$  induced by PLC coupled muscarinic receptors via  $Ca^{2+}$ /CM pathway in A9L(M1) and SH-SY5Y cells. Jansson et al demonstrated that muscarinic receptor linked elevation of cAMP was due to both  $Ca^{2+}$  and PKC. However, Baumgold and coworkers have shown that  $[Ca^{2+}]_i$  chelation does not effect carbachol stimulated rises in cAMP formation in SK-N-SH cells. It is interesting that these reports concentrate on  $Ca^{2+}$  and events due to PLC coupled receptor occupation, when other mechanisms for elevation of  $[Ca^{2+}]_i$  may also be important. None of these workers have studied the effect of VOCC gated  $Ca^{2+}$  influx following a depolarisation stimulus on AC activity. It is also important to know which particular isoform of AC is expressed in the different cells tested, as all isoforms have differential regulatory properties [Cooper et al, 1995].

The results from this thesis show a complete pharmacological picture of events which is shown in some detail in figure 8.1. AC in SH-SY5Y cells is stimulated some 2 fold over basal levels by carbachol ( $EC_{50}$ , 5 $\mu$ M), in agreement with a previous study [Jansson et al, 1991]. Activated PLC coupled  $M_3$  muscarinic receptors [Lambert et al, 1989] cause a biphasic increase in intra-cellular  $Ca^{2+}$  concentration. The pools of  $Ca^{2+}$  which are mobilised are of an intra- and extra-cellular origin. Both pools of  $Ca^{2+}$  influence the activity of a  $Ca^{2+}$  sensitive isoform of AC (figure 8.1).

Carbachol increased cAMP formation in the presence of  $Ni^{2+}$  at early time points but had no effect at later 5 and 10 minute time points (figure 3.3).  $Ni^{2+}$  blocks  $Ca^{2+}$  entry, and the

area under the curves represent the approximate contribution of intra- (+Ni<sup>2+</sup>) and extra-cellular (-Ni<sup>2+</sup>) Ca<sup>2+</sup> in the cAMP response. The area under the curve in the absence of Ni<sup>2+</sup> represents the maximal (100%) response to carbachol, whereas the area under the curve in the presence of Ni<sup>2+</sup> represents the response caused by intracellular Ca<sup>2+</sup> alone (approximately 33% of the total response). The difference (~66%) results from extracellular Ca<sup>2+</sup> entry (figure 8.1).

In Ca<sup>2+</sup> replacement experiments (figure 3.4) carbachol stimulated cAMP formation was 75% above basal levels even when incubated in nominally Ca<sup>2+</sup> free buffer, there was a subsequent increase in cAMP formation upon Ca<sup>2+</sup> re-addition totaling to a doubling of basal levels. However, from Ca<sup>2+</sup> replacement experiments, the relative proportion of extra- and intracellular Ca<sup>2+</sup> involved in this effect cannot be estimated, because nominally Ca<sup>2+</sup> free buffer contained  $\mu$ M levels of Ca<sup>2+</sup>, which could contribute to the intracellular Ca<sup>2+</sup> driven response. In addition, it may be argued that complete saturation of the response was not achieved at the 3 minute point when Ca<sup>2+</sup> was added to the buffer. Further experiments may reveal that the  $\mu$ M levels of [Ca<sup>2+</sup>]<sub>e</sub> can drive AC activation and hence may be the reason for not achieving a plateau effect at 3 minutes.

There have been no reports in the literature which have studied K<sup>+</sup> stimulated cAMP formation in any detail, even though it is well known that depolarisation of a neuronal membrane causes opening of VOCCs leading to a elevation of [Ca<sup>2+</sup>]<sub>i</sub> [Lambert et al, 1990 ; Morton et al, 1992; Hirota and Lambert, 1997].

The results show that potassium depolarisation also results in a similar (to carbachol) two fold activation of AC (EC<sub>50</sub>, 34mM) an effect which is blocked by co-incubation with Ni<sup>2+</sup>, therefore the Ca<sup>2+</sup> stimulus results solely from an extracellular pool, and probably via opening of VOCCs in the plasma membrane [Morton et al, 1992](figure 8.1).

The EC<sub>50</sub> for carbachol activated AC activity in SH-SY5Y cells correlates very closely with carbachol stimulated increases in Ins(1,4,5)P<sub>3</sub> formation [Smart et al, 1994] and

[Ca<sup>2+</sup>]<sub>i</sub> [Lambert and Nahorski, 1990]. Moreover, the EC<sub>50</sub> for potassium stimulated AC activity correlates closely with that for potassium stimulated intracellular Ca<sup>2+</sup> increases [Lambert et al, 1992]. Both observations indicate that Ca<sup>2+</sup> stimulated cAMP formation is tightly coupled to changes in intracellular Ca<sup>2+</sup> concentrations.

The role of PKC in the muscarinic activation of AC was excluded by the result which showed that the PKC inhibitor RO318220 did not affect the overall response. The bioactivity of this compound has been proven in previous studies from our laboratory [Smart et al, 1995]. This finding is inconsistent with the study by Jansson et al (1991), who showed that muscarinic receptor linked elevation in SH-SY5Y cells was mediated at least in part by PKC. The reasons for these contradictory findings are unclear. They could be due to differences in SH-SY5Y cell culture and hence differential AC, muscarinic receptor, or PKC isoenzyme expression, or could simply be due to experimental design differences.

The active role of calmodulin in both carbachol and potassium stimulated increases in cAMP formation was confirmed with the abolition of the response using the calmodulin antagonist trifluoperazine. This is in agreement with other reports in the literature [Baumgold et al, 1992; Felder et al, 1989; Nakagawa-Yagi et al, 1991]. In addition, calmodulin enhanced the production of cAMP in membranes prepared from SH-SY5Y cells (table 3.4). These findings are similar to other workers [Baumgold et al, 1992; Felder et al, 1989; Nakagawa-Yagi et al, 1991], and implicate neuronal Ca<sup>2+</sup>/CaM sensitive isoform(s) of AC are expressed in SH-SY5Y cells. Indeed, the isoform of AC which is predominantly expressed in SH-SY5Y cells is type 1 (Gilman, A. University Department of Pharmacology, Dallas, Texas, USA. Personal communication).

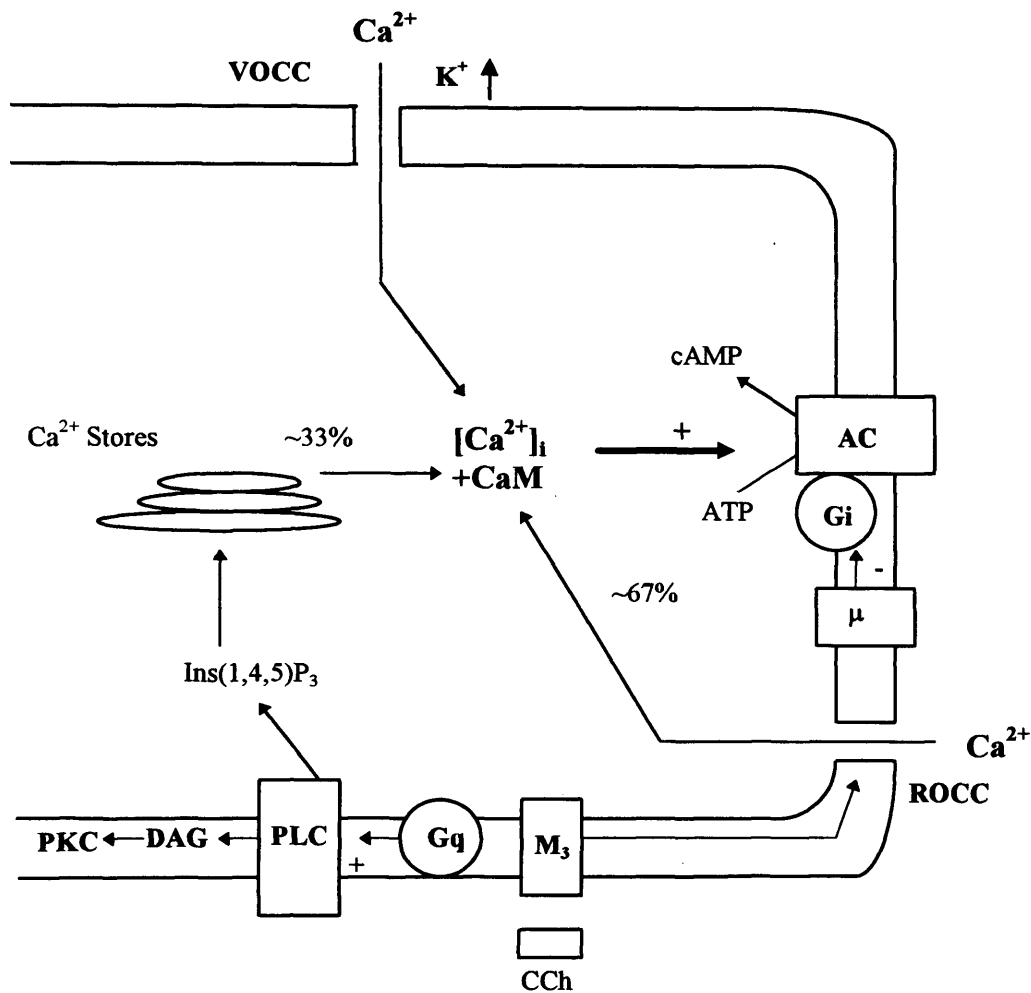


Figure 8.1. Calcium/calmodulin (CaM) activation of adenylyl cyclase in SH-SY5Y cells. Carbachol (CCh) binds to a M<sub>3</sub> muscarinic receptor which causes activation of phospholipase C (PLC) via Gq. PLC hydrolyses phosphoinositide to form inositol 1,4,5 triphosphate (Ins(1,4,5)P<sub>3</sub>) and diacylglycerol (DAG). DAG activates protein kinase C (PKC). Ins(1,4,5)P<sub>3</sub> releases Ca<sup>2+</sup> from internal stores and when it binds Calmodulin (CaM) is able to activate AC. Receptor (ROCC) or voltage operated Ca<sup>2+</sup> channels (VOCC) also increase intracellular Ca<sup>2+</sup> concentration, and this also binds CaM to activate AC. Approximately 33% of total AC activation via muscarinic receptor occupation results from intracellular release of Ca<sup>2+</sup> whereas approximately 67% comes from extracellular pools.

It is clear that receptor-effector cross-talk exists between muscarinic receptors coupled to PLC and AC activation in neurones. The physiological relevance of this phenomenon remains to be elucidated and should present new challenges for future researchers.

### **8.3. Opioid Receptor Agonist Affinity and Potency - Effect of Assay Conditions.**

As early as 1974, Pert and Snyder showed that the presence of  $\text{Na}^+$  in the binding medium reduced the affinity of opioid agonists while having no effect on the binding of opioid antagonists. In addition to effects of  $\text{Na}^+$  on opioid receptor binding, agonist binding is also influenced by GTP, the rate of agonist dissociation was shown to be increased in the presence of GTP [Blume, 1978]. Ions and nucleotides are thought to induce a conformational change in the opioid receptor, whereas agonists display high ( $-\text{Na}^+/\text{GTP}$ ) and low ( $+\text{Na}^+/\text{GTP}$ ) affinity for the two receptor states [Simon et al, 1975].

Nijssen et al (1988) showed that in the absence of  $\text{Na}^+$  and GTP opioid agonists displayed affinity values in the nM range whereas in the presence of  $\text{Na}^+$  and GTP the same agonists caused functional inhibition of adenylyl cyclase in the  $\mu\text{M}$  range. In the same study these workers hypothesised about the lack of correlation between opioid inhibited AC and high affinity opioid receptor binding site and concluded that the low affinity state of the receptor was able to cause functional inhibition of AC in agreement with other studies [Werling et al, 1985; Puttfarcken and Cox, 1989].

The binding data in this thesis was performed on membranes in Tris buffer in the absence of GTP and  $\text{Na}^+$  whereas the inhibition of cAMP formation was performed on whole cells ( $+\text{[GTP]}_i$ ) in Krebs buffer containing mM concentrations of extracellular  $\text{Na}^+$ . Therefore, the correlation between high affinity sites and functional inhibition of AC is difficult to make. However, the majority of the  $\text{IC}_{50}$  values for inhibition of AC do correlate well with high affinity sites revealed from displacement studies, but the physiological relevance of

this correlation cannot be extrapolated due to the ionic and nucleotide imbalances which exist in the membrane displacement studies performed in Tris buffer.

Well washed membranes (in the absence of GTP) have stable high affinity conformations which exist in varying proportions [Simon et al, 1975]. Indeed, the data in this thesis for agonist displacement curves show that opioid receptors do exist in high and low affinity states. The proportions of these receptor states differ considerably, and this is likely to be as a result of the different receptors at the point of membrane preparation. Receptors are influenced by many factors, such as receptor/G protein phosphorylation by various cell kinase enzymes, ionic balance of the buffer, proportion of receptors bound to endogenous agonist or the size of the receptor reserve.

#### **8.4. Opioid Receptor Pharmacology.**

Endogenous  $\mu$ - (SH-SY5Y) and  $\delta$ -opioid (NG108-15) receptors have been shown to bind [<sup>3</sup>H]DPN in a dose dependent and saturable manner, indicating a  $B_{max}$  value for SH-SY5Y cells three fold lower than NG108-15 cells (table 4.2). Literature  $B_{max}$  and  $K_d$  values in each cell vary depending on the paper, Table 8.2 shows this variation, SH-SY5Y  $B_{max}$ =35-527fmol/mg protein, DAMGO  $K_i/K_d$ =1.0-178nM and NG108-15  $B_{max}$ =431-1900 fmol/mg protein, DADLE  $K_i/K_d$ =1.7-2.9.

This variation is probably a result of different tissue culture methodology, which may cause differential gene expression. The differences may also result from receptor down-regulation or may be affected by extracellular  $Na^+$  levels [Carroll et al, 1988; Yabaluri and Medzihradsky, 1997]. In addition, these findings may be a result of rapid receptor phosphorylation events, however the specific kinase enzyme which may be involved requires further study.

Fentanyl and DAMGO, DPDPE and DADLE displace [<sup>3</sup>H]DPN from SH-SY5Y ( $\mu$ ) and NG108-15 ( $\delta$ ) cells demonstrating high affinity receptor sites (table 4.3). There are numerous studies where opioid receptor binding has been studied (see table 8.2, 8.3), however, two site analysis of agonist displacement curves is rarely presented. These high affinity receptors are coupled to a G-protein and are thought to mediate functional coupling to effector enzymes, however, this remains controversial for opioid inhibition of AC [Nijssen et al, 1992; Carrol et al, 1988].

Endogenous  $\mu$ -Opioid receptors on SH-SY5Y cells have been shown to couple to an inhibition of AC (table 4.4, figure 8.1). Fentanyl and DAMGO inhibited forskolin stimulated cAMP formation with IC<sub>50</sub> values of 17 and 200nM respectively. In addition,  $\delta$ -opioid receptors on NG108-15 cells also couple to an inhibition of AC, DPDPE and DADLE reducing forskolin stimulated cAMP formation with respective IC<sub>50</sub> values of 0.78 and 0.53nM (table 4.4).

Cloned  $\mu$ - and  $\delta$ -opioid receptors, when expressed in CHO cells, dose dependently and saturably bind [<sup>3</sup>H]DPN. Fentanyl, DAMGO, DPDPE and DADLE displace [<sup>3</sup>H]DPN revealing a high affinity binding site and the same agonists inhibit forskolin stimulated cAMP formation. The high affinity binding sites and functional inhibition of AC for each agonist can be compared for both endogenous and recombinant  $\mu$ - and  $\delta$ -opioid receptors (table 8.1).

Opioid receptor- Selective agonist	Endogenous		Cloned	
	K <sub>i</sub> H (nM)	cAMP IC <sub>50</sub> (nM)	K <sub>i</sub> H (nM)	cAMP IC <sub>50</sub> (nM)
μ- Fentanyl	0.1	18	0.4	11.4
μ- DAMGO	0.3	202	5.4	55
δ- DPDPE	0.1	0.8	9.6	2
δ- DADLE	0.2	0.5	1	0.8

Table 8.1. Comparison of endogenous (μ-, SH-SY5Y and δ-, NG108-15) and cloned μ- and δ-opioid receptor high affinity binding and functional inhibition of AC.

Fentanyl binds to endogenous and cloned μ-opioid receptors with a similar affinity, whereas DAMGO binds to endogenous receptors on SH-SY5Y cells with a higher (17 fold) affinity over cloned μ-opioid receptors expressed in CHO cells. This may be due to differences in membrane lipids, Na<sup>+</sup> sensitive binding, receptor desensitisation/down regulation in CHO cells which may affect the orientation of the receptor, and thereby reducing agonist binding affinity.

The IC<sub>50</sub> value for fentanyl inhibition of forskolin stimulated cAMP formation was similar in both SH-SY5Y and CHOμ cells. However, DAMGO IC<sub>50</sub> value in CHOμ cells was slightly more (4 fold) potent than in SH-SY5Y cells. Fentanyl binding affinity (K<sub>i</sub>H) was approximately 70-200 fold lower than IC<sub>50</sub> values in both SH-SY5Y and CHOμ cells. The K<sub>i</sub>H for DAMGO in SH-SY5Y cells was 673 fold lower than the IC<sub>50</sub> value (table 8.1). These differences may suggest that the high affinity G-protein coupled receptors are not solely responsible for the full inhibition of AC [Nijssen et al, 1992].

Cell Type	Opioid receptor	agonist/ antagonist	K <sub>i</sub> /K <sub>d</sub> (nM)	B <sub>max</sub> (fmol/mgP)	Group/year
SH-SY5Y	μ	DAMGO	4.0	43	Yabaluri and Medzihradsky, 1995
SH-SY5Y	μ	DAMGO	2.6	-	Yu et al, 1986
	δ	DADLE	2.7	-	
SH-SY5Y	μ	DAMGO	high 3.9 low 160	high 34 low 527	Carter and Medzihradsky, 1992
SH-SY5Y	μ	DAMGO	1.0	76	Kazmi and Mishra, 1987
	δ	DPDPE	1.2	35	
SH-SY5Y	μ	DAMGO	178	-	Toll, 1990
	δ	DADLE	130	-	
SH-SY5Y	μ	Fentanyl	0.4	-	Costa et al, 1992
NG108-15	δ	DADLE	1.75	1900	Law et al, 1985
NG108-15	δ	DPN	0.5	431	Polastron et al, 1992
NG108-15	δ	DADLE	2.9	-	Law et al, 1992

Table 8.2. Table showing the differences in cited literature K<sub>i</sub>/K<sub>d</sub> values for ligands acting at the opioid receptors in SH-SY5Y and NG108-15 cells.

Cell Type	Opioid receptor	agonist/ antagonist	K <sub>i</sub> /K <sub>d</sub> (nM)	B <sub>max</sub> (fmol/mgP)	Group/year
CHO	μ	DAMGO	2	-	Raynor et al, 1994
	δ	DPDPE	14	-	
	δ	DADLE	0.7	-	
	κ	Spiradoline	0.4	-	
CHO	δ	DPDPE	2.8	-	Law et al, 1994
	δ	DADLE	1.3	-	
COS1	κ	Spiradoline	4.8	-	Xue et al, 1994
COS7	μ	DAMGO	1.1	300	Surrat et al, 1994
COS7	μ	DAMGO	15	-	Fukuda et al, 1995
	δ	DPDPE	19	-	
COS7	δ	DPDPE	245	-	Kong et al, 1993

Table 8.3. Table showing the differences in cited literature K<sub>i</sub>/K<sub>d</sub> values for ligands acting at the cloned opioid receptors in CHO and COS cells.

Endogenous and cloned  $\delta$ -opioid receptors bind DADLE with similar high affinity, however, DPDPE binds with an approximate 100 fold higher affinity to endogenous over cloned  $\delta$ -opioid receptors.

The  $IC_{50}$  values for DADLE and DPDPE inhibition of forskolin stimulated cAMP formation are similar for both endogenous and cloned  $\delta$ -opioid receptors. The cloned  $\delta$ -opioid receptor in COS cell membranes has been shown to bind DPDPE and DADLE with respective affinities of 17.5 and 4.8nM [Evans et al, 1992]. The values of 9.6 (DPDPE) and 1nM (DADLE) reported here in CHO $\delta$  cell membranes is in general agreement with the findings of Evans et al [1992].

Endogenous  $\delta$ -opioid receptors display slightly lower (2-8 fold)  $K_i$  values than  $IC_{50}$  values for both agonists, whereas in cloned  $\delta$ -opioid receptors, using both DPDPE and DADLE,  $IC_{50}$  values were lower than  $K_i$  values. This may result from differences in surrounding membrane lipid micro-environment, G-protein/AC isoforms or as a direct result of receptor/G protein phosphorylation or  $Na^+$  sensitive binding in CHO cells.

SH-SY5Y cells have recently been shown to express ORL-1 receptors, with nociceptin causing a pertussis toxin sensitive inhibition of the N-type calcium current with an  $IC_{50}$  of 42nM [Connor et al, 1996]. In the same study, nociceptin was shown to cause a dose dependent enhancement of carbachol stimulated increase in  $[Ca^{2+}]_i$  with an  $EC_{50}$  of 60nM [Connor et al, 1996]. In our hands, endogenous ORL-1 receptor agonist nociceptin caused a dose dependent inhibition of forskolin stimulated cAMP formation in SH-SY5Y cells with an  $IC_{50}$  value of 72nM. This potency of nociceptin is similar to the finding of Connor et al [1996] and confirms the presence of ORL-1 receptors on our batch of SH-SY5Y cells.

$[^3H]$ DPN binds to CHO $\kappa$  cell membranes yielding  $K_d$  and  $B_{max}$  values of 0.15nM and 231fmol/mg protein.  $[^3H]$ DPN was displaced by the  $\kappa$ -opioid agonist spiradoline, revealing

a high affinity site (0.6nM). Spiradoline high affinity binding site being comparable to the affinity reported by Yasuda and coworkers (1nM) [1993] using COS-1 cells expressing the cloned  $\kappa$ -opioid receptor. Spiradoline also caused an inhibition of forskolin stimulated cAMP formation in CHO $\kappa$  cells yielding an IC<sub>50</sub> value of 3.3nM.

### **8.5. Central Cannabinoid Receptor Pharmacology.**

The successful development of a cannabinoid binding assay has enabled characterisation of the CB1 receptor using SR141716A, the first CB1 selective antagonist. During the preparation of this thesis, Rinaldi-Carmona et al, [1996], published a paper describing the binding characteristics of [<sup>3</sup>H]SR141716A. The binding characteristics of [<sup>3</sup>H]SR141716A published by Rinaldi-Carmona et al, [1996] were almost identical to the data presented in this thesis, thereby validating the method and its results.

Using an ATP regenerating buffer with rat cerebella membranes the cannabinoid receptor agonist WIN55212-2 caused a dose dependent inhibition of cAMP formation. This effect was abolished by SR141716A. In NG108-15 and SH-SY5Y cells nabilone caused a dose dependent inhibition of forskolin stimulated cAMP formation. IC<sub>50</sub> and I<sub>max</sub> values for the inhibition curves in NG108-15, SH-SY5Y and rat CBM could be demonstrated using various methods (Table 8.4). Inhibition of cAMP formation measured in membranes is seldom reported, indeed WIN55212-2 inhibition of cAMP formation in cerebella membranes could not be successfully demonstrated [Sexton, INRC personal communication].

	IC <sub>50</sub> (nM)	I <sub>max</sub> (%)
WIN55212-2, Rat CBM	24.0	33.2
Nabilone, NG108-15	11.9	30.1
Nabilone, SH-SY5Y	18.9	36.4

Table 8.4. The cannabinoid agonists WIN55212-2 and nabilone display similar IC<sub>50</sub> and I<sub>max</sub> values for the inhibition of cAMP formation.

Cloned CB1 receptor expression in CHO cells, resulted in the production of a cell line which bound [<sup>3</sup>H]SR141716A, this was displaced dose dependently by unlabelled SR141716A. In addition, nabilone caused a dose dependent inhibition of forskolin stimulated cAMP formation in the CHO CB1 cell line. A comparison can now be made of the binding and cAMP inhibition in cloned and endogenous CB1 receptors (table 8.5).

	Endogenous (rat CBM, NG108-15)		Cloned (CHO CB1)	
	SR141716A (CBM) K <sub>i</sub> (nM)	Nabilone (NG) cAMP IC <sub>50</sub> (nM)	SR141716A K <sub>i</sub> (nM)	Nabilone cAMP IC <sub>50</sub> (nM)
CB1	4.2	11.9	2.1	3.4

Table 8.5. Comparison of the pharmacology of cloned and endogenous central cannabinoid receptors.

Although a direct comparison made between K<sub>i</sub> and IC<sub>50</sub> values obtained using separate ligands in different tissues is difficult, endogenous and cloned receptors show similar pharmacological responses to SR141716A and Nabilone (table 8.5).

## **8.6. Future work.**

The work presented in this thesis has made a valuable contribution to our understanding of opioid and cannabinoid receptor pharmacology. However, more studies are required in order to further elucidate the second messenger pathways of these receptor systems.

Molecular biological techniques allow mutated or chimeric opioid and cannabinoid receptors to be constructed, and when these are transfected and expressed, a detailed picture of their pharmacology can be obtained. When the profiles of these receptors are compared with wild type receptors, any pharmacological differences may suggest important information about the altered regions of the receptor.

The novel ORL-1 receptor in SH-SY5Y cells requires further classification, with reference to its coupling to other effector proteins.

In addition, co-expression of the cloned ORL-1 receptors alongside  $\mu$ -,  $\delta$ -, or  $\kappa$ -opioid receptors in CHO cells may yield information about the nature of their coupling to AC in the presence of multiple agonists. For example, does the  $I_{\max}$  value double in the presence of nociceptin and fentanyl in CHO cells expressing ORL-1 and  $\mu$ -opioid receptors. These responses could be compared with endogenous ORL-1,  $\mu$ -opioid receptors in SH-SY5Y cells. Using these cells the effects of receptor desensitisation can also be studied in the prolonged presence of agonist. How long do the desensitisation effects of opioids take to recover in the presence of nociceptin?

Other work which is required includes, cloning out populations of CHO CB1 cells which express different levels of receptor so that receptor-effector coupling can be studied in high and low expressing cells.  $IC_{50}$  and  $I_{\max}$  values for cAMP inhibition may change with a decrease in  $B_{\max}$ .

These studies will present new challenges for future research.

## CHAPTER 9. REFERENCES

- Abood, M. E. and Tao, Q. 1995 *Journal of Pharmacology and Experimental Therapeutics*. 274:3: 1566-1573.
- Adem, A., Mattesson, M. E., Nordberg, A., Pahlman, S., 1987 *Brain Research*. 430:235-242.
- Atcheson, R. and Lambert, D. G. 1994 *British Journal of Anaesthesia*. 73:2: 132-134.
- Bakalyar, D. and Reed R. 1990 *Science*. 250:4986: 1403-1406.
- Baumgold, J. and Fishman, P. H. 1988 *Biochemical and Biophysical Research Communications*. 154:3: 1137-1143.
- Baumgold, J. Paek, R. and Fiskum, G. 1992 *Journal of Neurochemistry*. 58:5: 1754-1759.
- Beavo, J. A. 1996 *Physiological Reviews*. 75:4: 725-748.
- Beidler, J. L., Helson, L. and Spengler, B.A. 1973 *Cancer Research*. 33: 2643-2652.
- Besse, D., Lombard, M. C. and Besson, J. M. 1991 *Brain Research*. 548: 287-291.
- Bertilino, D. G. and Llinas, A. 1992 *Annual Review of Pharmacology and Toxicology* 32: 399-421.
- Berridge, M. J. 1993 *Nature (London)*. 361: 315-325.
- Bhat, S. V., Bajwa, B. S., Dornauer, H. and De Souza, N. J. 1977 *Tetrahedron Letters*. 19: 1669-1672.
- Birnbaumer, L., Abramowitz, J. and Brown, A. M. 1990 *Biochemica et Biophysica Acta*. 1031:163-224.

Birnbaumer, L. 1992 *Cell*. 71: 1069-1072.

Bitensky, M. W., Wheeler, G. L., Yamazaki, A., Rasenick, M. M. and Stein, P. J. 1981  
*Current Topics in Membrane Transport*. 15: 237-271.

Blaney, L. M., Gapper, P. W., and Newby, A. C. 1996 *British Journal of Pharmacology*. 118: 1003-1011.

Bliss, T. V. P. and Collingridge, G. L. 1993 *Nature*. 361: 31-39.

Bloom, A. S., Haavik, C. O., and Strehlow, D. 1978 *Life Sciences*. 23: 1399-1404.

Blume, A. J. 1978 *Proceedings of the National Academy of Sciences USA*. 75: 1713-1717.

Borsodi, A. 1991 *Towards a New Pharmacotherapy of Pain*. John Wiley, Chichester. 241-255.

Bouaboula, M., Poinot-Chazel, C., Bourrie, B., Canat, X., Calandra, B., Rinaldi-Carmona, M. Le Fur, G. and Casellas, P. 1995 *Biochemical Journal*. 312: 637-641.

Bourne, H. 1993 *Nature*. 366:628-629.

Bradbury, A. F., Smythe, D. G. and Snell, C. R. 1976 *Nature*. 260: 793-795.

Bronstrom, C. O., Huang, Y. C., Breckenridge, B. M. and Wolff, D. J. 1975  
*Proceedings of the National Academy of Sciences USA*. 72:1: 64-68.

Brown, B. L., Albano, J. D. M., Ekins, R. D. and Sgherzi, A. M. 1971 *Biochemical Journal*. 121: 516-552.

- Bunzow, J. R., Saez, C., Mortrud, M., Bouvier, C., Williams, J. T., Low, M. and Grandy, D. K. 1994 *FEBS Letters*. 347: 284-288.
- Burgisser, E. 1984 *Trends in Pharmacological Sciences*. 142-144.
- Burnstein, S. H. and Hunter, A. A. 1995 *Boichemical Pharmacology*. 49:6: 855-858.
- Butour, J. L., Moisand, C., Mazarguil, H., Mollereau, C. and Meunier, J. C. 1997 *European Journal of Pharmacology*. 321: 97-103.
- Cali, J. J., Zaagstra, J.C., Mons, N., Cooper, D.M.F. and Krupinski, J. 1994 *Journal of Biological Chemistry*. 269:16: 12190-12195.
- Carroll, J. A., Shaw, J. S., and Wickenden, A. D. 1988 *British Journal of Pharmacology*. 94:625-631.
- Carrol, J. A., Miller, L., Shaw, J. S., and Downes, C. P. 1984 *Neuropeptides*. 5: 89-92.
- Carter, B. D. and Medzihradsky, F. 1992 *Journal of Neurochemistry*. 58: 5: 1611-1619.
- Catterall, W. A. 1988 *Science*. 2: 50-60.
- Catterall, W. A. 1994 *Current Opinions in Cell Biology*. 6: 607-615.
- Caulfield, M. P. and Brown, D. A. 1992 *British Journal of Pharmacology*. 106: 231-232.
- Chavkin, C., James, I. F. and Goldstein, A. 1982 *Nature*. 215: 413-415.
- Chen, Y., Mestek, A., Liu, J., Hurley, J. A. and Yu, L. 1993 *Molecular Pharmacology*. 44: 8-12.

- Cheng, Y. C. and Prusoff, W. H. 1973 *Biochemical Pharmacology*. 22: 3099-3108.
- Cheng, J., Standifer, M. S., Tublin, P. R., Su, W. and Pasternak, G. W. 1995 *Journal of Neurochemistry*. 65:1: 170-175.
- Chang, K. J. and Cautrecasas, P. 1979 *Journal of Biological Chemistry*. 254: 2610-2618.
- Chetcovitch, D. M., Gray, R., Johnson, D. and Sweatt, J. D. 1991 *Proceedings of the National Sciences USA*. 88: 6467-6471.
- Cheung, Y. W., Bradham, L. S., Lynch, T. J., Lin, Y. M. and Tallant, E. A. 1975 *Biochemical and Biophysical Research Communications*. 66:3: 1055-1062.
- Childers, S. R., Pachco, M. A., Bennett, B. A., Edwards, T. A., Hampson, R. E., Mu, J. and Deadwyler, S. A. 1993 *Biochemical Society Symposium*. 59: 27-50.
- Choi, E. J., Xia, Z. and Storm, D. R. 1992 *Biochemistry*. 31: 6492-6498.
- Clarke, P. B. S. 1993 *Biochemical Society Symposium*. 59: 83-96.
- Clementi, E. and Meldolisi, J. 1996 *Cell Calcium*. 19: 4: 269-279.
- Cobbold, P. H. and Rink, R. J. 1987 *Biochemical Journal*. 248: 313-328.
- Codina, J., Hildebrandt, J. D., Sekura, E. D., Birnbaumer, M., Bryan, J., Manclark, C. R., Iyanger, R. and Birnbaumer, L. 1984 *Journal of Biological Chemistry*. 259: 5871-5886.
- Collins, D. R., Pertwee, R. G. and Davies, S. N. 1995 *British Journal of Pharmacology*. 115: 869-870.

- Compton, D. R., Rice, K. C., DeCosta, B. R., Razdan, R. K., Melvin, L. S., Johnson, M. R. and Martin, B. R. 1993 *Journal of Pharmacology and Experimental Therapeutics*. 265: 218-226.
- Connor, M., Yeo, A. and Hendeson, G. 1996 *British Journal of Pharmacology*. 118: 205-207.
- Connor, M. and Henderson, G. 1996 *British Journal of Pharmacology*. 117: 333-340.
- Cooper, D. M. F., Yoshimura, M., Zhang, Y., Chiono, M. and Mahey, R. 1994 *Biochemical Journal*. 297: 437-440.
- Cooper, D. M. F., Mons, N. and Karpen, J. W. 1995 *Nature*. 374:421-424.
- Costa, E. M., Hoffman, B. B. and Loew, G. H. 1992 *Life Sciences*. 50: 73-81.
- Cote, T. E., Izenwasser, S. and Weems, H. B. 1993 *Journal of Pharmacology and Experimental Therapeutics*. 267:1: 2389-2394.
- Crain, S. M. and Shen, K. F. 1990 *Trends in Pharmacological Sciences*. 11: 77-81.
- Cruciani, R. A., Dvorkin, B., Klinger, H. P. and Makman, M. H. 1994 *Brain Research*. 667: 229-237.
- Cvejic, S., Trapaidze, N., Cyr, C. and Devi, L. A. 1996 *Journal of Biological Chemistry*. 271: 4073-4076.
- Davis, P. D., Hill, C. H., Keech, E., Lawton, G., Nixon, J. S., Sedgewick, A. D., Wadsworth, J., Westmacot, D. and Wilkinson, S. E. 1989 *FEBS Letters*. 259:1: 61-63.

- Deadwyler, S. A., Hampson, R. E., Mu, J., Whyte, A and Childers, S. 1995 *Journal of Pharmacology and Experimental Therapeutics*. 273: 734-743.
- DeBernardi, M. A., Seki, T. and Brooker, G. 1991 *Proceedings of the National Academy of Sciences USA*. 88: 9257-9261.
- Deneris, E. S., Connolly, J., Rogers, S. W. and Duvoisin, R. 1991 *Trends in Pharmacological Sciences*. 12: 34-40.
- Devane, W. A., Hanus, L., Breuer, A., Pertwee, R. G., Stevenson, L. A., Griffen, G., Gibson, D., Mandelbaum, A., Etinger, A. and Mechoulam, R. 1992 *Science*. 258:1946-1949.
- Devane, W. A., Dysarz, F. A., Johnson, R., Melvin, L. S. and Howlett, A. C. 1988 *Molecular Pharmacology*. 34: 605-613.
- Dickenson, A. H. 1995 *British Journal of Anaesthesia*. 75: 193-200.
- Dickenson, J. M., Camps, M., Gierschlik, P. and Hill, S. J. 1995 *European Journal of Pharmacology*. 288: 393-398.
- Dolphin, A. C. 1991 *Biochimica Biophysica Acta*. 1091: 68-80.
- Evans, C. J., Keith, D. E., Morrison, H., Magendzo, K. and Edwards, R. H. 1992 *Science*. 258: 1952-1955.
- Felder, C. C., Joyce, K. E., Brieley, E. M., Mansouri, J., Mackie, K., Blond, O., Lai, Y, Ma, a. L. and Mitchell, R. L. 1995 *Molecular Pharmacology*. 48: 443-450.
- Felder, C. C., Veluz, J. S., Williams, H. L., Brieley, E. M. and Matsuda, L. A. 1992 *Molecular Pharmacology*. 42: 838-845.

- Felder, C. C., Kanterman, R. Y., Ma. A. L. and Axlerod, J. 1989 *Journal of Biological Chemistry*. 264: 20356-20362.
- Fukuda, K., Kato, S., Mori, K., Nishi, M. and Takeshima, H. 1993 *FEBS Letters*. 327: 311-314.
- Fukuda, K., Kato, S., Mori, K., Nishi, M., Takeshima, H., Iwabe, N., Miyata, T. and Sugimoto, T. 1994 *FEBS Letters*. 343: 42-46.
- Fukuda, K., Kato, S., and Mori, K. 1995 *Journal of Biological Chemistry*. 270:12:6702-6709.
- Furuichi, T. and Mikoshiba, K. 1995 *Journal of Neurochemistry*. 64:3: 953-961.
- Gaoni, Y. and Mechoulam, R. 1964 *Journal of the American Chemical Society*. 86: 1646-1647.
- Gerard, C. M., Mollereau, G., Vassart, H. and Parmentier, M. 1991 *Biochemical Journal*. 279: 129-134.
- Gilman, A. G. 1987 *Annual Review of Biochemistry*. 56: 615-649.
- Gilman, A. G., Rall, T. W., Nies, A. S., Taylor, P. 1990 *The Pharmacological Basis of Therapeutics*. Pergamon Press.
- Glat, C. E. and Snyder, S. H. 1993 *Nature*. 361: 536-538.
- Godchaux, W., and Zimmerman, W. F. 1979 *Journal of Biological Chemistry*. 254: 7874-7884.
- Goldstein, A., Tachibana, S., Lowney, L. I., Hunkapiller, M. and Hood, L. 1979 *Proceedings of the National Academy of Sciences USA*. 76: 6666-6670.

- Gross, R. A., Moises, H. C., Uhler, M. D. and Macdonald, R. L. 1990 Proceedings of the National Academy of Sciences USA. 87: 7025-7029.
- Grynkiewicz, G., Poenie, M. and Tsien, R. Y. 1985 Journal of Biological Chemistry. 260: 3440-3449.
- Grudt, T. J., Usowicz, M. M. and Henderson, G. 1995 Molecular Brain Research. 36:1: 93-100.
- Herkenham, M., Groen, B. G. S., Lynn, A. B., DeCosta, B. R. and Richfield, E. K. 1991 Brain Research. 552: 301-310.
- Hildebrandt, J. D., Sekura, R. D., Codina, J., Iyengar, R., Manclark, C. R. and Birnbaumer, L. 1983 Nature. 302: 706-709.
- Hillard, C. J., Adron Harris, R. and Bloom, A. S. 1985 Journal of Pharmacology and Experimental Therapeutics. 232:2: 579-588.
- Hillard, C. J., Edgmond, W. S. and Campbell, W. B. 1995 Journal of Neurochemistry. 64:2: 677-683.
- Hirota, K. and Lambert, D. G. 1997 Neuroscience Letters. 223: 169-172.
- Holister, L. E. 1986 Pharmacological Review. 38:1: 1-20.
- Howlett, A. C. Bidaut-Russell, M., Devane, W. A., Melvin, L. S., Johnson, M. R. and Herkenham, M. 1990 Trends in Neuroscience. 13: 420-423.
- Howlett, A. C. and Flemming, R. M. 1984 Molecular Pharmacology. 26: 532-538.

- Howlett, A. C., Qualey, J. M. and Khachatrian, L. L. 1986 *Molecular Pharmacology*. 29: 307-313.
- Howlett, A. C. 1984 *Life Sciences*. 35: 1803-1810.
- Hughes, J., Smith, T. W., Kosterlitz, H. W., Fothergill, L. A., Morgan, B. A. and Morris, H. R. 1975 *Nature*. 258: 577-579.
- Hughes, J. 1975 *Brain Research*. 88: 295-308.
- Hulme, E. C., Birdsall, N. J. M. and Buckley, N. J. 1990 *Annual Review of Toxicology*. 30: 633-673.
- Ingram, S. L. and Williams, J. T. 1994 *Neuron*. 13: 179-186.
- Ito, H. 1992 *Journal of General Physiology*. 99: 961-983.
- Iyengar, R. 1993 *FASEB Journal*. 7: 768-775.
- Jacobowitz, O., Chen, J., Premont, R. T. and Iyenger, R. 1993 *Journal of Biological Chemistry*. 268: 3829-3832.
- Jansson, C. C., Kukkonen, J. and Akkerman, K. E. O. 1991 *Biochemica et Biophysica Acta*. 1095: 255-260.
- Johnson, M., Devane, W., Howlett, A., Melvin, L. and Milne, G. 1988 *NIDA Research Monogram*. 90: 129-135.
- Kaminski, N. E., Abood, M. E., Kessler, F. K., Martin, B. R. and Schatz, A. R. 1992 *Molecular Pharmacology*. 42: 736-742.

- Karnik, S. S., Sakmar, T. P., Chen, H. B. and Khoranga, H. G. 1988 Proceedings of the National Academy of Sciences USA. 85: 8459-8463.
- Kawabe, J. 1994 Journal of Biological Chemistry. 269: 16554-16558.
- Kazmi, S. M. I. and Mishra, R. K. 1987 Molecular Pharmacology. 32: 109-118.
- Kennedy, C. and Henderson, G. 1991 Molecular Pharmacology. 40: 1000-1005.
- Kieffer, B., Befort, K., Gaveriaux-Ruff, C. and Hirth, C. G. 1992 Proceedings of the National Academy of Sciences USA. 89:12048-12052.
- Klotz, I. M. 1982 Science. 217: 1247-1249.
- Knapp, R. J., Malatynska, E., Fang, L., Li, X., Babin, E., Nguyen, M., Santoro, G., Varga, E. V., Hruby, V. J., Roeske, R. and Yamamura, H. I. 1994 Life Sciences. 54: 463-469.
- Kong, H., Raynor, K., Yasuda, K., Moe, S. T., Portoghese, P. S., Bell, G. I. and Resine, T. 1993 Journal of Biological Chemistry. 268: 23055-23058.
- Kreil, G., Barra, D., Simmaco, M., Erspammer, G., Negri, L., Severini, C., Corsi, R. and Melchiorri, P. 1989 European Journal of Pharmacology. 162: 123-128.
- Krupinski, J., Coussen, F., Bakalyer, H. A., Tang, W. J., Feinstein, P. G., Orth, K., Slaughter, C., Reed, R. R. and Gilman, A. G. 1989 Science. 244: 1558-1563.
- Kuhn, H. 1980 Nature. 283: 587-589.
- Kuster, J. E., Stevenson, J. I., Ward, S. J., D'Ambara, T. E. and Haycock, D. A. 1993 Journal of Pharmacology and Experimental Therapeutics. 264:3: 1352-1362.

- Kyte, J. and Doolittle, R. F. 1982 *Journal of Molecular Biology*. 157: 105-132.
- Lai, J., Bilsky, E. J., Bernstein, R. N., Rothman, R. B., Pasternak, G. W. and Porreca, F. 1994 *Regulatory Peptides*. 54: 159-160.
- Lambert, D. G. and Nahorski, S. R. 1992 *Journal of Physiology*. 86: 77-82.
- Lambert, D. G., Whitham, E. M., Baird, J. G. and Nahorski, S. R. 1990 *Molecular Brain Research*. 8: 263-266.
- Lambert, D. G., Wojcikiewicz, R. J. H., Safrany, S. T., Whitham, E. M. and Nahorski, S. R. 1992 *Progress in Neuro-psychopharmacology and Biological Psychiatry*. 16: 253-270.
- Lambert, D. G. 1993 *British Journal of Anaesthesia*. 71: 86-95.
- Lambert, D. G., Atcheson, R., Hirst, R. A., and Rowbotham, D. J. 1994 *Biochemical Pharmacology*. 46: 1145-1150.
- Larkman, P. M., Kelly, J. S. and Takahashi, T. 1995 *Pfluegers Archives-European Journal of Physiology*. 430: 5: 763-769.
- Law, P. Y., McGinn, M. J., Erikson, L. J., Evans, C. and Loh, H. 1994 *Journal of Pharmacology and Experimental Therapeutics*. 271:1686-1694.
- Law, P. Y., Koehler, J. E. and Loh, H. 1982 *Molecular Pharmacology*. 21: 483-491.
- Law, P. Y., Hom, D. S. and Loh, H. H. 1985 *Journal of Biological Chemistry*. 260; 6: 3561-3569.
- Lawrence, D. K. and Gill, E. W. 1975 *Molecular Pharmacology*. 11: 595-602.

- Lee, C., Park, D. J., Lee, K., Kim, C. G., and Rhee, S. G. 1993 *Journal of Biological Chemistry*. 268: 21318-21327.
- Lewis, J. Mansour, A., Khachaturian, H., Watson, S. J. and Akil, H. 1987 *Pain and Headache*, Vol 9, Neurotransmitters and pain control p129-159.
- Lie-Chen, L. Y., Yang, H. H., Li, S. and Adams, J. 1995 *Journal of Pharmacology and Experimental Therapeutics*. 273: 1047-1056.
- Lipton, S. A. 1991 *Advances in Pharmacology*. 22: 271-297.
- Lord, J. A. H., Waterfield, A. A., Hughes, J. and Kosterlitz, H. W. 1977 *Nature*. 267: 495-499.
- Lowry, O. H., Rosebrough, N. J., Farr, A. L. and Randall, R. J. 1951 *Journal of Biological Chemistry*. 193: 265-275.
- Lustig, K. D., Conklin, B. R., Herzmark, P., Taussig, R. and Bourne, H. R. 1993 *Journal of Biological Chemistry*. 268: 13900-13905.
- Mackie, K. and Hille, B. 1992 *Proceedings of the National Sciences USA*. 89: 3825-3829.
- Magnuson, D. S. K. and Dickenson, A. H., 1991 *British Journal of Pharmacology*. 66: 6: 1941-1950.
- Mailleux, P. and Vanderhaeghen, J. J. 1992 *European Journal of Pharmacology*. 266: 193-196.
- Manning, D. R. and Gilman, A. G. 1983 *Journal of Biological Chemistry*. 258: 7059-7063.

- Martin, W. R., Eades, C. G., Thompson, J. A., Huppler, R. E. and Gilbert, P. E. 1976  
Journal of Pharmacology and Experimental Therapeutics. 197: 517-532.
- Martin, B. R. 1986 Pharmacological Reviews. 38:1:45-73.
- Matsuda, L. A., Lolait, S. J., Brownstein, M. J., Young, A. C. and Bonnet, T. I. 1990  
Nature. 346: 561-564.
- McClesky, F. W., Fox, A. P., Feldman, D. H., Cruz, L. J., Olivera, B. M., Tsien, R. W.  
and Yoshakami, D. 1987 Proceedings of the National Academy of Sciences USA.  
84: 4327-4331.
- Meldolesi, J. and Pozzan, T. 1987 Experimental Cell Research. 171: 271-283.
- Metzger, H. and Lindner, E. 1981 IRCS Medical Science Biochemistry. 9: 99-99.
- Meunier, J. C., Mollereau, C., Toll, L., Suaudeau, C., Moisand, C., Alvinerie, P.,  
Butour, J. L., Guillemot, J. C., Ferrara, P., Monsarrat, B., Mazarguil, H., Vassart, G.,  
Parmentier, M and Costentin, J. 1995 Nature. 377: 532-535.
- Minami, M., Toya, T., Katao, Y., Maekawa, K., Nakamura, S., Onogi, T., Kaneko, S  
and Satoh, M. 1993 FEBS Letters. 329: 291-295.
- Mollereau, C., Palmentier, M., Mailleux, P., Boutour, J. L., Moisand, C., Chalon, P.,  
Caput, D., Vassart, G. and Meunier, J. C. 1994 FEBS Letters. 341: 33-38.
- Mons, N., Yoshimura, M. and Cooper, D. M. F. 1993 Synapse. 14: 51-59.
- Morton, A. J., Hammond, C., Mason, W., and Henderson, G. 1992 Molecular Brain  
Research. 13: 53-61.
- Munro, S., Thomas, K. L. and Abu-Shaar, M. 1993 Nature. 365: 61-65.

- Munson, P. J. 1983 *Journal of Receptor Research*. 3: 249-259.
- Nakagawa-Yagi, Y., Saito, Y., Takada, Y. and Takayama, M. 1991 *Biochemical Biophysical Research Communications*. 178:1: 116-123.
- Ney, J. S., Seltzman, H. H., Pitt, C. G. and Snyder, S. 1985 *Journal of Pharmacology and Experimental Therapeutics*. 234:6: 784-791.
- Nijssen, P. C. G., Sexton, T. and Childers, S. R. 1992 *Journal of Neurochemistry*. 59:6: 2251-2262.
- Nirenberg, A. 1988 *Nature*. 336: 185-187.
- North, R. A., Williams, J. T., Suprenant, A. and Christie, M. J. 1987 *Proceedings of the National Academy of Sciences USA*. 84: 5487-5491.
- Northrup, J. K., Sternweis, P. C., Smigel, M. D., Schleifer, L. S., Ross, E. M. and Gilman, A. G. 1980 *Proceedings of the National Academy of Sciences USA*. 77: 6516-6520.
- Olianas, M. C. and Onali, P. 1994, *Journal of Neurochemistry*. 63:1: 161-168.
- Pasternak, G. W. and Wood, P. L. 1986 *Life Sciences*. 38: 1889-1898.
- Pasternak, G. W. 1993 *Clinical Neuropharmacology*. 16:1: 1-18.
- Pert, C. B. and Snyder, S. H. 1973 *Science*. 179: 1011-1014.
- Pertwee, R. G. 1988 *Pharmacological Therapeutics*. 36: 189-194.

Pei, G., Cai, Y., Yin, D., Chen, Z., Fan, G. H. and Ma, L. 1996 Proceedings of the INRC. Tu6.

Polastron, J., Jauzac, P. and Meunier, J. C. 1992 European Journal of Pharmacology. 226: 133-139.

Pranther, P. L., McGinn, T. M., Erickson, L. J., Evans, C. J., Loh, H. H. and Law, P. Y. 1994 Journal of Biological Chemistry. 269: 21293-21302.

Puck, A. S., Wemmer, G. R., and Sonnel, D. 1958 Journal of Experimental Medicine. 108: 945-950.

Puttfarcken, P. S. and Cox, B. M. 1989 Life Sciences. 45: 1937-1942.

Rall, T. W., Sutherland, E. W. and Wosilait, W. D. 1956 Journal of Biological Chemistry. 218: 483-495.

Rands, E., Candelore, M. R., Cheung, A. H., Hill, W. S., Strader, C. D. and Dixon, R. A. F. 1990 Journal of Biological Chemistry. 265: 10759-10764.

Rang, H. P. and Dale, M. M. 1987 Pharmacology. London: Churchill Livingstone.

Raynor, K., Kong, H., Chen, Y., Yasuda, K., Yu, L., Bell, G. I. and Reisine, T. 1994 Molecular Pharmacology. 45: 330-334.

Reeve, H. L., Vaughn, P. F. T. and Peers, C. 1994 European Journal of Neuroscience. 6: 943-952.

Reinscheid, R. K., Northacker, H. P., Bourson, A., Ardati, A., Henningsen, R. A., Bunzow, J. R., Grandy, D. K., Langen, H., Monsma, F. J. and Civelli, O. 1995 Science. 270: 792-794.

Reisine, T. and Bell, G. I. 1993 *Trends in Neurosciences*. 16: 506-509.

Reisine, T., Heerding, J. and Raynor, K. 1994 *Regulatory Peptides*. 54: 241-242.

Rhim, H. and Miller, R. J. 1994 *Journal of Neuroscience*. 14: 7608-7615.

Richards, M. H. 1991 *Biochemical Pharmacology*. 42: 1645-1653.

Rinaldi-Carmona, M., Barth, F., Heaulme, M., Alonso, R., Shire, D., Congy, C., Soubrie, P., Breliere, J. and Le-Fur, G. 1995 *Life Sciences*. 56: 1941-1947.

Rinaldi-Carmona, M., Barth, F., Heaulme, M., Shire, D., Calandra, B., Congy, C., Martinez, S., Maruani, J., Neliat, G., Caput, D., Ferrara, P., Soubrie, P., Breliere, J., and Le Fur, G. 1994 *FEBS Letters*, 350: 240-244.

Rinaldi-Carmona, M., Pialot, F., Congy, C., Redon, E., Barth, F., Bachy, A., Breliere, J., Soubrie, P. and Le Fur, G. 1996 *Life Sciences*. 58:15: 1239-1247.

Rinaldi-Carmona, M., Calandra, B., Shire, D., Bouaboula, M., Oustric, D., Barth, F., Casellas, P., Ferrara, P. and Le Fur, G. 1996a *Journal of Pharmacology and Experimental Therapeutics*. 278: 871-878.

Robison, G. A., Butcher, R. W. and Sutherland, E. W. 1968 *Annual Review of Biochemistry*. 37: 149-174.

Rodbell, M., Birnbaumer, L., Pohl, S. L. and Krans, H. M. J. 1971 *Journal of Biological Chemistry*. 246: 1877-1992.

Ross, E. M. and Gilman, A. G. 1977 *Journal of Biological Chemistry*. 252: 6966-6969.

Scatchard, G. 1949 *Annual New York Academy of Science*. 51: 660-672.

- Schaible, H. G. and Grubb, B. D. 1993 *Pain*. 55: 5-54.
- Seward, E., Hammond, C. and Henderson, G. 1991 *Proceedings of the Royal Society*.  
London. 244: 129-135.
- Seward, E. and Henderson, G. 1990 *Pfluegers Archieves European Journal of  
Physiology*. 417: 223-230.
- Shears, S. B. 1991 *Pharmacology and Therapeutics*. 49:1-2: 79-104.
- Shire, D., Carillon, C., Kaghad, M., Calindra, B., Rinaldi-Carmona, M., Le-Fur, G.,  
Caput, D. and Ferrara, P. 1995 *Journal of Biological Chemistry*. 270: 3726-  
3731.
- Shimohigashi, Y., Hatano, R., Fujita, T., Nakashima, R., Nose, T., Sujaku, T., Saigo,  
A., Shinjo, K. and Nagahisa, A. 1996 *Journal of Biological Chemistry*. 39: 27:  
23642-23645.
- Simon, E. J., Hiller, J. M., Groth, J., and Edelman, I. 1975 *Journal of Pharmacology  
and Experimental Therapeutics*. 192: 531-537.
- Simon, E. J., Hiller, J. M. and Edelman, I. 1973 *Proceedings of the National Academy  
of Sciences USA*. 70: 1947-1949.
- Simonin, F., Gaveriaux-Ruff, C., Befort, K., Matthes, H., Lannes, G., Micheletti, G.,  
Mattei, M. G., Charron, G., Bloch, B. and Kieffer, B. 1995 *Proceedings of the  
National Academy of Sciences USA*. 92: 7006-7010.
- Smart, D. and Lambert, D. G. 1995 *British Journal of Pharmacology*. 116: 2655-2660.
- Smart, D. and Lambert, D. G. 1996 *Trends in Pharmacological Sciences*. 17: 264-269.

- Smart, D., Smith, G. and Lambert, D. G. 1995 *Biochemical Journal*. 305: 577-582.
- Smart, D., Smith, G. and Lambert, D. G. 1994 *Journal of Neurochemistry*. 62: 1009-1014.
- Smrcka, A. V., Hepler, J. R., Brown, J. O. and Sternweis, P. C. 1991 *Science*. 251: 804-807.
- Standifer, K. M., Cheng, J., Brookes, A. I., Honrado, C. P., Su, W., Viconti, L. M., Biedler, J. L. and Pasternak, G. W. 1994 *Journal of Pharmacology and experimental Therapeutics*. 270:3: 1246-1255.
- Stanfa, L. C., Clapman, V., Kerr, N. and Dickenson, A. H. 1996 *British Journal of Pharmacology*. 118:1875-1877.
- Sternweis, P. C. and Robishaw, J. D. 1984 *Journal of Biological Chemistry*. 259: 13806-13813.
- Stojilkovic, S. S., Reinhart, J. and Catt, K. J. 1994 *Endocrine Reviews*. 15:4: 462-499.
- Stryer, L., Hurley, J. B. and Fung, B. K. 1981 *Current Topics in Membrane Transport*. 15: 93-108.
- Suh, B. C. and Kim, K. T. 1995 *Journal of Neurochemistry*. 64:6: 2500-2508.
- Surratt, C. K., Johnson, P. S., Moriwaki, A., Seidleck, B. K., Blaschak, C. J., Wang, J. B. and Uhl, G. R. 1994 *Journal of Biological Chemistry*. 269: 20548-20553.
- Taddese, A., Nah, S. Y. and McClesky, E. W. 1995 *Science*. 270: 1366-1369.
- Tang, T., Kiang, J. G., Cote, T. and Cox, B. M. 1995 *Journal of Neurochemistry*. 65:4: 1612-1621.

- Tang, W. J. and Gilman, A. G. 1991 *Science*. 254:1500-1503.
- Tang, W. J. and Gilman, A. G. 1992 *Cell*. 70: 869-872.
- Tang, W. J., Krupinski, J. and Gilman, A. G. 1991 *Journal of Biological Chemistry*. 266:13: 8595-8603.
- Taussig, R., Iniguez-Lluhi, J. A. and Gilman, A. G. 1993 *Science*. 261: 218-221.
- Taussig, R., Tang, W. J., Hepler, J. R. and Gilman, A. G. 1994 *Journal of Biological Chemistry*. 269:8: 6093-6100.
- Terenius, L. 1973 *Acta Pharmacology and Toxicology*. 32: 317-320.
- Tobin, A. B., Keys, B. and Nahorski, S. R. 1996 *Journal of Biological Chemistry*. 271:7: 3907-3916.
- Toll, L. 1990 *European Journal of Pharmacology*. 176: 213-217.
- Trapaizze, N., D. E. Keith, S. Cvejic, C. J. Evans, and L. A. Devi. 1996 *Journal of Biological Chemistry*. 271, 29279-29285.
- Traynor, J. and Elliott, J. 1993 *Trends in Pharmacological Sciences*. 14: 84-86.
- Tsein, R. W., Lipscombe, D., Madison, D. V., Bley, K. R. and Fox, A. P. 1988 *Trends in Neurochemical Sciences*. 11: 431-438.
- Ueda, N. and Tang, W. J. 1993 *Biochemical Society Transactions*. 21: 1132-1138.
- Vaughan, C. W. and Christie, M. J. 1996 *British Journal of Pharmacology*. 117: 1609-1611.

- Vaughan, P. F. T., Peers, C. and Walker, J. H. 1995 *General Pharmacology*. 26:6: 1191-1201.
- Vogel, Z., Barg, J., Levy, R., Saya, D., Heldman, E. and Mechoulam, R. 1993 *Journal of Neurochemistry*. 61: 352-355.
- Vorherr, T., James, P., Krebs, J., Penniston, J. T. and Carafio, E. 1993 *Biochemistry*. 32: 6081-6088.
- Wang, J. B., Imai, Y., Epler, M. C., Gregor, P., Spivak, C. and Uhl, G. R. 1993 *Proceedings of the National Academy of Sciences USA*. 90: 10230-10234.
- Wang, J. B., Johnson, P. S., Persico, A. M., Hawkins, A. L., Griffin, C. A. and Uhl, G. R. 1994 *FEBS Letters*. 338: 217-222.
- Watts, A. E., Williams, J. T. and Henderson, G. 1996 *Journal of Neurophysiology*. 76; 4: 2262-2270.
- Werling, L. L., Zarr, G. D., Brown, S. R., and Cox, B. M. 1985 *Journal of Pharmacology and Experimental Therapeutics*. 233: 722-728.
- Werling, L. L., Brown, S. R., Puttfarcken, P. and Cox, B. M. 1986 *Molecular Pharmacology*. 30: 90-95.
- Werz, M. A. and Macdonald, R. L. 1983 *Journal of Pharmacology and Experimental Therapeutics*. 227: 394-401.
- Wess, J., Brann, M. R. and Bonner, T. I. 1989 *FEBS Letters*. 258: 133-136.
- Wess, J., Bonner, T. I., Dorje, F. and Brann, M. R. 1990 *Molecular Pharmacology*. 38: 517-523.

- Wick, M. J., Minnerath, S. R., Lin, X., Elde, R., Law, P. Y. and Loh, H. H. 1994  
Molecular Brain Research. 27: 37-44.
- Wu, Z., Wong, S. T. and Storm, D. R. 1993 Journal of Biological Chemistry. 268:  
4604-4607.
- Wu, Z., Wong, S. T. and Storm, D. R. 1995 Proceedings of the National Academy of  
Sciences USA. 92: 220-224.
- Xai, Z., Refsdal, C. D., Merchant, K. M., Dorsa, D. M. and Storm, D. R. 1991 Neuron.  
6: 489-515.
- Xia, Z., Choi, E. J., Wang, F., Blazynski, C. and Storm, D. R. 1993 Journal of  
Neurochemistry. 60: 305-311.
- Xue, J. C., Chen, C., Zhu, J., Kunapuli, S., DeReil, J. K. and Liu-Chen, L. Y. 1994  
Journal of Biological Chemistry. 269: 30195-30199.
- Yabaluri, N. and Medzihradski, F. 1997 Journal of Neurochemistry. 68:3: 1053-1061.
- Yabaluri, N. and Medzihradski, F. 1995 Molecular Pharmacology. 48: 690-695.
- Yasuda, K., Raynor, K., Kong, H., Breder, C. D., Takeda, J., Reisine, T. and Bell, G. I.  
1993 Proceedings of the National Academy of Sciences USA. 90: 6736-6740.
- Yoshimasa, T., Silbey, D. R., Bouvier, M., Lefkowitz, R. J. and Caron, M. G. 1987  
Nature. 327: 67-70.
- Yoshimura, M. and Cooper, D. M. F. 1992 Proceedings of the National Academy of  
Sciences USA. 89: 6716-6720.

Yu, V. C., Richards, M. L. and Sadee, W. A. 1986 *Journal of Biological Chemistry*.  
261: 1065-1070.

Zadina, J. E., Hackler, L., Ge, L. J. and Kastin, A. J. 1997 *Nature*. 386: 499-502.

Zastawny, R. L., George, S. R., Nguyen, T., Chen, R., Tsatsos, J., Briones-Urbina, R.  
and O'Dowd, B. F. 1994 *Journal of Neurochemistry*. 62: 6: 2099-2105.

## **9.1. Publications Arising from this Thesis.**

### **Full Papers.**

- [1] **Hirst R. A.** and Lambert D. G. Adenylyl Cyclase in SH-SY5Y human neuroblastoma cells is regulated by intra- and extra-cellular calcium. (1995) *Biochemical Pharmacology*, 49:11, p1633-1640.
- [2] **Hirst R. A.**, Almond S.A. and Lambert D. G. Characterisation of the rat cerebella CB1 receptor using SR141716A, a central cannabinoid receptor antagonist. (In-press) *Neuroscience Letters*.
- [3] **Hirst R. A.**, Smart D., Devi L. A. and Lambert D. G. Effects of C-terminal truncation of the recombinant  $\delta$ -opioid receptor on ligand binding, cAMP and Ins(1,4,5)P<sub>3</sub> formation. (in-preparation) *Journal of Biological Chemistry*.
- [4] **Hirst R. A.**, Hirota, K., Grandy, D. K. and Lambert, D. G. Coupling of the cloned rat  $\kappa$ -opioid receptor to adenylyl cyclase is dependent on receptor expression. (Submitted) *Neuroscience Letters*.
- [5] Lambert D. G., Atcheson R., **Hirst R. A.** and Rowbotham D. J. The effects of morphine and its metabolites on opiate receptor binding, cAMP formation and [<sup>3</sup>H]-noradrenaline release from SH-SY5Y cells. (1993) *Biochemical Pharmacology*, 46: 7, p1145-1150.
- [6] Smart D., **Hirst R. A.**, Grandy D. K. and Lambert D. G. The effects of recombinant rat  $\mu$ -Opioid receptor activation in CHO cells on phospholipase C, [Ca<sup>2+</sup>]<sub>i</sub> and adenylyl cyclase. (In-press) *British Journal of Pharmacology*.
- [7] Atcheson R., Lambert D. G., **Hirst R. A.** and Rowbotham D.J. Studies on the mechanism of [<sup>3</sup>H]-noradrenaline release from SH-SY5Y cells: The role of Ca<sup>2+</sup> and cAMP. (1994) *British Journal of Pharmacology*, 111, p787-792.

### **Book Chapter.**

**Hirst R. A.,** Harrison, C. and Lambert, D. G. Measurement of  $[Ca^{2+}]_i$  in cell suspensions using Fura-2. (in-preparation) Calcium signalling protocols, Humana Press. USA.

### **Abstracts.** (P= Poster and O= Oral presentation)

[A1] **Hirst R. A.** and Lambert D. G. Do SH-SY5Y Cells possess cannabis receptors? (1995) Biochemical Society Transactions. 418S. (P)

[A2] **Hirst R. A.,** Devi L., and Lambert D.G. Is the C-terminus of the recombinant  $\delta$ -opioid receptor important for adenylyl cyclase coupling? (1996) British Journal of Pharmacology. 118, 27P. (O)

[A3] **Hirst R. A.** and Lambert D. G. Carbachol stimulated cAMP formation in SH-SY5Y cells is dependent on both intra- and extra-cellular calcium. (1993) Biochemical Society Transactions, 21: 431S. (O, by special invitation from the Biochemical Society)

[A4] **Hirst R. A.,** Hirota K., Grandy D. K. and Lambert D. G. Coupling of the cloned  $\kappa$ -opioid receptor to adenylyl cyclase is dependent on receptor expression. (1996) International Narcotics Research Conference Proceedings, Long Beach, CA (P).

[A5] **Hirst R. A.,** Lambert D. G., Smart D. and McKnight A.T. Effects of Nociceptin on cAMP and  $Ins(1,4,5)P_3$ - $[Ca^{2+}]_i$  signaling in SH-SY5Y human neuroblastoma cells. (in-press) British Journal of Pharmacology, (P).

[A6] Lambert D.G., **Hirst R. A.,** Smart D. And Grandy D. K. Characterization of CHO cells expressing the cloned rat  $\mu$  opioid receptor. (1996) British Journal of Pharmacology 117, 6P. (O)

[A7] Lambert D. G. and **Hirst R. A.** Effects of morphine and its metabolites on opiate receptor binding and cAMP formation. (1993) British Journal of Anaesthesia, 70:475-476P. (O)

[A8] Atcheson R., **Hirst R. A.**, Rowbotham D. J. and Lambert D. G. Studies on the mechanisms of fentanyl-induced depression of evoked [<sup>3</sup>H]-noradrenaline release in SH-SY5Y human neuroblastoma cells. (1994) Proceedings of the world pain congress, Paris. (P)